PREVENTING THROMBOSIS AND INFECTION OF MEDICAL DEVICES USING NON-FOULING COATINGS COUPLED WITH NITRIC OXIDE RELEASE

by

MARCUS JAMES GOUDIE

(Under the Direction of Hitesh Handa)

ABSTRACT

Blood contacting medical devices, such as catheters, stents, vascular grafts, and extracorporeal artificial organs, are used in thousands of patients every day. Despite decades of research on developing biocompatible materials, infection and thrombus formation continue to be two of the leading complications with blood contacting medical devices. Thrombus formation can result in significant consequences such as medical device failure, embolism, inaccurate results from sensors, and death; while an estimated 1.7 million healthcare associated infections result in 99,000 deaths per year in the United States alone. The combination of frequent use and the need for higher dosage of antibiotics has led to the development of antibiotic resistant strains of bacteria, further increasing treatment costs and suffering for the patients. A variety of approaches have been used to create materials that can resist protein and bacterial adhesion that leads to infection and thrombosis, including super hydrophilic surfaces, liquid-infused materials, or coating with zwitterionic compounds. However, these materials can be further improved by the addition of active release of bactericidal and antithrombotic agents.

Nitric oxide (NO) is naturally produced from healthy endothelium cells, macrophages, and in our sinuses, and is involved in regulating several biological processes such as platelet activation and adhesion, and is a potent broad spectrum antibacterial agent, effective in killing common pathogens associated with hospital acquired infections such as *Staphylococcus aureus*, *Staphylococcus epidermidis*, *Pseudomonas aeruginosa*, *Escherichia coli*, and *Acinetobacter baumanii*. Integrating the active release of NO into polymeric materials can provide a biomimetic approach for preventing thrombosis while reducing risks associated with infection. In this dissertation, NO releasing materials are evaluated for their ability to reduce thrombus formation *in vivo*, and are characterized for several key challenges associated with clinically relevant materials. The efficacy of these materials is then further improved upon by coupling NO releasing materials with novel approaches for creating non-fouling surfaces, for materials that can both passively reduce protein and bacterial adhesion while having bactericidal and antithrombotic properties.

INDEX WORDS: Nitric oxide, non-fouling, hemocompatible, antimicrobial, biomaterials

# PREVENTING THROMBOSIS AND INFECTION OF MEDICAL DEVICES USING NON-FOULING COATINGS COUPLED WITH NITRIC OXIDE RELEASE

by

MARCUS JAMES GOUDIE

BS, University of Michigan, 2012

MS, University of Pennsylvania, 2013

A Dissertation Submitted to the Graduate Faculty of The University of Georgia in Partial Fulfillment of the Requirements for the Degree

DOCTOR OF PHILOSOPHY

ATHENS, GEORGIA

2017

# PREVENTING THROMBOSIS AND INFECTION OF MEDICAL DEVICES USING NON-FOULING COATINGS COUPLED WITH NITRIC OXIDE RELEASE

by

MARCUS JAMES GOUDIE

| | |
|---|---|
| Major Professor: | Hitesh Handa |
| Committee: | Ramana Pidaparti |
| | Benjamin Brainard |

Electronic Version Approved:

Suzanne Barbour
Dean of the Graduate School
The University of Georgia
December 2017

DEDICATION

To my family, for always supporting me in whatever I choose to pursue, and always encouraging me to follow my dreams.

ACKNOWLEDGEMENTS

First, I would like to thank Dr. Hitesh Handa for taking a chance and taking me as his first student, and being a great advisor over the past four years. Your level of flexibility, understanding, and desire for your students to succeed provides a great atmosphere for research, where students have the freedom to pursue their passions and grow as independent scientists.

Second, I would like to thank my fellow lab members, especially Jitendra Pant, Priya Singha, Dr. Sean Hopkins, Dani Workman, and Katie Homeyer, for making my time as a graduate student fun, both inside and outside of the lab. Having such driven and knowledgeable lab mates really makes the work more enjoyable and exciting.

Next, I would like to thank Dr. Scott Merz and MC3 Inc. for the number of internships I held in the company, helping me develop my knowledge and passion for biomedical engineering. I would like thank Dr. Kathy Osterholzer, Dan Mazur, and Brian Price for all their mentoring, and helping me develop understanding and expertise in biomedical device design and always pushing me to go outside of my comfort zone.

Thank you to my committee members, Drs. Benjamin Brainard and Ramana Pidaparti for their time and direction during my doctoral studies. It was great not only to have their support in my thesis work, but in a variety of collaborations throughout my studies.

Thank you to Dr. Chad Schmiedt for your mentoring and training in developing my surgical skills for all of my *in vivo* work, and Tara Denley, Ethan Karstedt, and Melissa Martin for all of their hard work in monitoring and caring for the animals.

I would like to thank Dr. Jason Locklin and his lab for being so welcoming to the University of Georgia, and their willingness to always lend a helping hand. Their training on a number of laboratory instruments helped tremendously.

Lastly, I would like to thank a number of funding institutions for their support throughout my graduate studies. I would like to thank the ARCS Foundation of Atlanta for their selection of me as an ARCS scholar. Their support not only gave me extra resources to develop my surgical skills, but helped me present my work at highly focused conferences in my field. I would also like to thank the National Institutes of Health and the Center for Disease Control for funding this work.

TABLE OF CONTENTS

Page

LIST OF TABLES

Page

LIST OF FIGURES

Page

# CHAPTER 1

# INTRODUCTION AND LITERATURE REVIEW

## Introduction

The goal of creating a truly hemocompatible material has troubled researchers for decades, despite a deep understanding of the coagulation cascade. Fouling of these devices, either through adsorption of protein leading to thrombus formation, or the adhesion of bacteria resulting in infection, are two of the most common complications seen clinically today.[1-3] While tremendous advances have been made in preventing thrombosis through the systemic administration of anticoagulants such as heparin, systemic anticoagulation has several consequences such as uncontrolled hemorrhage and thrombocytopenia.[4] In the case of extracorporeal circuits, while systemic anticoagulation is required to preserve the patency of the circuit, platelet consumption is still observed and can drop to <40% of the initial value during the first 1-2 h of use.[5] Due to these complications, the systemic administration of anticoagulants is the leading cause of drug-related deaths from adverse clinical events in the United States.[6] Prevention of thrombosis is critical to the functionality of medical devices, such as catheters, stents, vascular grafts, heart valve prosthesis, and extracorporeal membrane oxygenation systems, that are used in thousands of patients every day.[7] Therefore, developing materials that can prevent thrombosis locally at the material surface can reduce the levels of systemic anticoagulation needed, or remove the need for systemic anticoagulants all together.

Although preventing thrombosis is critical for the functionality of the device to be maintained, the implantation of these devices provides a substantial risk for infection to occur due to openings in the body from surgery, or through contamination issues associated with the

procedure. In the US alone there are over 1.7 million hospital acquired infections (HAIs) annually resulting in 100,000 death.[8, 9] There is an exponential increase in nosocomial infections due to rapid development of multi-drug resistant strains and failure of the current antimicrobial strategies to prevent this.[10] As the infection occurs, bacteria form biofilm, an extracellular matrix that encompasses the bacterial network, providing protection from antimicrobial compounds in the surrounding. It is this biofilm formation that calls for high dosages of antibiotic to be administered once the infection has been diagnosed, as biofilm can require 1000 times the concentration of antibiotics when compared to bacteria in a dispersed state.[11, 12] These high levels of antibiotics have resulted in the emergence of antibiotic resistant strains, and demonstrate the need for preventative approaches to limit infection and aid in reducing the frequency of antibiotic administration.

This chapter provides and introduction to two classes of materials used for limiting thrombosis and infection of medical devices: i) non-fouling and ii) nitric oxide (NO) releasing materials.

**Non-fouling materials**

When materials are exposed to biological environments (such as blood) proteins adsorb to the surface within minutes.[7, 13] The adsorption of these proteins facilitates the binding of both bacteria and platelets to the material surface, and the attachment of these proteins and bacteria is referred to as fouling or biofouling. The blood protein fibrinogen is the key protein involved in thrombosis, leading to the formation of fibrin which provides structure to the thrombus. The adsorption of fibrinogen also results in conformational changes in the protein structure, allowing for binding to platelets through the glycoprotein GPIIb/IIIa.[14] Therefore, limiting the degree of

protein and bacterial adhesion to materials can provide a passive approach for limiting both thrombosis and infection.

*Hydrophilic and super-hydrophobic materials*

One approach to limit the adsorption of proteins to a medical implant in aqueous environments has been to develop materials with strongly favorable or unfavorable interactions with water. A variety of surface parameters can influence the interactions between the material surface and the surround water, such as surface charge, free energy, and roughness. The most common way to assess the degree of hydrophilicity is through the contact angle, where a small volume of water is placed on the surface. The energy balance between surface tensions of the air-water and water-material interfaces results in an angle between the material surface and the water drop, where low angles represent "wetting" or spreading of the water drop over the surface, and high angles where unfavorable interactions between the water and surface leave the droplet in a rounded state. The highly favorable interactions between the water molecules and the materials surface provide an energy barrier for protein to adsorb, acting as a mechanism for reducing thrombus formation.

While hydrophilic materials may be beneficial at reducing protein adhesion, their high water uptake often coincides with poor mechanical properties. These materials with high water adsorption are typically referred to as hydrogels, and can be prepared from a variety of materials; such as poly(vinyl alcohol) (PVA), polyacrylamides (PAAm), poly(N-vinyl pyrrolidone) (PNVP), poly(hydroxymethyl methacrylate) (PHEMA), poly(ethylene oxide) (PEO), poly(ethylene glycol) (PEG), and cellulose.[15] Due to their poor mechanical properties, these materials have been immobilized onto or coated on to other polymeric substrates to improve their surface properties, where hydrogen bonding between water and the polymer backbone prevents

cells and protein from adhering.[16-18] The two most common surface modification using these hydrogels has been PEG and PEO.[16, 18-20] While these approaches generally provide reductions in protein adhesion by > 90% when compared to unmodified polymers, adhesion of platelets has been observed when these materials are used i*n vivo*.[21]

Zwitterionic materials, containing both a positive and negative charge, are a specialized class of grafted molecules that possess high affinity for water, and can exhibit contact angles less than 10 degrees. Examples of commonly used zwitterionic groups are phosphobetaine, sulfobetaine, and carboxylbetaine (Figure 1.1). The hemocompatible and non-fouling nature of these materials stems from their phophorylcholine-like groups which are present on the lipid bilayers of cell membranes.[22, 23] While the hydrophilic molecules above (such as PEG) have strong interactions with water through hydrogen bonding, the electrostatic interaction between the anionic and cationic charges within the zwitterionic group bind to water even more strongly through induced electrostatics.[22, 24] These materials have shown excellent non-fouling capabilities *in vitro*, but have not yet been shown to prevent thrombosis *in vivo*.

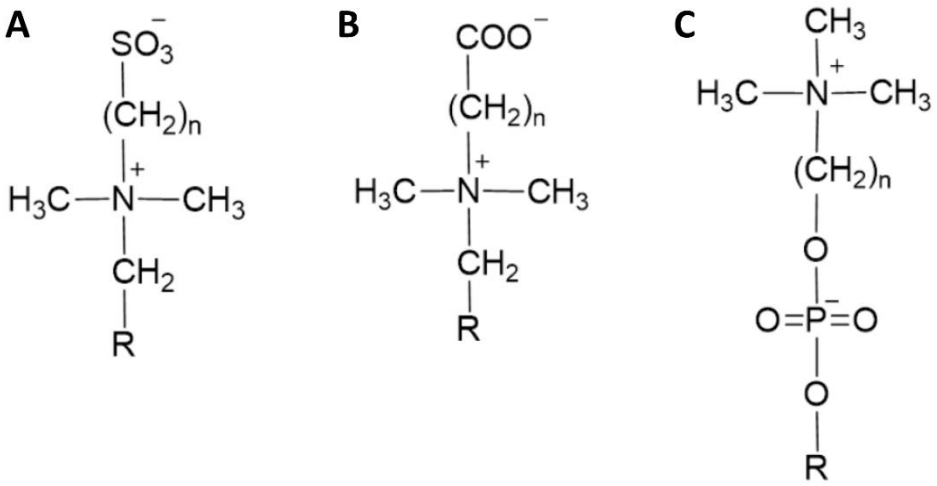


Figure 1.1: Structures of A) sulfobetaines, B) carboxylbetaines, and C) phosphobetaines.

While hydrophilic materials typically reduce protein adsorption, this does not necessarily translate to decreases in platelet adhesion and hemocompatibility due to the structural confirmation of the protein on the surface.[25, 26] For this reason, strongly hydrophobic materials can demonstrate good hemocompatibility as well. These can include silicones, polyurethanes, polytetrafluorethylene (PTFE), poly(vinyl chloride) (PVC), and polyethylene. While these materials do not have a high affinity for water, adsorption of the most abundant blood protein, albumin, can bind to the surface more strongly. This strong binding reduces what is observed as the Vroman effect, where the highly concentrated albumin protein is replaced over time by fibrinogen, which is responsible for thrombus formation.[27, 28] As roughness can become a factor in the hydrophilicity of a material, patterning of surfaces with ordered topography has been used to create super hydrophobic materials (contact angle >150 degrees). While these materials are excellent at repelling water under atmospheric conditions, their efficacy has not been observed *in vivo*. This is due to the transition of the droplet on the surface from the Cassie-Baxter to Wenzel state, where wetting within the patterned geometry greatly increases the surface area, promoting thrombus formation.[29]

*Liquid infused materials*

Liquid-infused materials, or sometimes referred to as slippery liquid infused porous surfaces (SLIPS), utilize the interactions of a liquid with either the bulk polymer matrix or a thin surface modification like the polymer brush as noted above.[30, 31] These materials address the issues associated with super hydrophobic surfaces that utilize surface patterning to achieve the non-wetting status, while providing a robust self-healing coating.[32] The first of these SLIPS materials utilized for medical application was the addition of a tethered perfluorocarbon via silane chemistry to a variety of polymers commonly used in the medical field.[33] Following the

surface modification, the medical tubing is primed using a liquid perfluorocarbon, which has been used in a variety of medical applications such as liquid ventilation, ophthalmic surgery, and is a US Food and Drug Administration approved blood substitute. However, as the liquid layer separating the material surface from its environment is incredibly thin, the longevity of the slippery nature can be an issue. However, these materials have shown drastic decreases in bacterial adhesion *in vivo* in a murine subcutaneous model.[34] To provide a replenishing of the liquid layer, infusion of a commonly used medical polymer silicone with silicone oil provides a large reservoir to replenish the slippery nature of the surface as the material is exposed to shear forces.[31] While these materials are excellent at drastically reducing the adhesion of proteins and bacteria to the material surface, the interaction of these thin films in bacterial rich environments is not fully understood. It is hypothesized that bacteria can penetrate this thin film and form "beachheads", where local cocolonization and biofilm formation can begin to occur.[32] These materials can also lead to complications associated with platelet activation.[33, 35] To address issues related with bacterial penetration of the liquid layer, incorporation of an antimicrobial Triclosan has been shown to provide both bactericidal activity while having the ultra-low fouling characteristics of SLIPS.[32] While this is excellent for non-blood-contacting medical devices, issues associated with platelet activation are yet to be addressed.

**Nitric oxide releasing materials**

Nitric oxide (NO) is a free radical, water soluble, ubiquitous gas, which influences various biological functions. It is a cellular signaling molecule naturally secreted by vascular endothelial cells, and is involved in many physiological and pathological processes.[36] As shown in **Figure 1.2**, nitric oxide is enzymatically synthesized endogenously from L-arginine by nitric oxide synthase (NOS). There are 3 NOS synthase isoforms: eNOS (endothelial NOS, generates

NO from the endothelial lining of blood vessels), nNOS (neuronal NOS, present in neurons and produces NO that acts as a neurotransmitter) and iNOS (inducible NOS, present in macrophages as a response to bacterial/viral infections).[37, 38] The eNOS and nNOS isoforms are calcium dependent and increased NO production occurs when there is an increase in $Ca^{2+}$. The iNOS isoform is calcium independent and is involved in immune responses, including autoimmune diseases, and is the predominate cause of septic shock.[39]

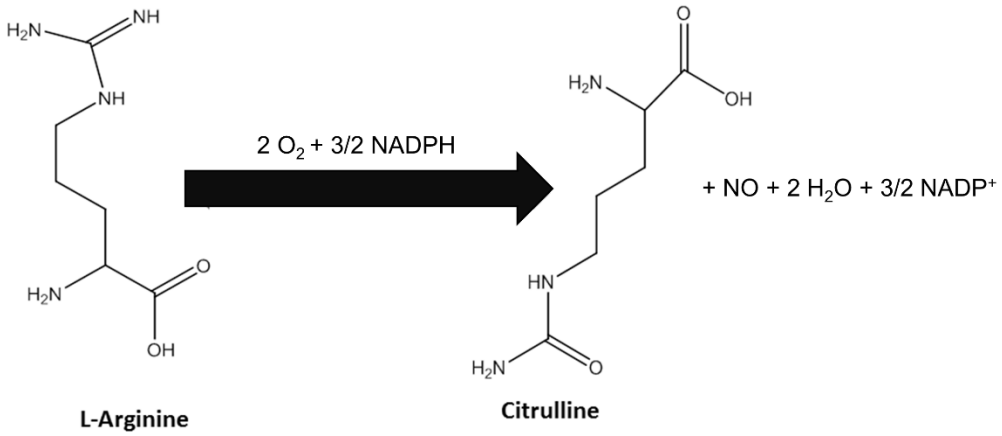


Figure 1.2: Enzymatic (nitric oxide synthase, NOS) conversion of L-arginine to citrulline resulting in nitric oxide (NO) release.

Radomski et al. first described NO as a potent vasodilator secreted by the normal endothelium that has the ability to inhibit platelet adhesion and aggregation to the blood vessel wall.[40, 41] In 1992, the free radical NO was approbated as 'molecule of the year' by the journal Science and was the subject of Nobel Prize in 1998. Numerous published reviews have been devoted to a comprehensive discussion of different NO-releasing/generating materials and their many potential biomedical applications.[42-48]

Nitric oxide offers great potential to be utilized in biomedical applications due to its impact on wide ranging biological functions including infection, angiogenesis, inflammation, vasodilation, thrombosis, smooth muscle cell proliferation and migration, wound healing,

cardiovascular diseases, nervous system diseases, mammalian cell growth and tumor formation [49-55]. Nitric oxide is known to be a potent inhibitor of platelet activation and adhesion. Healthy endothelial cells exhibit an NO flux of $0.5–4.0 \times 10^{-10}$ mol $cm^{-2}$ $min^{-1}$. [56] In addition, NO released within the sinus cavities and macrophages functions as a natural antimicrobial agent.[47, 57] Mullin et al. showed that gaseous NO is bactericidal against several strains of bacteria derived from tracheal aspirates of mechanically ventilated patients in the intensive care unit (ICU). [58] Therefore, using NO-releasing polymers that can locally delivery NO at or above physiologically relevant levels has the advantage of creating implantable devices that can possess both antithrombotic and antibacterial properties.

Due to the fact that NO is highly reactive under physiological conditions, many molecules with functional groups that can store and release NO have been studied. Among various NO donors, diazoniumdiolates and S-nitrosothiols (RSNOs) have been studied widely. [42, 59-68] Diazeniumdiolates are synthetic NO donors that undergo proton or thermally driven mechanism to release 2 moles of NO per diazeniumdiolate molecule (**Figure 1.3**). [69-71] Both endogenous and synthetic *S*-nitrosothiols (RSNOs) have been studied (**Figure 1.4**). Some of the endogenous RSNOs include *S*-nitrosoglutathione (GSNO), *S*-nitrosocysteine (CysNO), and *S*-nitrosoalbumin. *S*-nitroso-*N*-acetylpenicillamine (SNAP) and *S*-nitroso-*N*-acetylcysteine (SNAC) are two examples of synthetic RSNOs. These RSNOs can release NO via thermal decomposition, catalysis (using metals ions such as $Cu^{+}$), or by exposure to light (wavelengths of 340 and/or 590 nm) resulting in disulfide species (RSSR) formation.[38, 72-75]

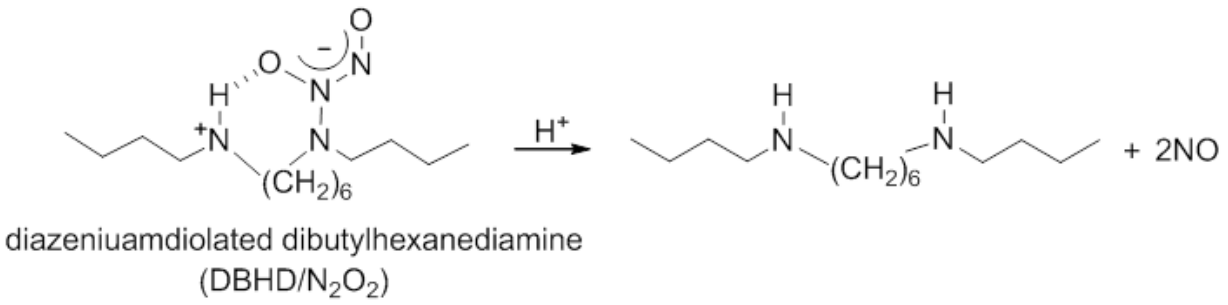


Figure 1.3: Mechanism of NO release from diazeniumdiolated dibutylhexanediamine ($DBHD/N_2O_2$).

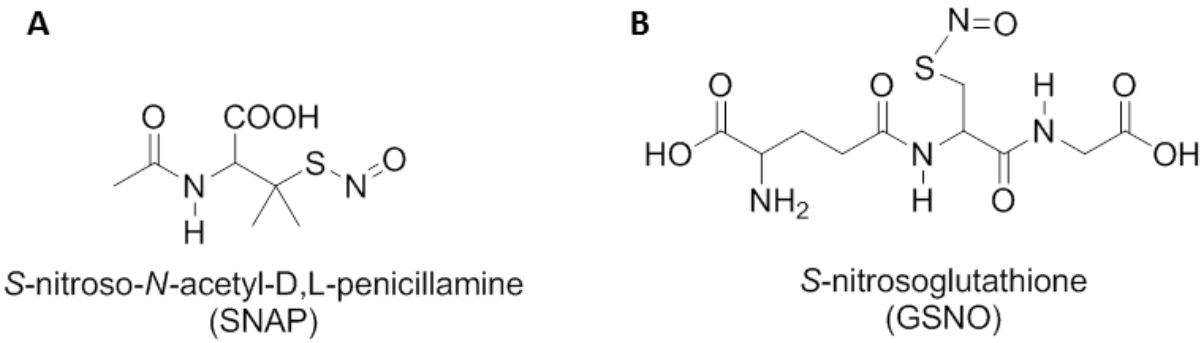


Figure 1.4: Structures of example synthetic (A) and endogenous (B) *S*-nitrosothiol species.

Brisbois et al. incorporated SNAP into Elast-eon E2As; a copolymer of poly(dimethylsiloxane), poly(hexamethylene oxide), and methylene diphenyl isocyanate.[62] The SNAP and control catheters were prepared by dip coating polymer solutions on stainless steel mandrels. The SNAP-doped E2As catheters had a trilayer configuration, with base and top E2As coats and a 10 wt% SNAP containing middle active layer. These SNAP/E2As catheters were able to withstand the EO sterilization process, retaining 88.8 ± 0.7% of the original SNAP. The NO lost during sterilization can be attributed to the elevated temperature and exposure to humidity used in the EO sterilization procedure. The SNAP/E2As catheters were able to continually release NO at physiological levels (greater than $0.5 \times 10^{-10}$ mol $cm^{-2}$ $min^{-1}$) for up to

20 d. The catheters exhibited a higher NO flux on the first day of soaking due to the initial water uptake of the polymer and slight leaching of SNAP that is on the surface. Even though NO release from the catheters reaches the lower end of endothelial NO release, it continues to reduce intravascular thrombosis and bacterial adhesion. The SNAP and control catheters were implanted in the jugular veins of sheep for 7 d. The SNAP/E2As catheters had significantly less thrombus formation than controls ($1.56 \pm 0.34$ cm$^2$ and $5.06 \pm 0.64$ cm$^2$ respectively) as well as had a 90% reduction in adherence of living bacteria to the surface as compared to control E2As catheters.

Various additives have been used to facilitate the release of NO from both diazeniumdiolates and nitrosothiol donors. For diazeniumdiolates, the release of NO leads to the polymer matrix becoming basic over time due to free amines, effectively shutting off the NO release. The addition of poly(lactic-co-glycolic acid) (PLGA) to the polymer matrix controls the pH through the decomposition of the PLGA species, and increases the longevity of NO release to over 14 d.[76] The degradation rate and chemical termination of the PLGA can be adjusted to provide various NO release profiles, allowing for high controllability of the release profile. This approach drastically reduced thrombus formation of central venous catheters *in vivo* over 9 d in a rabbit model, while also providing a 95% reduction in viable bacteria. For nitrosothiols, photoinitiated release has been shown to provide excellent control of NO release from polydimethylsilioxane films, the use of light can be limited for implanted applications.[73] Integration of metallic complexes such as copper into polymer networks with SNAP has been shown to provide not only a method to increase the observed NO release levels, but provide a secondary antimicrobial activity due to the oligodynamic effect while remaining non-cytotoxity to mammalian cells.[77] Incorporation of copper nanoparticles has also been used as a method to

provide catalytic release of systemically administered and endogenous NO donors, signifying that these materials can continue to release NO in the presence of blood even after all of the NO has been released from the NO donor in the polymer matrix.[78]

## Conclusion

Many approaches have been used to improve the biocompatibility of materials over the past few decades. One of the most common approaches has been the development of non-fouling materials, which provide a passive mechanism to limit protein and bacterial adhesion, leading to reductions in thrombus formation and infection, where this non-fouling nature is achieved by altering the surface chemistry of the base material. Nitric oxide releasing materials are the first materials to date that actively reduce thrombosis and infection simultaneously by preventing platelet activation while acting as a bactericidal agent. While both approaches have made substantial improvements in reduced viable bacterial attachment and thrombosis in the laboratory setting, it is clear that there is no single approach capable of providing a completely biocompatible material. However, further improvements can be made by developing multi-functional materials that can use multiple mechanism to prevent thrombosis and infection.

## Organization of the Dissertation

This dissertation describes the development of materials that possess non-fouling characteristics with an active release of NO. The NO donor S-nitroso-acetylpenicillamine (SNAP) is integrated into several medical materials as method to develop antithrombotic and antimicrobial materials. The remaining of the dissertation is organized as follows:

Chapter 2 investigates the properties of NO releasing materials as they relate to the translation from benchtop to bedside, and addresses key issues associated with medical applicability.

Chapter 3 demonstrates the efficacy of NO releasing materials in reducing thrombus formation *in vivo*. Various metrics were used to indicate the hemocompatibility of these materials, including platelet and clotting factor consumption over time.

Chapter 4 describes the development of an ultra-low fowling NO releasing surface, that is achieved through using liquid-infused materials. The NO donor was incorporated into medical grade silicone tubing using a solvent swelling process. After solvent removal, the NO releasing silicone was then infused with a biocompatible oil, providing a lubricious protective layer. The effect of this oil on NO release kinetics, as well as biological activity are investigated.

Chapter 5 describes the development of a surface immobilized NO donors that as a source for exogenous NO while decreasing the fouling of the material surface. As a drawback to materials that actively release compounds to achieve antimicrobial or antithrombotic properties, efficacy of the material may be limited or decrease over time. The addition of NO donors immobilized at the surface provides non-fouling capabilities after all NO is released, and can be easily combined with existing NO releasing materials as an alternative to augment NO release.

Chapter 6 provides conclusions based on this work, and outlines future directions researchers may pursue based on the materials developed here.

**References**

1. A. Vertes, V. Hitchins and K. S. Phillips, Analytical chemistry, 2012, 84, 3858-3866.
2. N. P. O'Grady, M. Alexander, E. P. Dellinger, et al., Clinical infectious diseases, 2002, 35, 1281-1307.

3. M. L. Paden, S. A. Conrad, P. T. Rycus, et al., ASAIO journal, 2013, 59, 202-210.

4. R. E. Cronin and R. F. Reilly, 2010.

5. G. Annich, Journal of Thrombosis and Haemostasis, 2015, 13.

6. G. Shepherd, P. Mohorn, K. Yacoub, et al., Annals of Pharmacotherapy, 2012, 46, 169-175.

7. E. J. Brisbois, H. Handa and M. E. Meyerhoff, in Advanced Polymers in Medicine, Springer, 2015, pp. 481-511.

8. C. A. Welsh, M. E. Flanagan, S. C. Hoke, et al., American journal of infection control, 2012, 40, 29-34.

9. R. M. Donlan, Clinical Infectious Diseases, 2001, 33, 1387-1392.

10. A. Pegalajar-Jurado, K. A. Wold, J. M. Joslin, et al., Journal of Controlled Release, 2015, 217, 228-234.

11. P. S. Stewart and J. W. Costerton, The lancet, 2001, 358, 135-138.

12. K. K. Jefferson, D. A. Goldmann and G. B. Pier, Antimicrobial agents and chemotherapy, 2005, 49, 2467-2473.

13. J. Pant, M. Goudie, E. Brisbois, et al., in Advances in Polyurethane Biomaterials, Elsevier, 2016, pp. 471-550.

14. M. B. Gorbet and M. V. Sefton, Biomaterials, 2004, 25, 5681-5703.

15. N. Peppas, Y. Huang, M. Torres-Lugo, et al., Annual review of biomedical engineering, 2000, 2, 9-29.

16. J. Andrade, V. Hlady and S.-I. Jeon, Polymeric Materials: Science and Engineering, 1993, 60-61.

17. C.-G. Gölander, J. N. Herron, K. Lim, et al., in Poly (ethylene glycol) Chemistry, Springer, 1992, pp. 221-245.
18. J. H. Lee, H. B. Lee and J. D. Andrade, Progress in Polymer Science, 1995, 20, 1043-1079.
19. N. A. Alcantar, E. S. Aydil and J. N. Israelachvili, Journal of biomedical materials research, 2000, 51, 343-351.
20. J. M. Harris, Poly (ethylene glycol) chemistry: biotechnical and biomedical applications, Springer Science & Business Media, 1992.
21. G. R. Llanos and M. V. Sefton, Journal of Biomedical Materials Research Part A, 1993, 27, 1383-1391.
22. S. Jiang and Z. Cao, Advanced Materials, 2010, 22, 920-932.
23. L. Wu, Z. Guo, S. Meng, et al., ACS applied materials & interfaces, 2010, 2, 2781-2788.
24. Z. Zhang, M. Zhang, S. Chen, et al., Biomaterials, 2008, 29, 4285-4291.
25. M. Sefton, C. Gemmell and M. Gorbet, BD Ratner, AS Hoffman, FJ Schoen, JE Lemons, Biomaterials Science Elsevier, 2004.
26. B. Sivaraman and R. A. Latour, Biomaterials, 2010, 31, 832-839.
27. L. Vroman and A. L. Adams, Surface Science, 1969, 16, 438-446.
28. H. Noh and E. A. Vogler, Biomaterials, 2007, 28, 405-422.
29. D. Murakami, H. Jinnai and A. Takahara, Langmuir, 2014, 30, 2061-2067.
30. J. W. Costerton, Z. Lewandowski, D. E. Caldwell, et al., Annual Reviews in Microbiology, 1995, 49, 711-745.
31. N. MacCallum, C. Howell, P. Kim, et al., ACS Biomaterials Science & Engineering, 2014, 1, 43-51.

32. U. Manna, N. Raman, M. A. Welsh, et al., Advanced Functional Materials, 2016, 26, 3599-3611.

33. D. C. Leslie, A. Waterhouse, J. B. Berthet, et al., Nature biotechnology, 2014, 32, 1134-1140.

34. J. Chen, C. Howell, C. A. Haller, et al., Biomaterials, 2017, 113, 80-92.

35. R. C. Hartmann, C. L. Conley and E. L. Poole, Journal of Clinical Investigation, 1952, 31, 685.

36. Y. Hou, A. Janczuk and P. Wang, Current Pharmaceutical Design, 1999, 5, 417-442.

37. R. G. Knowles and S. Moncada, Biochemical Journal, 1994, 298, 249.

38. A. Dicks, H. Swift, D. Williams, et al., Journal of the Chemical Society, Perkin Transactions 2, 1996, 481-487.

39. D. J. Stuehr, Biochimica et Biophysica Acta (BBA)-Bioenergetics, 1999, 1411, 217-230.

40. M. W. Radomski, R. M. Palmer and S. Moncada, Biochemical and biophysical research communications, 1987, 148, 1482-1489.

41. M. W. Radomski and S. Moncada, in Mechanisms of Platelet Activation and Control, Springer, 1993, pp. 251-264.

42. M. C. Frost, M. M. Reynolds and M. E. Meyerhoff, Biomaterials, 2005, 26, 1685-1693.

43. A. B. Seabra, P. D. Marcato, L. B. de Paula, et al., 2012.

44. D. A. Riccio and M. H. Schoenfisch, Chemical Society Reviews, 2012, 41, 3731-3741.

45. J. Kim, G. Saravanakumar, H. W. Choi, et al., Journal of Materials Chemistry B, 2014, 2, 341-356.

46. M. C. Jen, M. C. Serrano, R. van Lith, et al., Advanced Functional Materials, 2012, 22, 239-260.

47. G. M. Halpenny and P. K. Mascharak, Anti-Infective Agents in Medicinal Chemistry (Formerly Current Medicinal Chemistry-Anti-Infective Agents), 2010, 9, 187-197.

48. A. W. Carpenter and M. H. Schoenfisch, Chemical Society Reviews, 2012, 41, 3742-3752.

49. J. Marín and M. A. Rodríguez-Martínez, Pharmacology & Therapeutics, 1997, 75, 111-134.

50. K. Vural and M. Bayazit, European Journal of Vascular and Endovascular Surgery, 2001, 22, 285-293.

51. M. W. Radomski and S. Moncada, Thrombosis and Haemostasis, 1993, 70, 36-41.

52. T. B. Cai, P. G. Wang and A. A. Holder, NO and NO donors for pharmaceutical and biological applications., Weinheim: Wiley VCH, 2005.

53. A. F. Chen, Acta Pharmacologica Sinica, 2005, 26, 259-264.

54. P. L. Feldman, Chem. Eng. News, 1993, 71, 26-38.

55. P. C. Kuo and R. A. Schroeder, Annals of Surgery, 1995, 221, 220.

56. M. W. Vaughn, L. Kuo and J. C. Liao, American Journal of Physiology-Heart and Circulatory Physiology, 1998, 274, H2163-H2176.

57. J. J. Rouby, American Journal of Respiratory and Critical Care Medicine, 2003, 168, 265-266.

58. B. B. McMullin, D. R. Chittock, D. L. Roscoe, et al., Respiratory care, 2005, 50, 1451-1456.

59. J. H. Shin and M. H. Schoenfisch, Analyst, 2006, 131, 609-615.

60. E. M. Hetrick and M. H. Schoenfisch, Chemical Society Reviews, 2006, 35, 780-789.

61. H. Handa, T. C. Major, E. J. Brisbois, et al., Journal of Materials Chemistry B, 2014, 2, 1059-1067.

62. E. J. Brisbois, R. P. Davis, A. M. Jones, et al., Journal of Materials Chemistry B, 2015.

63. E. J. Brisbois, H. Handa, T. C. Major, et al., Biomaterials, 2013, 34, 6957-6966.

64. E. J. Brisbois, J. Bayliss, J. Wu, et al., Acta Biomaterialia, 2014, 10, 4136-4142.

65. M. M. Reynolds, J. A. Hrabie, B. K. Oh, et al., Biomacromolecules, 2006, 7, 987-994.

66. T. C. Major, D. O. Brant, M. M. Reynolds, et al., Biomaterials, 2010, 31, 2736-2745.

67. T. C. Major, H. Handa, E. J. Brisbois, et al., Biomaterials, 2013, 34, 8086-8096.

68. M. Frost and M. E. Meyerhoff, Analytical Chemistry, 2006, 78, 7370-7377.

69. M. M. Batchelor, S. L. Reoma, P. S. Fleser, et al., Journal of Medicinal Chemistry, 2003, 46, 5153-5161.

70. K. A. Mowery, M. H Schoenfisch, J. E. Saavedra, et al., Biomaterials, 2000, 21, 9-21.

71. D. J. Smith, D. Chakravarthy, S. Pulfer, et al., Journal of Medicinal Chemistry, 1996, 39, 1148-1156.

72. P. D. Wood, B. Mutus and R. W. Redmond, Photochemistry and Photobiology, 1996, 64, 518-524.

73. M. C. Frost and M. E. Meyerhoff, Journal of the American Chemical Society, 2004, 126, 1348-1349.

74. R. J. Singh, N. Hogg, J. Joseph, et al., Journal of Biological Chemistry, 1996, 271, 18596-18603.

75. D. L. H. Williams, Accounts of Chemical Research, 1999, 32, 869-876.

76. E. J. Brisbois, T. C. Major, M. J. Goudie, et al., Acta Biomaterialia, 2016.

77. J. Pant, M. J. Goudie, S. P. Hopkins, et al., ACS Applied Materials & Interfaces, 2017.

78. T. C. Major, D. O. Brant, C. P. Burney, et al., Biomaterials, 2011, 32, 5957-5969.

# CHAPTER 2

# CHARACTERIZATION OF A NITRIC OXIDE RELEASING POLYMER FROM A TRANSLATION PERSPECTIVE[1]

[1] Goudie, M.J., Brisbois, E.J., Pant, J., Thompson, A., Potkay, J., Handa, H. 2016. *International Journal of Polymeric Materials and Polymeric Biomaterials* 65.15: 769-778

Reprinted here with permission of the publisher

**Abstract**

Due to the role of nitric oxide (NO) in regulating a variety of biological functions in humans, numerous studies on different NO releasing/generating materials have been published over the past two decades. Although NO has been demonstrated to be a strong antimicrobial and potent antithrombotic agent, NO-releasing (NOrel) polymers have not reached the clinical setting. While increasing the concentration of the NO donor in the polymer is a common method to prolong the NO-release, this should not be at the cost of mechanical strength or biocompatibility of the original material. In this work, it was shown that the incorporation of S-nitroso-penicillamine (SNAP), an NO donor molecule, into Elast-eon E2As (a copolymer of mixed soft segments of polydimethylsiloxane and poly(hexamethylene oxide)), does not adversely impact the physical and biological attributes of the base polymer. Incorporating 10 wt % of SNAP into E2As reduces the ultimate tensile strength by only 20%. The inclusion of SNAP did not significantly affect the surface chemistry or roughness of E2As polymer. Ultraviolet radiation, ethylene oxide, and hydrogen peroxide vapor sterilization techniques retained approximately 90% of the active SNAP content, where sterilization of these materials did not affect the NO-release profile over an 18 day period. Furthermore, these NOrel materials were shown to be biocompatible with the host tissues as observed through hemocompatibility and cytotoxicity analysis. In addition, the stability of SNAP in E2As was studied under a variety of storage conditions, as they pertain to translational potential of these materials. SNAP-incorporated E2As stored at room temperature for over 6 months retained 87% of its initial SNAP content. Stored and fresh films exhibited similar NO release kinetics over an 18 day period. Combined, the results from this study suggest that SNAP-doped E2As polymer is

suitable for commercial biomedical applications due to the reported physical and biological characteristics that are important for commercial and clinical success.

## Introduction

Over the past 20 years, nitric oxide (NO) has emerged as a key player in regulating a number of biological functions, including angiogenesis, inflammation, vasodilation, thrombosis, smooth muscle cell proliferation and migration, wound healing, cardiovascular diseases, nervous system diseases, prevention of infection, cell growth and tumor formation in humans and other mammals.[1-7] It has been shown that NO is the primary regulator in inhibiting platelet activation and adhesion [8-11], and is naturally released from vasculature at an estimated rate of $0.5 – 4 \times 10^{-10}$ mol $min^{-1}$ $cm^{-2}$.[12] In addition, NO has broad-spectrum antibacterial properties, and is effective against both gram-positive and gram-negative bacteria.[13-18] These research results show the potential of using NO-releasing materials for biomedical device applications with improved biocompatibility and reduced foreign body response. In order to translate the NO research from benchtop to bedside, there is an urgent need to understand the physical and biological characteristics of NO-releasing polymers.

Nitric oxide is a free radical, water soluble, ubiquitous gas with a very short half-life and hence acts in a localized manner.[19] The NO exposure to a biological system can have significant consequences in a dose dependent manner; therefore, concentration of NO must be controlled carefully to provide reproducible results. For instance, micromolar concentrations of NO are required for inhibiting the growth of tumor cells, while picomolar concentrations have an angiogenic effect.[20] Recently, the development of NO donor molecules has allowed for localized delivery of NO, drastically increasing the possible applications for NO-releasing (NOrel) materials. Among various NO donors that have been investigated, synthetic *S*-nitrosothiols

(RSNOs) have been studied extensively.[10, 11, 18, 21-29] Release of NO from these materials can occur through thermal decomposition, catalysis (using metals ions such as $Cu^{+}$) [30], or by exposure to light [29, 31, 32], resulting in disulfide species (RSSR) formation. *S*-nitroso-acetylpenicillamine (SNAP) is a synthetic RSNO which has shown to exhibit significant antimicrobial and antithrombotic effects in various medical grade polymers.[11, 14, 23, 33] One advantage of using SNAP as an NO-donor is that any slight leaching of SNAP, or more likely N-acetyl-penicillamine (NAP) or NAP disulfide species, would ultimately hydrolyze to penicillamine and acetic acid.[23] Low levels of these species are not a major concern, since penicillamine is an FDA approved agent used for treating heavy metal ion poisoning (Pb(II), etc.) in humans.[34] Among different polymers studied, Elast-eon E2As polymer (a copolymer of mixed soft segments of polydimethylsiloxane and poly(hexamethylene oxide)), possesses excellent intrinsic biocompatibility properties, exhibiting low levels of blood protein adhesion.[35, 36] In a previous study, diazeniumdiolates (NONOate) added to the E2As coating was able to retain 97 ± 10% of platelet counts *in vivo* in a 4 hour extracorporeal circuit (ECC) in a rabbit model.[10] These promising *in* vivo results have prompted the study of SNAP as the NO donor in E2As, where E2As-SNAP ECC loops preserved 100 ± 7% of the platelet count in a 4 hour ECC study in rabbits, while showing great stability of the NO donor after 2 months of storage.[23] Longer terms studies have been reported recently of SNAP-E2As catheters, and showed reduce bacterial adhesion and thrombus formation for 7 days in sheep.[11]

As evident from the previous studies described above, SNAP-doped E2As possesses great potential for biomedical applications. However, in the absence of fundamental research focusing on characterization of NO-releasing polymers in terms of mechanical strength, hemocompatibility, cytotoxicity, and ability to be stored and sterilized, the true potential of this

novel strategy cannot be realized. While NO-releasing polymers have been shown to give excellent results in research settings, antibacterial activity and prevention of thrombus formation are not the only properties to consider when moving towards clinically relevant polymers. Due to the reactivity of NO donors with heat and light, sterilization and storage of these materials continue to limit use of these polymers in clinical devices. [23] Furthermore, the addition of NO donors into polymers should not have cytotoxic effects on cells or induce hemolysis, while maintaining the mechanical and surface properties of the base polymer.

In this work, the effects of incorporating the NO donor SNAP into Elast-eon E2As were investigated in terms of its physical and biological properties. The effects of the addition of various levels of SNAP on the physical and mechanical properties (surface roughness, wettability, and maximum loading) are also shown through atomic force microscopy, static contact angle measurements, and tensile strength testing respectively. Standard methods were used to measure the hemolytic activity (ASTM F756 and ISO 10993-4) and cytotoxicity (ISO 10993-5) to determine biocompatibility of these NO-releasing materials. Furthermore, various levels of SNAP doped films (5 and 10 wt%) were stored under various conditions (ranging from -20°C to 37°C) to examine the shelf life of these materials for up to 6 months, as well as the effect of storage on the release kinetics of NO over a period of 18 days. The SNAP content of these materials was examined before and after a number of common sterilization techniques, including ultraviolet light exposure, autoclaving, hydrogen peroxide vapor, and ethylene oxide.

**Materials and Methods**

N-Acetyl-D-penicillamine (NAP), sodium chloride, ethylenediaminetetraacetic acid (EDTA), potassium chloride, sodium phosphate dibasic, potassium phosphate monobasic, tetrahydrofuran (THF), sulfuric acid and N,N-dimethylacetamide (DMAc) were purchased from

Sigma Aldrich (St. Louis, MO). Methanol, hydrochloric acid and sulfuric acid were obtained from Fisher Scientific (Pittsburgh, PA). Elast-eon E2As was obtained from AorTech International, plc (Scoresby, Victoria, Australia). Phosphate buffered saline (PBS), pH 7.4, containing 138 mM NaCl, 2.7 mM KCl, 10 mM sodium phosphate, and 100 mM EDTA was used for all *in vitro* experiments. Atomic force microscopy Tap 300-G tips were purchased from NanoandMore.

*SNAP Synthesis*

A modified version of a previously reported method was used to synthesize SNAP [28]. Equimolar ratios of NAP and sodium nitrite were added to a 1:1 mixture of water and methanol containing 2 M HCl and 2 M $H_2SO_4$. After 30 min of stirring, the reaction vessel was cooled in an ice bath to precipitate the SNAP crystals. The crystals were collected by filtration, washed with water, and allowed to air dry. The reaction and crystals were protected from light at all the times.

*Preparation of SNAP-based polymer films*

Polymer films containing 5, 10, and 15 wt% SNAP were prepared by solvent evaporation method. The casting solutions were prepared by dissolving 190, 180, or 170 mg Elast-eon E2As in 3 mL THF. SNAP (10, 20, 30 mg, respectively) was then added to the polymer solution and the mixture was stirred for 10 min to give 5, 10, and 15 wt% SNAP solutions. The film solution was casted in Teflon ring (d = 2.5 cm) and dried overnight under ambient conditions. Small disks (d = 0.7 cm) were cut from the parent films and were dip coated with a topcoat solution (200 mg polymer (no SNAP added) in 4 mL THF) and dried over-night under ambient conditions, followed by 48 h of drying under vacuum to remove any residual solvent. The weight of each

small disk was recorded prior to top coating. All films and film solutions were protected from light throughout.

*Tensile testing*

Control and SNAP-loaded E2As films (5 wt%, 10 wt%, 15 wt%) were cast in dumbbell-shaped Teflon™ molds with an active area length of 4.5 cm and width of 1 cm using similar concentrations described in film preparation section. Tensile testing was performed by clamping samples in place on the jaws of the Instron tensile tester. The polymer was pulled with a constant cross-head speed of 20 mm/min and the force at break (N) was recorded. Tensile testing was conducted at room temperature (23 °C).

*Surface characterization*

Film preparation: Films were spin coated onto glass slides using a CHEMAT Technology KW-4A spin coater at a fixed E2As concentration of 50 mg/mL and 15 wt% of SNAP in THF, and spun for 60 seconds at 2000 rpm. A common approach for limiting NO release from SNAP loaded films is the addition of a top coat. E2As solution (50 mg/mL) was applied over the primary E2As layer to match the top coat thickness from dip coated top coats on SNAP-doped films.

*Wettability*: Static contact angle was measured using Kruss DA 100 drop shape analyzer. A 1 µL droplet of water was placed on E2As and E2As-SNAP films that were spin coated on glass slides, and the average of left and right contact angles were measured via the Kruss software.

*Surface Roughness:* Films were then analyzed using Bruker Multimode atomic force microscopy (AFM) to determine surface roughness over a 4 $\mu m^2$ square region using tapping mode. Each film was analyzed in three random areas, with n=3 for each condition (E2As, SNAP-

E2As). The average surface roughness value was taken as the *Ra* parameter, which is the centerline average between the highest and lowest point of the surface irregularities, and was calculated by built in software (Nanoscope, Digitial Instruments, CA, USA).[37]

*Storage Stability of SNAP/E2As Films*

SNAP/E2As films (consisting of 5 wt% or 10 wt% SNAP) were placed under the following conditions in vials with desiccant: 23°C, 37°C in dark, refrigerator (4°C), and in the freezer (-20°C). The amount of SNAP remaining in the films was measured after 1, 3, and 6 months of storage at each condition. Films were dissolved in DMAc and the UV-Vis spectra were recorded to determine the % SNAP remaining in the film, as compared to the initial SNAP films. The NO release kinetics of the films stored for 6 months at 23°C were compared to the freshly made films containing 5 and 10 wt% SNAP.

*Nitric Oxide release measurements*

Nitric oxide released from the films was measured using a Sievers Chemiluminescence Nitric Oxide Analyzer (NOA) 280 (Boulder, CO). Films were placed in the sample vessel immersed in PBS (pH 7.4) containing 100 mM EDTA. Nitric oxide was continuously purged from the buffer and swept from the headspace using nitrogen sweep gas and bubbler into the chemiluminescence detection chamber. Films were submerged in PBS with EDTA and stored in glass vials and kept at 37°C between NO-release measurements. Fresh PBS solution was used for each NO-release measurement, and films were kept in fresh PBS solution for storage after each measurement.

*UV-Vis spectra*

All UV-Vis spectra were recorded in the wavelength range of 200-700 nm using a UV-Vis spectrophotometer (Lambda 35, Perkin Elmer, MA) at room temperature. The presence of the S-NO group of SNAP provides characteristic absorbance maxima at 340 and 590 nm.[29, 38, 39] E2As films were dissolved in DMAc and absorbance values were measured at 340nm.

*In vitro Cytotoxicity Study Using the ISO Elution Method*

To ascertain whether leachable extracted from the 10 wt% SNAP-E2As films would cause any toxic effects on mammalian cells, cytotoxicity testing using ISO 10993-5 Elution Method was used. The cytotoxicity testing was performed by NAMSA® following aseptic Standard Operating Procedures. A single preparation of the 10 wt% SNAP-E2As films was extracted in single strength Minimum Essential Medium (1X MEM) supplemented with 5% fetal bovine serum, 2% antibiotics (100 units/mL penicillin, 100 µg/mL streptomycin and 2.5 µg/mL amphotericin B) and 1% (2 mM) L-glutamine (1X MEM) at 37°C for 24 hours. The negative control (high density polyethylene), reagent control (1X MEM), and positive control (Powder-Free Latex Gloves) were similarly prepared using MEM medium. The 10 wt% SNAP-E2As films were prepared and returned to the freezer until testing. The extracts were not centrifuged, filtered, or otherwise altered prior to dosing. However, the extracts were continuously agitated during extraction. The 1X MEM extraction was performed using serum to optimize extraction of both polar and non-polar components. Mouse fibroblast cells (L-929) were propagated and maintained in flasks containing 1X MEM at 37°C with 5% carbon dioxide ($CO_2$). Thereafter, cells were seeded in 10 $cm^2$ cell culture wells and incubated at 37°C in the presence of 5% $CO_2$ to obtain subconfluent monolayers of cells. Triplicate cultures with subconfluent cell monolayer

were then used for leachate exposure. The growth medium contained in the triplicate cultures was replaced with 2.0 mL of the test extract, reagent control, negative control, or positive control extract depending on the experiment. The wells were incubated at 37°C in 5% $CO_2$ for 48 hours. The color of the test medium was observed to determine any change in pH. In general, a color shift toward yellow indicates an acidic pH range, and a color shift toward magenta to purple indicates an alkaline pH range.

*Hemolysis*

The potential of 10 wt% SNAP-E2As films to cause hemolysis was studied *in vitro* by NAMSA®. The films were tested using ASTM F756, Standard Practice for Assessment of Hemolytic Properties of Materials and ISO 10993-4. Whole blood samples collected from four New Zealand White rabbits into vacuum tubes containing EDTA as the anticoagulant were maintained at room temperature and used within four hours of collection. Anticoagulated whole rabbit blood was pooled, diluted, and added to tubes with the test sample in calcium and magnesium-free phosphate buffered saline (CMF-PBS). Negative controls, positive controls, and blanks were prepared in the same manner. Sterile water for injection (SWFI) and CMF-PBS were used as blanks and positive controls respectively while high density polyethylene (HDPE) was used as the negative control for this study. Clot-free blood samples were collected from each animal into 7 mL vacuum tubes containing 12 mg of EDTA on the same day the test was performed. The blood collected from each animal was pooled into a borosilicate screw cap tube and mixed gently to prevent mechanical hemolysis. The pooled blood was diluted with CMF-PBS to a total hemoglobin concentration of 10 ± 1.0 mg/mL. In a ratio of 1.0 mL diluted blood to 7.0 mL CMF-PBS, samples were prepared in triplicates both for direct contact as well as

extraction. The samples were capped, inverted gently to mix the contents, and then maintained for at least 3 hours at 37°C with periodic inversions at approximately 30-minute intervals. Following incubation, the blood-CMF-PBS mixtures were transferred to separate disposable centrifuge tubes. These tubes were centrifuged for 15 minutes at 700-800 x g. The condition of the supernatant was recorded and a 1.0 mL aliquot of each test article, negative control, positive control, and blank supernatant was added to individual 1.0 mL portions of Drabkin's reagent (hemoglobin reagent) and allowed to stand for 15 minutes at room temperature. The condition of the test article supernatants were recorded a second time. The absorbance of each test article, negative control, positive control, and blank solution was measured at 540 nm using a spectrophotometer. The condition of the test article supernatants was then recorded a third, and the final time.

The hemoglobin concentration of each test article, negative control, positive control and blank solution was then calculated from the standard curve. The blank corrected percent hemolysis was calculated for each test article and the negative and positive controls as follows (where ABS = absorbance):

$$\textit{Blank Corrected \% Hemolysis} = \frac{\textit{ABS (Sample) - ABS (Blank)}}{\textit{ABS (Diluted Blood) - ABS (Blank)}} \textit{ X 100}$$

For the suitability of the system to be confirmed, the negative control must have had a blank corrected % hemolysis value <2% and the positive control must have had a blank corrected % hemolysis value of >5%. If either of these values were not within the acceptable range, the test was repeated with fresh blood.

The mean blank corrected % hemolysis (BCH) was calculated by averaging the blank corrected % hemolysis values of the triplicate test samples. In the event the BCH resulted in a value less than zero, the value was reported as 0.00. The standard deviation for the replicates was determined. An average hemolytic index of the triplicate test samples was also calculated as follows:

*Hemolytic Index = Mean BCH (Test Article) - Mean BCH (Negative Control)*

*Sterilization methods of E2As-SNAP films*

A number of sterilization techniques have become common practice in the fields of medical devices and bacteria/cell culture. Various commonly used sterilization techniques were compared to sterilize 10 wt% SNAP containing E2As films. Autoclaving, hydrogen peroxide vapor, ethylene-oxide (EO), as well as ultra-violet light exposure were investigated. The samples were tested for the wt% SNAP content before and after each sterilization method by UV-Vis analysis. Polymer samples were weighed and rapidly dissolved in DMAc for determination of SNAP by UV-Vis. Details of each sterilization method is described below.

*Autoclave:* The films were steam sterilized at 121°C for 30 min in a Steris 3033 steam sterilizer.

*Hydrogen Peroxide vapor:* SNAP-loaded polymer samples were sterilized using a Steris VHP MD140X for 28 minutes at the University Of Georgia College of Veterinary Medicine. The sterilization chamber is evacuated and hydrogen peroxide solution is injected from a cassette and is vaporized in the sterilization chamber to a concentration of 6 mg/L.

*Ethylene Oxide Sterilization:* SNAP-loaded polymers samples were sterilized by ethylene oxide at the University of Michigan Hospital Central Sterile Processing Department. The EO

sterilization procedure is conducted at 54 °C and 40–80% humidity. Samples were conditioned for 1 h, exposed to EO gas for 2-3 h, and aerated for 14 h.

*UV Sterilization:* SNAP-loaded polymer samples were sterilized using ultra-violet light administered from a 1300 Series A2 Thermo Scientific Biosafety cabinet for 1.5 hours.

*Statistical Analysis*

Results are expressed as mean ± standard error of the mean (SEM). Comparison of SNAP-doped E2As films to control was done using Student's t-test, where $p < 0.05$ was considered statistically significant for all tests.

**Results and Discussions**

One of the prime objectives in developing NOrel materials is to control as well as prolong the NO-release from these devices. Increasing the lifetime of these materials is generally done through increasing the amount of NO donor that is incorporated in the host material. However, the increase in NO donor concentration can also provide an initial burst of NO. Similarly, leaching of NO donors from their base material is a common metric to determine how effective the NO is being delivered. Leaching of SNAP from E2As has been studied previously, and shows how the application of top coats of pure E2As to SNAP-E2As devices will prevent the leaching of SNAP over a period of time.[23] This technique for preventing leaching of SNAP has also been described for other polymeric materials as well.[40] For this reason, the characterization of SNAP-E2As was solely done in combination with pure E2As top coats.

*Tensile Strength*

The use of additives in polymers can have a detrimental effect on a number of the mechanical properties of the base material, such as the tensile strength. The addition of SNAP

was seen to reduce the ultimate tensile strength (UTS) of E2As, and is shown as a percentage of the pure polymer UTS in Figure 2.1. Base polymer E2As was found to have an UTS of 55.8 ± 4.3 N. Films of E2As with 5 wt% SNAP had a ultimate tensile strength of 47.0 ± 10.4 N, and were shown to not be significantly different than the pure E2As films ($p$=0.13). The UTS of SNAP-E2As between 5 and10 wt% was not found to change significantly ($p$=0.31), where 10 wt% SNAP-E2As had an UTS of 45.0 ± 4.4 N. However, as SNAP concentrations are increased past 10 wt%, sharp decreases in material strength were observed, with an UTS of 35.1 ± 5.6 N for films with 15 wt% SNAP (64% of pure E2As). Therefore, concentrations between 5 and 10 wt% SNAP are optimal for retaining the properties of the base material. Optimization of these materials will need to be performed for each type of device, as NO-release characteristics and physical strength requirements can vary drastically from application to application. As the sharp decrease in UTS was seen for SNAP concentration at 15 wt%, only SNAP concentration of 5 wt% and 10 wt% were used in the subsequent studies.

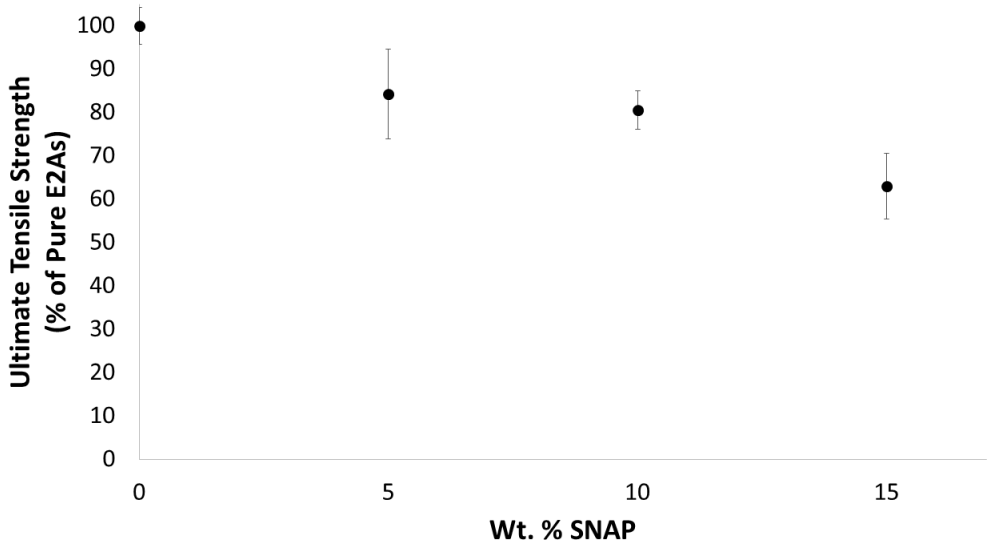


Figure 2.1: Ultimate tensile strength of E2As films with various concentrations of SNAP at break point, as measured by Instron tensile strength instrument.

*Surface characterization*

Surfaces properties of medical devices, blood contacting devices in particular, are some of the most important characteristics of the device in determining biocompatibility. It is well known that increasing roughness as well as hydrophobicity of surfaces can potentially lead to higher amounts of protein adsorption on the surface.[41-43] Therefore, increasing the wettability and decreasing the roughness of these materials is desirable, or any modifications to existing materials should not decrease wettability or increase roughness. Results for the surface characteristics are shown in Table 2.1, and show the addition of SNAP has no noticeable effect on the surface roughness or wettability of the base polymer.

Table 2.1: Effect of SNAP on surface characteristics of E2As films as measured using atomic force microscopy (AFM) and contact angle measurements.

| Film | Surface Roughness (nm) | Contact Angle (Degrees) |
|---|---|---|
| Elast-eon E2As | 11.04 ± 1.97 | 111.7 ± 3.30 |
| 10 Wt % SNAP | 11.65 ± 1.08 | 110.7 ± 0.47 |

The high biocompatibility of the pure E2As polymer can partially be attributed to the higher affinity of albumin binding to the surface when compared to fibrinogen, which has been determined to be the primary protein to initiate the coagulation cascade and induce clot formation.[36, 44] Therefore, altering the surface chemistry of E2As can have large implication on the effectiveness of the material to resist clot formation. Contact angle was measured for pure E2As (111.7 °± 3.3) and 10 wt% SNAP-E2As films (110.7° ± 0.4) ($p$= 0.20). Therefore, it is

predicted that interactions between blood proteins and the surface will remain unchanged by the addition of SNAP.

Increasing surface roughness has been shown to increase the adsorption of fibrinogen.[41] This stems from geometrical changes in the arrangement of the adsorbed fibrinogen, as it is a non-globular protein. Therefore, it is important to ensure that the addition of the NO donor will not have a detrimental effect on the average surface roughness. Surface roughness of E2As and SNAP-E2As films were measured using AFM over a 4 $\mu m^2$ region. Pure E2As films were found to have an average roughness value of 11.04 ± 1.97 nm, while SNAP-E2As films had a roughness value of 11.65 ± 1.08 nm ($p$=0.38). As the addition of SNAP was insignificant in changing the wettability or surface morphology, it is expected the interactions of blood proteins with the E2As surface remain unchanged.

*Storage Stability of SNAP-doped E2As*

While a number of NO donors have been studied, all share a similar sensitivity to heat. The ability for these products to be stored will play a critical role in the feasibility of these materials to be clinically applicable. Films with 10 wt% SNAP were stored at a variety of temperatures (-20°C to 37°C) to mimic possible storage conditions. Even after 6 months at the elevated temperature (37°C), 81.2 ± 4.3 % of SNAP remained in the E2As films. This amount increased as storage temperature decreased. Room temperature conditions being most realistic for commercial/clinical applications, retained 88.4 ± 2.7 % SNAP after 1 month, and 87.1 ± 2.8 % SNAP after 6 months. Optimum storage conditions were found to be at -20 °C, where 100% ± 3.1 SNAP was remaining after 3 months, and 95 ± 2.1% remained after 6 months. A complete description of the storage data for all temperatures can be found in Figure 2.2. Films containing 5

wt% SNAP were also stored at these conditions, with 57.4 ± 2.8 % (37°C), 61.1 ± 3.5 % (25°C), 90.8 ± 0.9 % (4°C), and 94.7 ± 6.5 % (-20°C) remaining after 6 months. This increased stability of SNAP at higher concentrations was recently discovered to be due to the solubility of SNAP (ca. 3.4 – 4.0 wt%) when preparing polymer films through solvent evaporation [40]. While SNAP concentration at 5 wt% have less effect on the mechanical properties, but do not contain enough crystalline SNAP to maintain NO during storage. Higher concentrations (e.g., 10 wt%) allow for increased crystal formation within the polymer matrix through intermolecular hydrogen bonding, resulting in the enhanced storage stability. This crystallization processes also plays an important role in determining the release kinetics of NO from the polymer, as discussed below.

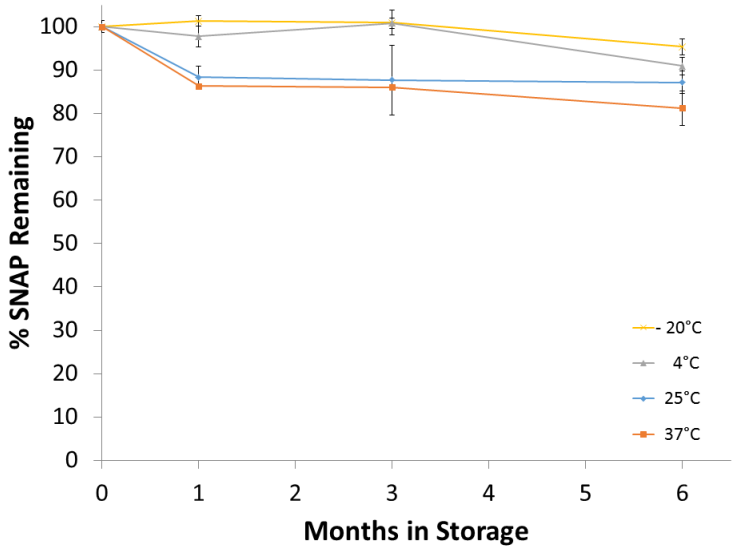


Figure 2.2 Storage stability of SNAP in E2As. Films were stored under various conditions and evaluated for SNAP content by dissolving in DMAc and measuring absorbance at 340 nm via UV-Vis.

While stability of SNAP in the polymer films is important, maintaining the release profile from the films is equally critical for controlled release. NO-release from 5 and 10 wt% SNAP-E2As films were measured directly after film preparation, as well as after 6 months storage at

room temperature. While the initial 24 hour release rates of NO from both 5 and 10 wt% stored films after 6 month storage are significantly lower, the release rates for both compositions after 24 hours maintain similar profiles over the remaining lifetime of the fresh films. While the release rates for stored films are lower on day 0, they remain in the physiological range of NO released from the natural endothelium ($0.5 – 4 \times 10^{-10}$ mol $min^{-1}$ $cm^{-2}$ ).[12] The higher levels of NO-release from films on Day 0 can be attributed to the SNAP soluble in the polymer, which is unstable and rapidly releases its NO payload. During storage, this soluble SNAP decomposes, while the crystalline SNAP is stabilized by intermolecular hydrogen bonding. The SNAP in crystalline form provides the long-term NO-release and is minimally affected by the shelf storage. This increased crystallinity not only is important for the storage of the material, but also plays a pivotal role in the control of the release. This lower NO-flux for the 6 month stored films can be attributed to the loss of SNAP that is observed in the UV-vis results. Release measurements of films stored for 6 months as compared to control films are shown in Figure 2.3.

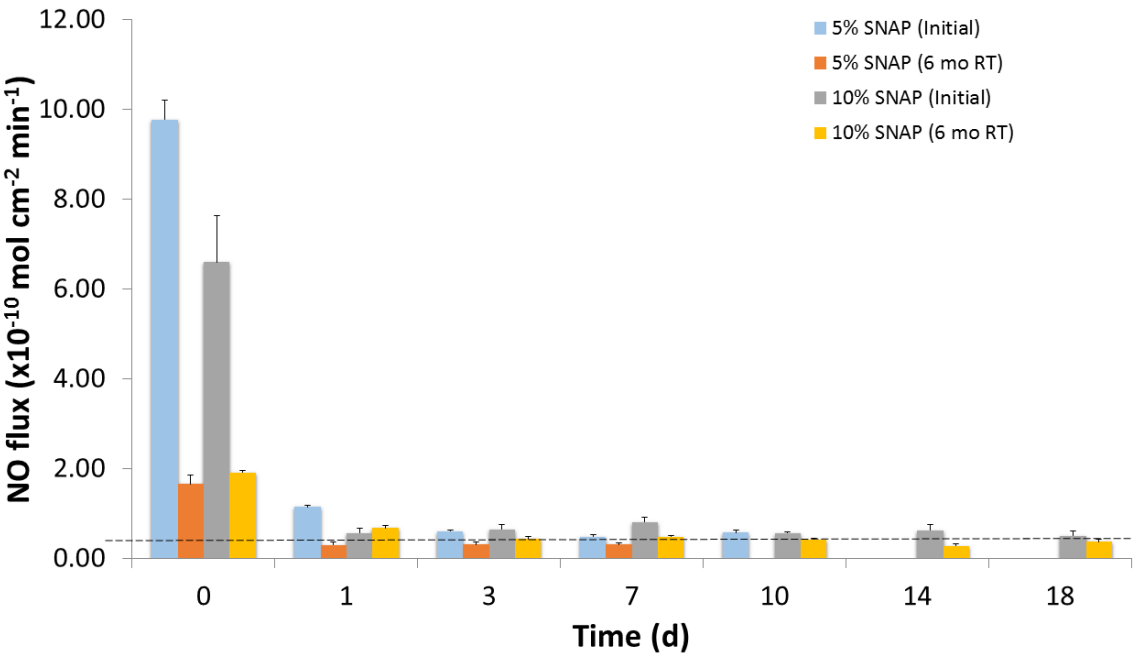

Figure 2.3: Nitric oxide release profiles of stored SNAP-E2As films (6 months) and fresh/new films as measured by chemiluminescence in PBS buffer at 37°C. The dotted line represents lower limit to physiological levels.

*Cytotoxicity*

Treating cells with a chemical agent can result in a variety of cell fates like altered metabolism, decrease in cell viability, necrosis death and change in the genetic program of cells ultimately resulting in apoptosis (programed cell death). After incubation with the SNAP-E2As, L-929 mouse fibroblast cells were examined microscopically (100X) following the cytotoxicity testing using ISO 10993-5 elution method to evaluate cellular characteristics (abnormal morphology and cellular degeneration) and percent lysis. For the test to be valid, the reagent control and the negative control must have had a reactivity of none (grade 0) and the positive control must have moderate (grade 3) or severe (grade 4) reactivity. In the event of 100% cell lysis, percent rounding and percent cells without intracytoplasmic granules were not evaluated. The reagent control, negative control, and the positive control performed as anticipated (grade 0, grade 0, and grade 4 respectively). The 10 wt% SNAP-E2As films showed no evidence of causing cell lysis or toxicity when tested for 48 hours on L-929 mouse fibroblast cells (grade 0), where the positive control showed 100% cell death.

*Hemolysis*

Hemolysis testing is considered to be the most common method to evaluate the hemolytic properties of any blood contacting biomaterial or device. The test is based on erythrocyte (red blood cells) lysis induced by contact, toxins, metal ions, leachables, and surface charge or any other cause of red blood cells lysis. The hemolytic potential of 10 wt% SNAP-E2As films was

tested *in vitro* for 3 hours at 37°C on blood samples sourced from rabbit using ISO 10993-4 protocol. In the event the hemolytic index resulted in a value less than zero, the value was reported as 0.0. The hemolytic index for 10 wt% SNAP-E2As films in direct contact with blood was 0.05 ± 0.1% when compared to negative and positive controls (0%, 102 ± 1.7% respectively). Extract from the films were also tested, where and the hemolytic index for SNAP-E2As was 0.05 ± 0.1%, with negative and positive controls of 0.23 ± 0.1% and 99.77 ± 2.3%. Thus, 10 wt% SNAP-E2As films in direct contact with blood and the sample extract were found to be non-hemolytic in a 3 h study.

*Sterilization of SNAP-doped E2As*

Infection continues to be a serious problem in clinical settings, where 1.7 million healthcare associated infections result in 99,000 deaths per year in the United States alone.[45] Providing a sterile environment is necessary for surgical procedures to be successful. For device related infections, bacteria congregate at the device site, or have adhered to the device itself prior to implantation. While various sterilization techniques have greatly reduced the risk of infection, the threat of infection has yet to be eliminated. Active antibacterial materials have been developed to help reduce the attachment of bacteria throughout the lifetime of the device. However, sterilization of these materials must be plausible for their implementation into clinical use. As mentioned above, SNAP is both heat and light sensitive, and is a limiting factor in the sterilization of these materials. A number of common sterilization techniques were evaluated to determine the best sterilization method for materials incorporating SNAP.

*Autoclave*: Autoclaving is a widely used technique to sterilize any equipment/material using a high pressure saturated steam at 121°C for around 30 minutes.[46] Sterilization autoclaves

are commonly used in microbiology, veterinary science, mycology, prosthetics fabrication, and medicine. Only 7.2 ± 0.1 wt% of the initial SNAP concentration was retained after autoclaving and hence is not recommended to sterilize SNAP-doped polymers.

*Ethylene Oxide*: Ethylene oxide gas has been used since the 1950s for heat-sensitive and moisture-sensitive medical devices.[46] Films exposed to EO sterilization retained 89.4 ± 2.0 % of SNAP. The ability for SNAP to withstand EO sterilization is very important as it is a standard method used in many healthcare facilities for heat sensitive products. The ability for these products to be sterilized without the need for specialized equipment will make SNAP-E2As an easily implemented material.

*Hydrogen peroxide vapor*: Hydrogen peroxide sterilization works by producing destructive hydroxyl free radicals that can attack the membrane lipids, DNA, and other essential cell components, and is effective against bacteria, yeasts, fungi, viruses, and spores.[46] Hydrogen peroxide sterilization was able to retain 89.4 ± 6.7 wt%. This can be a promising alternative for facilities lacking EO sterilization.

*UV Exposure*: Ultra-violet radiation has been become a common technique for sterilization, providing a bactericidal effect between 210 and 328 nm, with the maximum bactericidal effect using light between 240 and 280 nm.[47] Numerous health studies have shown that ultraviolet (UV) light is very effective against bacteria, spores, mold, fungi, mildew and viruses by breaking down their RNA or DNA. Ultra-violet radiation has been implanted in the disinfection of drinking water[48], air[47], titanium implants[49], and contact lenses[50].UV sterilization for 1.5 hours was found to retain the highest amount of SNAP at 99 ± 0.003 wt%. Effects of UV exposure on the retention of SNAP in the polymer will have an increasingly detrimental effect as you approach 340 nm (corresponding to the S-NO bond within SNAP).[29]

A summary of the various sterilization techniques on the retention of SNAP is found in Figure 2.4. Autoclaving the SNAP-doped E2As films was the most detrimental to the NO release properties of the films due to the prolonged exposure to high temperatures. While UV sterilization may be not be applicable for all applications, such as ECC tubing or catheter-type applications, it remains a viable option for devices requiring surface coatings. For devices requiring more intensive sterilization, EO and $H_2O_2$ methods are viable approaches. Similarly to storage, the sterilization of these materials should not alter the NO-release profile. As EO sterilization is the most clinically accepted method for sterilization of heat sensitive products, NO-release from sterilized and nonsterilized 10 wt% SNAP-E2As films were measured over 18 day period. The sterilization of the SNAP-E2As films had minimal effects on the NO-release profile, as shown in Figure 2.5.

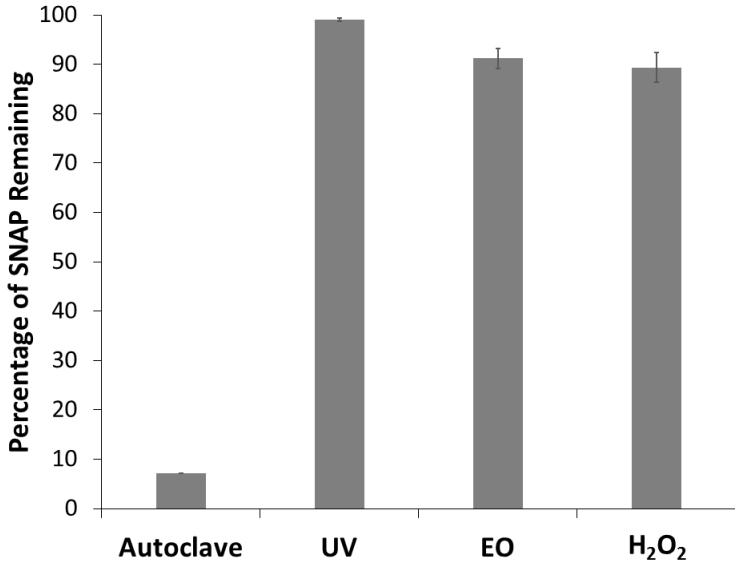


Figure 2.4: Effect of various sterilization methods on retention of SNAP in E2As films. Films were sterilized by the various methods, and then dissolved in DMAc for rapid determination of the SNAP content via UV-Vis.

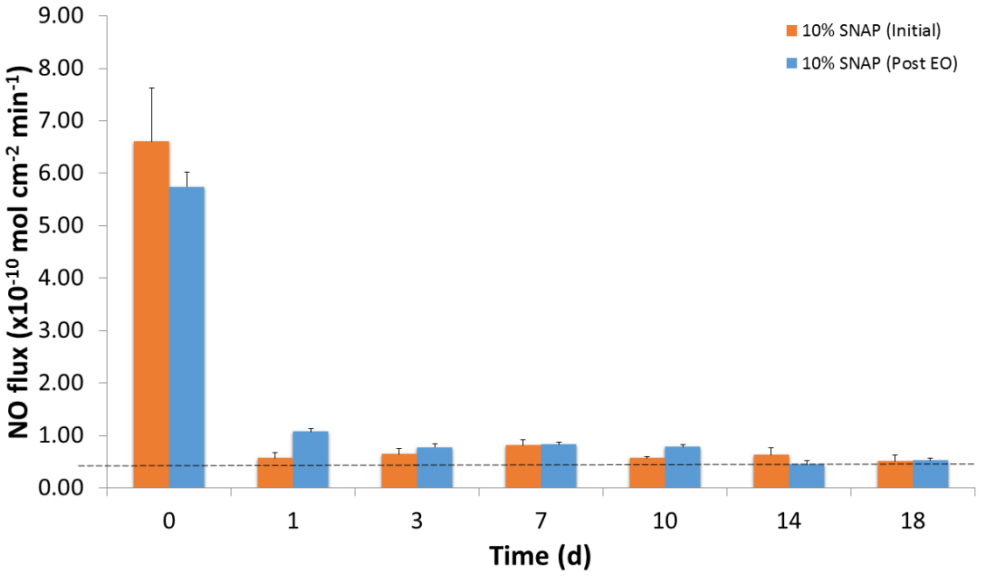


Figure 2.5: Effect of EO sterilization on NO-release profile from 10 wt% SNAP-E2As films measured by chemiluminescence in PBS buffer at 37°C.The dotted line represents lower limit to physiological levels.

**Conclusions**

As researchers look to extend the lifetime of NOrel devices, the physical properties and biomcompatibility of these materials hold precedent on the clinical feasibility of medical devices utilizing these polymers. In this study, different aspects of a SNAP doped polymer as they pertain to commercialization and clinical application were investigated, including the effects of SNAP on mechanical and physical properties, hemocompatibility, and cytotoxicity. In addition, stability of SNAP during shelf storage and exposure to various sterilization techniques was evaluated. Ultimate tensile strength of SNAP-doped E2As films was 80% of the pure polymer when used at a concentration from 5-10 wt%, declining rapidly at SNAP concentrations of 15 wt% (~63% of pure E2As). Further mechanical testing of SNAP incorporated polymers is recommended for medical devices that undergo high or cyclical loading, such as roller pump tubing for rotary blood pumps. The addition of SNAP did not alter the surface roughness or

surface chemistry, as measured using AFM and contact angle. Concentrations of SNAP at and below 10 wt% have been shown in previous works to adequately prevent platelet adhesion and activation, as well as antimicrobial properties *in vivo*. These biological attributes are complemented by our current work, demonstrating the non-cytotoxic and hemocompatible properties of SNAP-doped E2As polymer. Furthermore, the present study demonstrated NO releasing E2As (10 wt% SNAP) can be stored for 6 months at room temperature while retaining 87.1 ± 2.8 % of initial SNAP content, and retained 81.2 ± 4.3 % at harsh conditions (37°C). Films containing 5 wt% SNAP were found to be less stable (61.1 ± 3.5 % after 6 months at room temperature), and are consistent with previous findings on SNAP-doped polymers. Furthermore, these stored materials maintain similar release kinetics over an 18 day period as compared to freshly prepared SNAP-doped E2As. Various sterilization methods were tested, and showed $H_2O_2$, EO, and UV sterilization methods all to be promising methods for sterilization (>90% SNAP retained). To confirm the sterilization of the SNAP-E2As films had minimal effects on the NO-release profile, NO-release from EO sterilized films were compared to fresh films over an 18 day period.

While adding increasing amounts of SNAP may seem to be an attractive approach for increasing and prolonging the NO-release from polymeric materials, this can have detrimental effects on the mechanical properties of the device. Contrarily, reducing the amount of SNAP below 5 wt % will have detrimental effects in terms of stability and shelf-life. It is observed that polymers with low water uptake containing SNAP in the range of 5-10 wt% provide high stability, long durations of NO release, with minimal effects on strength. To conclude, the successful demonstration of NO-releasing E2As as a stable, and physically and biologically

compatible material, makes it a potential material for biomedical device and implant applications.

**References**


1. J. Marín and M. A. Rodríguez-Martínez, Pharmacology & Therapeutics, 1997, 75, 111-134.
2. K. Vural and M. Bayazit, European Journal of Vascular and Endovascular Surgery, 2001, 22, 285-293.
3. M. W. Radomski and S. Moncada, Thrombosis and Haemostasis, 1993, 70, 36-41.
4. A. F. Chen, Acta Pharmacologica Sinica, 2005, 26, 259-264.
5. P. L. Feldman, Chem. Eng. News, 1993, 71, 26-38.
6. P. C. Kuo and R. A. Schroeder, Annals of Surgery, 1995, 221, 220.
7. T. B. Cai, P. G. Wang and A. A. Holder, NO and NO donors for pharmaceutical and biological applications., Weinheim: Wiley VCH, 2005.
8. M. W. Radomski, R. M. Palmer and S. Moncada, Biochemical and biophysical research communications, 1987, 148, 1482-1489.
9. M. W. Radomski and S. Moncada, in Mechanisms of Platelet Activation and Control, Springer, 1993, pp. 251-264.
10. H. Handa, T. C. Major, E. J. Brisbois, et al., Journal of Materials Chemistry B, 2014, 2, 1059-1067.
11. E. J. Brisbois, R. P. Davis, A. M. Jones, et al., Journal of Materials Chemistry B, 2015.
12. M. W. Vaughn, L. Kuo and J. C. Liao, American Journal of Physiology-Heart and Circulatory Physiology, 1998, 274, H2163-H2176.

13. G. Regev-Shoshani, M. Ko, C. Miller, et al., Antimicrobial Agents and Chemotherapy, 2010, 54, 273-279.

14. H. Ren, A. Colletta, D. Koley, et al., Bioelectrochemistry, 2014.

15. B. J. Nablo, T.-Y. Chen and M. H. Schoenfisch, Journal of the American Chemical Society, 2001, 123, 9712-9713.

16. B. J. Nablo and M. H. Schoenfisch, Journal of Biomedical Materials Research Part A, 2003, 67, 1276-1283.

17. L. R. Martinez, G. Han, M. Chacko, et al., Journal of Investigative Dermatology, 2009, 129, 2463-2469.

18. A. Pegalajar-Jurado, K. A. Wold, J. M. Joslin, et al., Journal of Controlled Release, 2015, 217, 228-234.

19. L. J. Ignarro, Nitric oxide: biology and pathobiology, Academic press, 2000.

20. S. Mocellin, V. Bronte and D. Nitti, Medicinal research reviews, 2007, 27, 317-352.

21. J. H. Shin and M. H. Schoenfisch, Analyst, 2006, 131, 609-615.

22. E. M. Hetrick and M. H. Schoenfisch, Chemical Society Reviews, 2006, 35, 780-789.

23. E. J. Brisbois, H. Handa, T. C. Major, et al., Biomaterials, 2013, 34, 6957-6966.

24. M. Frost and M. E. Meyerhoff, Analytical Chemistry, 2006, 78, 7370-7377.

25. M. C. Frost, M. M. Reynolds and M. E. Meyerhoff, Biomaterials, 2005, 26, 1685-1693.

26. M. C. Frost and M. E. Meyerhoff, Journal of Biomedical Materials Research Part A, 2005, 72, 409-419.

27. W. Cha and M. E. Meyerhoff, Biomaterials, 2007, 28, 19-27.

28. I. Chipinda and R. H. Simoyi, The Journal of Physical Chemistry B, 2006, 110, 5052-5061.

29. M. C. Frost and M. E. Meyerhoff, Journal of the American Chemical Society, 2004, 126, 1348-1349.

30. A. Dicks, H. Swift, D. Williams, et al., Journal of the Chemical Society, Perkin Transactions 2, 1996, 481-487.

31. D. J. Sexton, A. Muruganandam, D. J. McKenney, et al., Photochemistry and Photobiology, 1994, 59, 463-467.

32. P. D. Wood, B. Mutus and R. W. Redmond, Photochemistry and Photobiology, 1996, 64, 518-524.

33. E. Salas, M. Moro, S. Askew, et al., British Journal of Pharmacology, 1994, 112, 1071-1076.

34. R. P. Kark, D. C. Poskanzer, J. D. Bullock, et al., New England Journal of Medicine, 1971, 285, 10-16.

35. A. Simmons, A. D. Padsalgikar, L. M. Ferris, et al., Biomaterials, 2008, 29, 2987-2995.

36. D. Cozzens, A. Luk, U. Ojha, et al., Langmuir, 2011, 27, 14160-14168.

37. T.-W. Chung, D.-Z. Liu, S.-Y. Wang, et al., Biomaterials, 2003, 24, 4655-4661.

38. E. M. Hetrick and M. H. Schoenfisch, Annual review of analytical chemistry (Palo Alto, Calif.), 2009, 2, 409.

39. P. N. Coneski and M. H. Schoenfisch, Chemical Society Reviews, 2012, 41, 3753-3758.

40. S. l. M. Shishido, A. B. Seabra, W. Loh, et al., Biomaterials, 2003, 24, 3543-3553.

41. Y. Li and P. I. Lee, Molecular Pharmaceutics, 2010, 7, 254-266.

42. Y. Wo, Z. Li, E. J. Brisbois, et al., ACS applied materials & interfaces, 2015.

43. K. Rechendorff, M. B. Hovgaard, M. Foss, et al., Langmuir, 2006, 22, 10885-10888.

44. J.-H. Elam and H. Nygren, Biomaterials, 1992, 13, 3-8.

45. D. Lyman, J. Brash, S. Chaikin, et al., ASAIO Journal, 1968, 14, 250-255.

46. B. Sivaraman and R. A. Latour, Biomaterials, 2011, 32, 5365-5370.

47. A. Vertes, V. Hitchins and K. S. Phillips, Analytical chemistry, 2012, 84, 3858-3866.

48. W. A. Rutala, D. J. Weber and C. f. D. Control, Journal, 2008.

49. A. P. Fraise, P. A. Lambert and J.-Y. Maillard, Russell, Hugo & Ayliffe's Principles and Practice of Disinfection, Preservation & Sterilization, John Wiley & Sons, 2008.

50. K. K. Hall, E. T. Giannetta, S. I. Getchell-White, et al., Infection Control, 2003, 24, 580-583.

51. S. Singh and N. G. Schaaf, Internat. J. Oral Maxillofac. Implants, 1989, 4, 139-146.

52. P. J. Dolman and M. J. Dobrogowski, American journal of ophthalmology, 1989, 108, 665-669.

# CHAPTER 3

# CHARACTERIZATION AND IN VIVO PERFORMANCE OF NITRIC OXIDE-RELEASING EXTRACORPOREAL CIRCUITS IN A FELINE MODEL OF THROMBOGENICITY[2]

[2] Goudie, M.J., Brainard, B.C., Schmiedt, C.W., Handa, H. 2017. *Journal of Biomedical Materials Research Part A.* 105.2: 539-546.

Reprinted with permission of the publisher

**Abstract**

Infection and thrombosis are the two leading complications associated with blood contacting medical devices, and have led to active materials that can delivery antibiotics or antithrombotic agents. Two key characteristics of these materials are the ability to produce controlled delivery, as well as minimal systemic delivery of the agent outside of the device site. Nitric oxide (NO) releasing materials are attractive as NO plays pivotal roles in the body's natural defense against bacterial infection, as well as regulation of platelet adhesion and activation. This work characterizes an NO-releasing extracorporeal circuit (ECC) under flow conditions for the first time, examining the effect of incubation and application of the top coating on leaching of NO donor and NO-release kinetics. Top coated ECCs with incubation delivered ca. 1% of the total NO potential over the 4-hour period, whereas uncoated ECCs delivered over 4.5% of the total NO. Incubated ECC loops maintained a flux of $1.83 \pm 0.50 \times 10^{-10}$ mol $min^{-1}$ $cm^{-2}$ for the full 4 h duration. The NO-releasing ECC loops significantly increased the time-to-clot as compared to the corresponding control (11 ± 3.6 min control, 132 ± 93.0 min NO-releasing) when evaluated *in vivo* in a feline animal model.

**Introduction**

Nitric oxide (NO) has been shown to be a major contributor in several key physiological roles, such as regulating platelet adhesion and activation, fighting against bacterial infection, and enhancing wound healing through promoting angiogenesis.[1-4] The concentrations of NO delivered can range drastically through each of these roles. Researchers have developed NO-releasing materials as a way to increase hemocompatibility of blood contacting devices such as vascular grafts, stents, intravascular catheters, and extracorporeal life support circuits.[5-7] One method to improve the hemocompatibility of these existing materials is through the use of

coatings, where the coating can more closely mimic the natural NO release from the endothelium.[8-12]

Nitric oxide is highly reactive under physiological conditions, having a half-life in the range of seconds to minutes.[13] Due to this high reactivity, NO donor molecules utilizing functional groups to store and release NO have been developed as a way to localize, store, and release NO. One of the most common classes of NO donors are *S*-nitrosothiols (RSNO) as these materials can be found naturally in the blood stream (such as *S*-nitrosohemoglobin and *S*-nitrosoglutathione), and are considered to be an endogenous reservoir for NO.[14-16] Synthetic RSNOs have been developed, such as *S*-nitroso-*N*-acetylpenicillamine (SNAP), and have been shown to provide significant antimicrobial and antithrombotic effects when used both *in vitro* and *in vivo*.[7, 17, 18] The release of NO from the RSNO can occur through thermal decomposition, and be catalyzed using moisture, light, or metal ions such as copper (**Figure 3.1**).[19-21] The incorporation of these RSNOs into polymeric materials have led to the ability for NO-releasing coatings to improve the biocompatibility of blood contacting devices by locally administering NO at the material surface. However, one issue with the physical blending of the RSNO within the polymer matrix is the leaching of the RSNO from the polymer. This leaching can cause large burst-releases of NO from the material, deliver NO away from the material surface, and can result in significant decreases in the NO-release lifetime to only several hours.[17, 22, 23] One approach to limit RSNO leaching is by covalently linking the NO donor to the polymer matrix.[24, 25] While this approach is effective in decreasing leaching from the material, limitations of the total NO-donor content arise due to the chemical composition of the polymer used and can require complex synthesis processes. Physical incorporation of the NO donor allows for greater control over the overall NO donor content, as well as increasing the available possibilities for

applicable polymers. Efforts to limit leaching in these physically mixed systems have shown the use of a top coat of pure polymer as well as the incorporation of the RSNO into hydrophobic materials with little water uptake to be effective strategies. However, these approaches have yet to be studied in flow-based systems.[17, 18]

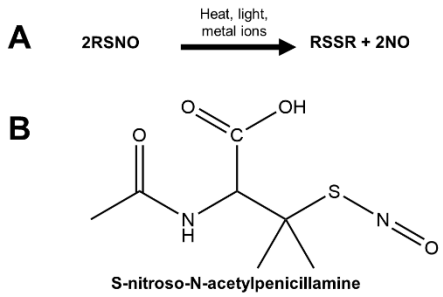


Figure 3.1: A) Release mechanism of NO and disulfide bond formation from RSNOs. B) Structure of the RSNO SNAP.

Ex vivo clot formation provides a mechanism to study the characteristics of thrombus formation, and may also be useful for the assessment of the efficacy of antithrombotic medications. The use of a flexible plastic extracorporeal circuit (ECC) has been reported in a rabbit model of thrombogenicity.[9, 10, 17, 26] The circuit connects the carotid artery to the contralateral external jugular vein to provide flow without the use of roller pumps or other mechanical assistance. This 'thrombo-chamber' is manufactured with a step in the internal diameter to induce regions of turbulence and recirculation, resulting in the activation of platelets, and the production of a thrombus in the ECC. Because the thrombus forms outside of the circulation of the animal, this presents the possibility of a model for high-throughput screening of anticoagulant compounds that does not require euthanasia of the subject following clot formation.

As described previously, the surface of the ECC tubing can be coated with polymers that can minimize the blood/biomaterial interaction, and decrease the thrombogenicity of the ECC.[10] Improving the hemocompatibility of the ECC surface may be used for various extracorporeal therapies such as hemodialysis, extracorporeal membrane oxygenation (ECMO), and cardiopulmonary bypass. A biocompatible ECC with low thrombogenicity can decrease the need for systemic anticoagulation, which otherwise places the patient at risk for bleeding-associated complications.

The objective of this study was to fully understand the delivery (both local and systemic) of NO from the SNAP-coated ECC tubing, as well as to determine if the increased platelet sensitivity in domestic short-hair felines could provide a more rigorous, survivable model for testing the hemocompatibility of materials. A systemic hypercoagulable state occurs in 50% of cardiomyopathic felines with spontaneous echocardiographic contrast (or "smoke") with or without a left atrial (LA) thrombus, and in 56% of felines with ATE and LA enlargement.[27] Thromboembolism in felines with CM is likely an effect resulting from platelet activation (due to altered blood flow and shear stress within the cardiovascular system)[28] and coagulation factors (in areas of blood stasis within the left atrium).[29] This increased platelet activity in felines could provide a more rigorous model for the evaluation of the biocompatibility of materials.

## Materials and Methods

### *Materials*

N-Acetyl-D-penicillamine (NAP), sodium chloride, ethylenediaminetetraacetic acid (EDTA), potassium chloride, sodium phosphate dibasic, potassium phosphate monobasic, tetrahydrofuran (THF), and sulfuric acid were purchased from Sigma Aldrich (St. Louis, MO). Methanol, hydrochloric acid and sulfuric acid were obtained from Fisher Scientific (Pittsburgh,

PA). Tygon™ tubing was purchased from Cole-Parmer. CarboSil® 20 80A was obtained from DSM. Phosphate buffered saline (PBS), pH 7.4, containing 138 mM NaCl, 2.7 mM KCl, 10 mM sodium phosphate, and 100 mM EDTA was used for in vitro NO release and SNAP leaching studies. CarboSil 20 80A (here on referred to as CarboSil) was obtained from DSM.

*SNAP Synthesis*

Synthesis of SNAP was done by mixing equimolar ratios of sodium nitrite and NAP in water and methanol containing 2.0 M HCl and 2.0 M $H_2SO_4$ as previously reported.[30] The reaction vessel was cooled in an ice bath after 30 min of stirring to precipitate the SNAP crystals. The crystals were collected by filtration, washed with water, and allowed to air dry. The reaction and crystals were protected from light at all times.

*Extracorporeal Circuit Fabrication*

ECC loops were fabricated as described previously.[9, 17, 31] The ECC loop consisted of two polyurethane angiocatheters (Kendall Monoject Tyco Healthcare Mansfield, MA), two sections of 16 cm long ¼'' inner diameter (ID) Tygon™ tubing, and an 8 cm long section of 3/8'' ID Tygon™ tubing. The step increase in tubing diameter is intended to create regions of circulation turbulence, promoting clot formation.

Nitric oxide releasing ECC loops were prepared with CarboSil coatings containing 5 wt% SNAP, as the NO donor. The NO-releasing solution was prepared by dissolving 2,250 mg CarboSil and 125 mg SNAP in 20 mL THF. Two coats of this solution were applied for all coating configurations. Coating of the ECC circuit was done as previously described.[17] Briefly, application of the coating was done by filling the tubing section completely with the polymer

solution for 5 s, followed by inverting the tubing to drain the polymer solution, and then rotated about the longitudinal axis horizontally for 1 min to aid in creating a uniform coating. To determine the optimal coating method, three coating configurations were tested in vitro before testing in the in vivo model: 5 wt% SNAP in CarboSil without a top coat, 5 wt% SNAP in CarboSil with a top coat of pure CarboSil, and 5 wt% SNAP in CarboSil with a top coat of CarboSil and incubation (**Figure 3.2**). Incubated ECC loops were filled with PBS with EDTA for 12 hours after the loop had fully dried. All ECC loops were air dried for 1 h between coats. Nitric oxide-releasing angiocatheters were coated with one coat of 5 wt% SNAP-CarboSil, followed by one top coat layer of pure CarboSil.

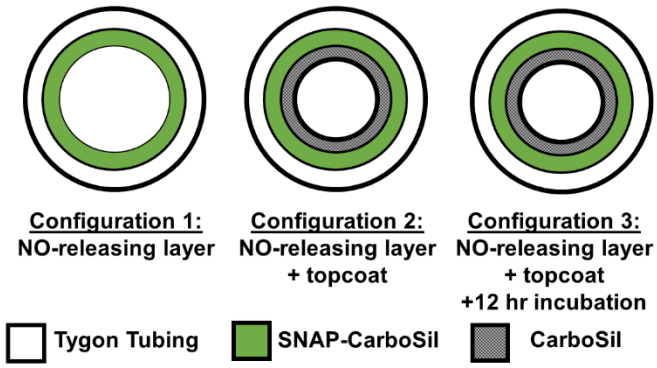


Figure 3.2: Cross sectional designs for *in vitro* characterization of NO-releasing ECC loops.

After coating, ECC loops were assembled using THF. Assembly was done starting with a luer-lock to ¼ in adaptor, one 16 cm long ¼ in ID tubing, the 8 cm long thrombogenicity chamber, the second 16 cm long ¼ in ID tubing, and a luer-lock to ¼ in adaptor. Assembled ECC loops were allowed to air dry for >24 h under ambient conditions, followed by drying under vacuum for 48 hours. One group of ECC loops were soaked in PBS buffer containing 100 mmol EDTA for 12 hours at 4°C prior to in vitro or in vivo testing to prevent burst release of NO.

*Characterization of ECC coatings*

Thrombo-chambers were massed prior to coating with CarboSil and SNAP-CarboSil, and massed after the application of two coats. After the drying process was complete, sections of the control and NO releasing thrombo-chambers were analyzed to determine the remaining concentration of SNAP within the coating as well as examine the thickness and morphology of the coating. Scanning electron microscopy was done using a FEI Inspect F FEG-SEM with a 10 kV excitation. Thickness and morphology of the coating was examined using optical and scanning electron microscopy. To determine the SNAP concentration within the coating, sections of the control and NO releasing thrombo-chambers were dissolved in DMAc and absorbance at 340 nm was measured via a GENYSIS spectrophotometer (ThermoScientfic), where 340 nm corresponds to the presence of the S-NO bond of nitrosothiols.[21] The concentration of SNAP was then calculated using a calibration curve from known concentrations of SNAP in DMAc.

*In vitro* SNAP leaching

Total leaching of SNAP over the 4-hour period was examined using a Chandler loop (**Figure 3.3**). Nitric oxide releasing ECC sections were coated in the same fashion as described in the NO releasing ECC section. Leaching was examined for ECC loops for each configuration shown in Figure 3.2. Phosphate buffered saline (PBS) with 100 mmol EDTA was adjusted to a pH of 7.4 and primed in the modified Chandler loop, where EDTA was used to ensure any metal ions in the PBS solution are neutralized as metallic ions can act as a catalyst for the decomposition of SNAP to release NO. Flow of PBS was done at room temperature to minimize NO release from SNAP that had been leached from the ECC tubing, and flowed at approximately 100 mL $min^{-1}$ to match the physiological flows previously seen in the *in vivo* model using a

Masterflex 77601-10 Easy Load peristaltic pump.[7, 9, 26, 31] Samples (~5 mL) were drawn every 30 minutes from a 3-way luer-lock port, where concentration of SNAP was measured using UV Vis, and reintroduced to the test loop so as to not alter the total volume of the circuit throughout the 4 h period. The SNAP molecule has maxima at 340 and 590 nm, corresponding to the S-NO bond.[17, 19, 21] Absorbance was recorded for each sample, and concentration was determined using a predetermined calibration curve for known concentrations of SNAP in the PBS/EDTA solution. The pure PBS/EDTA solution was used as a blank for all measurements.

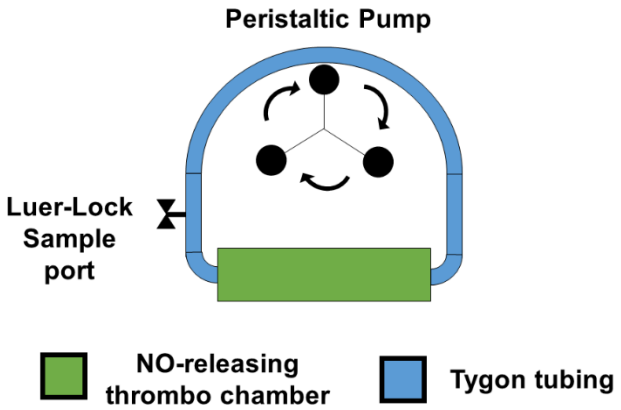


Figure 3.3: Modified Chandler loop for *in vitro* leaching measurement of SNAP from coated ECC circuits.

*Nitric oxide release measurements*

Nitric oxide release rates from the various configurations proposed for the ECC loop were measured using a Sievers chemiluminescence Nitric Oxide Analyzer (NOA), model 280i. (Boulder, CO). Sections of Tygon™ tubing (ID = ¼'') were coated in the same fashion as the NO-releasing ECC loops and placed in 4 mL PBS buffer with EDTA at 37°C. Nitric oxide released from the surface was continuously purged from the sample cell by bubbling of the PBS

with N2, along with a headspace flow of $N_2$ to carry NO-rich gas to the NOA detection chamber. Flow of $N_2$ through the cell was set to 200 mL $min^{-1}$.

*Feline thrombogenicity model*

The animal handling and surgical procedures were approved by the University of Georgia Committee on the Use and Care of Animals in accordance with university and federal regulations. A total of six domestic short hair felines were used in this study. All felines were premedicated with intramuscular injections of ketamine (7 mg/kg), acepromazine (0.01 mg/kg), midazolam (0.1 mg/kg), and buprenorphine (0.03 mg/kg). Anesthesia was induced using isoflurane in 100% oxygen, delivered by mask, until endotracheal intubation could be achieved. Following endotracheal intubation, anesthesia was maintained using isoflurane in 100% oxygen (from 0.5-1.5%). Ventilation at a rate of 12 breaths per minute and a tidal volume of 10-15 mL/kg was maintained using a mechanical ventilator (Hallowell EMC, Pittsfield, MA 01201). Blood pressure was monitored using a Doppler ultrasonic flow probe (Parks Medical, Las Vegas, NV 89119). Continuous ECG and heart rate were monitored using a multiparameter monitor (Grady Medical, Los Angeles CA). Body temperature was monitored with a rectal probe and maintained at 38°C using a circulating warm water heating blanket and forced air heater. Baseline blood samples were collected prior to the placement of the ECC circuit.

After the baseline blood measurements were taken, the ECC circuit, primed with 0.9% NaCl, was placed into position by cannulating the right jugular artery and the left jugular vein. Flow through the ECC was initiated via unclamping of the ECC loop, and monitored using an ultrasonic flow probe and flow meter (Transonic 400 Ithaca, NY). The endpoint of clotting of the ECC loop was determined as when the flow in the ECC loop reached 0 mL min-1, and remained

at no flow for 5 min. After no flow was established for 5 min, or after the 4-hour time period had been reached, the ECC loop was clamped, removed from the animal, and rinsed with 60 mL of normal saline to observe any clotting that occurred in the ECC loop during the test period. However, if zero flow was observed prior to the 1 h measurement, the ECC loop was clamped and the venous angiocatheter was disconnected from the ECC loop and flushed with 1-3 mL normal saline. This was done as to examine if thrombus formation within the thrombo chamber would prevent flow in the ECC circuit, as opposed to only obstructing the angiocatheter. Any clots that formed in the ECC loop were collected, massed, and stored and formalin. Animals were not systemically anticoagulated during the experiment.

*Blood sampling*

Whole blood was drawn from the femoral vein by direct venipuncture, collected in 3.2% sodium citrate (1:9 citrate:blood ratio, Becton, Dickinson. Franklin Lakes, NJ) for coagulation analysis, and EDTA for analysis of complete blood count (CBC; including platelet count). Following the initiation of the ECC circuit, blood samples were collected every hour for 4 h. Citrated whole blood was centrifuged at 1500 x g for 7 minutes, after which the plasma portion was decanted, and kept frozen at –80°C until analysis at the Cornell comparative coagulation laboratory. Coagulation parameters included the prothrombin time (PT), activated partial thromboplastin time (aPTT), thrombin clotting time (TCT), fibrinogen concentration, and vonWillebrand Factor (vWF) activity. CBC was performed using an impedance counter (CBC-Diff, Heska Corp. Loveland CO)

*Statistical analysis*

Data are expressed as mean ± standard deviation. Comparisons of the time to first clot and thrombus mass between control and NO-releasing ECC loops were analyzed using a two-tailed Student's t-test. Comparison of hourly coagulation parameters in the felines with the NO-releasing ECC was performed using a one-way ANOVA for repeated measures, with a Bonferroni correction for multiple comparisons. In addition to the 1-way ANOVA, pairwise multiple comparisons were made using the Holm-Sidak method. Values of $p < 0.05$ were considered statistically significant for all tests.

**Results and Discussion**

*Cumulative leaching of SNAP and physical characteristics of ECC loops*.

The ability for NO releasing materials to retain the NO donor in the polymer matrix is not only critical for providing controlled release rates from the material surface, but also in ensuring localized delivery of NO. Leaching of the NO donor can result in systemic delivery of NO, as well as uncontrolled bursts. These bursts can be detrimental to patient's safety resulting in large decreases in blood pressure or issues with toxicity, as the physiological levels of NO release are estimated to be 0.5-4 ×10-10 mol $min^{-1}$ $cm^{-2}$.[32] Therefore, *in vitro* characterization of the release of NO from the ECC circuits is essential prior to animal testing. Although SNAP has been reported to be slightly hydrophobic, therefore energetically favorable to stay within the polymer matrix, leaching of SNAP from low water-uptake/hydrophobic polymers has been seen experimentally under static conditions.[33] Efforts to limit leaching in these physically mixed systems have shown the use of a top coat of pure polymer, as well as incorporation of the RSNO into hydrophobic materials with little water uptake, can minimize leaching, but have yet to be studied in flow based systems.[17, 18] While the leaching of SNAP has been studied from various

hydrophilic and hydrophobic polymers, these studies have only been conducted under static conditions.[17, 18]

To mimic the flow conditions experienced *in vivo*¸ PBS/EDTA was flowed ca. 100 mL $min^{-1}$ through a modified Chandler loop where cumulative SNAP leaching was measured over the 4 h period. Leaching rates in term of the total SNAP loading of the coating are shown in **Figure 3.4**. As expected, coatings containing 5 wt% SNAP without a top coat throughout showed the largest leaching (0.11 ± 0.004 mg $cm^{-2}$) over the 4 h period, where nearly 40% of the total leached SNAP was observed within the first 30 min of exposure. The addition of a single polymer topcoat layer significantly decreased the total leaching of SNAP by over 40% (0.066 ± 0.006 mg $cm^{-2}$, p =0.005). Similar to the ECC loops with no application of a top coat, top-coated ECC sections showed approximately 38% of the total leaching within the first 30 min. A simple way to avoid these leaching characteristics when using these coatings *in vivo* is to soak the device prior to use.[17] While the 12-h incubation does not alter the overall leaching seen from the NO-releasing ECC sections, the observed leaching during 4 h of use (as would be seen by the patient) changes drastically. The application of a top coat, along with 12 hours of incubation in PBS/EDTA at room temperature, the observed leaching of SNAP was further reduced to 0.037 ± 0.009 mg $cm^{-2}$, and was significantly lower than the addition of the top coat alone (p = 0.02), providing over 66% reduction of leaching from non-top-coated ECCs. The leaching observed in the initial 30 min was also decreased to 33% of the total SNAP leached in the 4 h period.

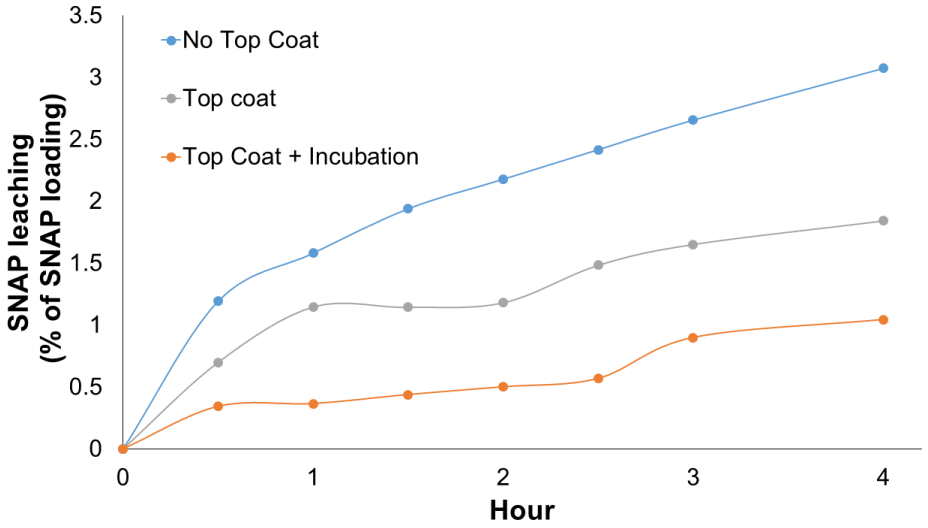


Figure 3.4: Cumulative leaching of SNAP from 5 wt% SNAP coated ECC circuits. Concentration of SNAP was measured using UV-Vis spectroscopy using absorbance recorded at 340 nm, corresponding to the S-NO bond.

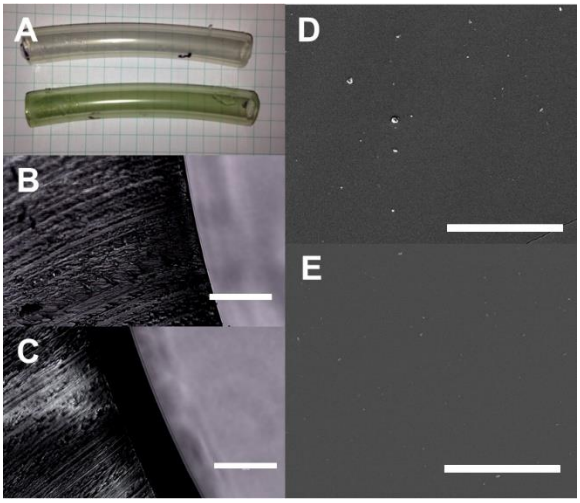


Figure 3.5: Images of ECC circuit tubing. A) Photograph of control (top) and NO releasing (bottom) thrombo chambers. Representative optical images of B) uncoated and C) coated Tygon tubing. Scale bar represents 200 µm. Morphology of the coating was examined using SEM D) Uncoated Tygon, E) 2 NO-releasing coats with a top coat. Images were taken at 1000 X magnification. Scale bar represents 100 µm.

These results are consistent with previous finding of coatings using silicone-polyurethane copolymers incorporating SNAP.[17] The addition of a top coat can drastically reduce leaching when the top coat is on the order of 50 μm. However, increasing the top coat thickness after this level was not observed to provide a substantial decrease in leaching. For this reason, the ECC circuits for this study utilized the top coat ca. 50 μm as observed through optical microscopy. Each coat of both SNAP-CarboSil and the CarboSil top coat applied ca. 60 μm as measured using imageJ (**Figure 3.5**). Solubility of SNAP in THF is >100 mg/mL, and is much higher than the concentration used in this study providing a very homogenous coating solution where this solvent casting method has been used for a number of NO-releasing materials utilizing the NO donor SNAP.[7, 17, 18, 34] Photograph of a thrombo chamber is shown in figure 5, and shows the macroscale homogeneity of the SNAP within the coating, providing a homogeneous green color. It was previously reported that solubility of the SNAP within the CarboSil matrix is ca. 3-4% by weight, where crystal regions of SNAP form within the matrix when used above this critical concentration.[18] It is said that the crystalized region of the SNAP within the polymer matrix is what leads to the long term stability of the donor and ability to release for extended periods of time. However, while majority of the SNAP in the CarboSil matrix is soluble when used at 5 wt%, the ability to predict the leaching kinetics and NO released from the coating is critical for creating reproducible coatings and patient outcomes. Once the drying process was complete for top coated ECCs, the remaining SNAP concentration was determined using UV-vis spectrophotometry, and found to be 90.1 ± 4.1% of the theoretical SNAP loading. The incubation of top coated films for 12 h in PBS with EDTA at 4°C prior to use resulted in 81.1 ± 2.3% SNAP remaining. Morphology of the surface was imaged using a FEI Inspect F FEG-SEM. Both control and coated ECC circuits show microscale smoothness, where the surface is non-porous in

nature. This is consistent with previous reports, as SNAP-CarboSil coatings have been found to have a roughness on the nm scale, even at 10 wt% SNAP, with the use of a top coat.[34]

*NO release profiles of coated ECC loops*

For a NO-releasing material to be considered applicable for clinical use, the product should show certain properties, including long-term NO release, release of NO at physiological conditions, release NO at rates similar to those experience physiologically (0.5-4.0 × $10^{-10}$ mol $min^{-1}$ $cm^{-2}$ [32]), reduce platelet activation and adhesion, as well as exhibit antibacterial properties. The ability for these materials to release NO for extended periods of time is directly related to the ability to control the release, as burst releases can be seen when incorporating RSNOs within the polymer matrix using solvent evaporation. Release rates for 10 wt% SNAP in CarboSil catheters have been reported to reach ca. 6 × $10^{-10}$ mol $min^{-1}$ $cm^{2}$ during the first day, decreasing to a constant release rate near 1-2 × $10^{-10}$ mol $min^{-1}$ $cm^{-2}$ after 24 hours.[18] This release can also be catalyzed using heat, light, or incorporation of metal ions, allowing other methods to control the release from the material.[21, 35-37] However, preventing such bursts of NO from the material, particularly during short-term applications where delivery of NO should be constant throughout the usage period, is critical for reproducibly preventing thrombus formation, as well as maintaining the safety of the patient.

The NO release from ECC loops were measured *in vitro* using chemiluminescence, which has become a gold standard for measurement of NO released from materials due to the ability to limit interference from molecules such as nitrates and nitrites. Release rate from incubated loops with the application of the top coat of CarboSil showed the preferred release characteristics, maintaining a flux of 1.83 ± 0.50 × $10^{-10}$ mol $min^{-1}$ $cm^{-2}$ for the full 4 h duration.

Along with this release showing to be constant, it is well within physiological range (0.5 - 4.0 × $10^{-10}$ mol $min^{-1}$ $cm^{-2}$). [32] To confirm that the NO release observed is coming from the material sample, at the end of the 4 h period, the incubating buffer was replaced with fresh buffer, and it was observed that the NO release level returned to the same level for the top-coat with incubation sample. However, non-incubated samples and those not utilizing a top coat both had leached SNAP into the solution as measured by UV vis spectroscopy. While these levels overestimate the levels of NO release that are occurring at the surface, they accurately quantify the amount of NO that would be delivered if used *in vivo*. This large burst of NO would be delivered systemically rather than remaining at the material surface, and can cause drastic vasodilation and decreases in blood pressure. Representative NO release profiles for the 4 h period for each of the ECC configurations is shown in **Figure 3.6**. Top coated ECCs with incubation delivered ca. 1% of the total NO potential over the 4-hour period, where uncoated ECCs delivered over 4.5% of the total NO. The constant NO-release from the ECC loops using the topcoat and 12 h of incubation, along with minimal leaching, proved to provide the desired characteristics for NO releasing blood contacting devices, and was further tested for biocompatibility in the feline *in vivo* model.

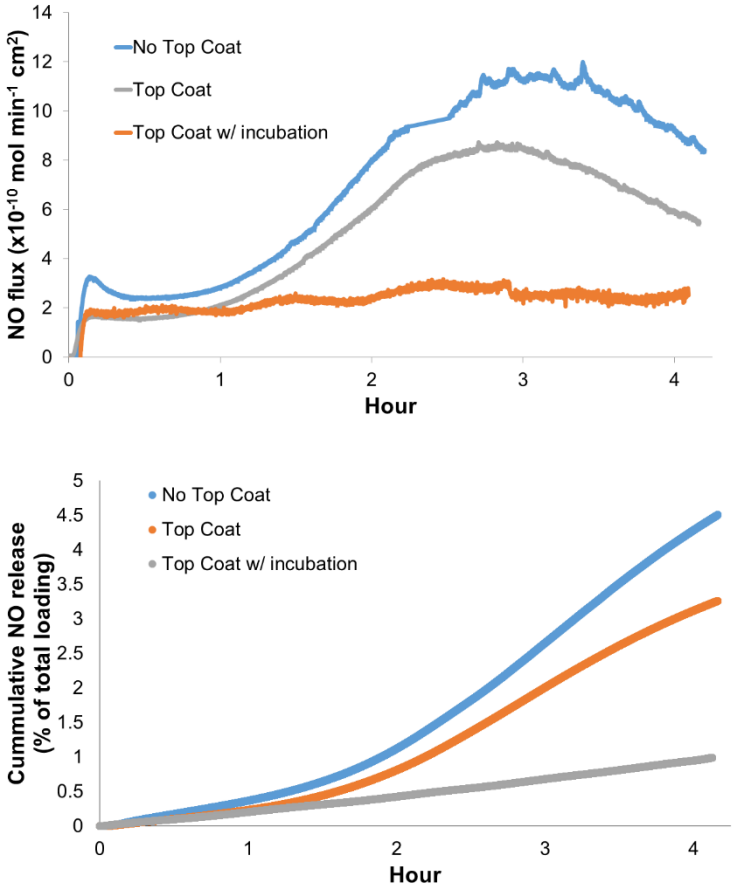


Figure 3.6: Real time NO-release from coated ECC sections of Tygon tubing as measured using Sievers Chemiluminescence Nitric Oxide Analyzer. All measurements were conducted at 37°C.

*In vivo* feline thrombogenicity model

The optimized ECC design (5 wt% SNAP with top coat and 12-h incubation in PBS/EDTA) was compared to control ECC loops in a feline model. The NO-releasing circuit was able to deliver a constant flux of NO at $1.83 \pm 0.50 \times 10^{-10}$ mol $min^{-1}$ $cm^{-2}$. The NO release from ECC surfaces have been shown to be unchanged after being exposed to blood.[26] Fibrinogen concentration, platelet count, as well as general coagulation factors were measured over a 4 h period when the felines were exposed to control and NO-releasing ECC loops. All felines in the control group clotted well before the one-hour measurement (11 ± 3.6 min). Due to the quick

clotting of the control ECC circuits, when zero flow was observed prior to the 1 h measurement, the ECC loop was clamped and then the venous angiocatheter was disconnected from the ECC loop and flushed with 1-3 mL normal saline. This was done as to examine if thrombus formation within the thrombo chamber would prevent flow in the ECC circuit, as opposed to only obstructing the angiocatheter, as well as prolong the exposure to the ECC to examine if changes could be seen from drawn blood. These results show the sensitivity of the feline model when compared to the rabbit model, as control rabbit ECC loops have been seen to not clot even after 4 hours using similar commercial biomedical grade polymers.[9] By contrast, NO releasing ECC loops showed much greater time to clot (132 ± 93 min), with N=1 loops showing no clotting in the 4 h period. Flow rates through the ECC circuit were observed to be comparable to that of the rabbit model, with flows fluctuating around 100 mL $min^{-1}$ on initial placement of the ECC loop. However, the rapid clotting in the feline model lead to sharp decreases in flow, contrary to the rabbit model where flow has been observed to decrease slowly over time. Thrombi were collected from the ECC either after 5 minutes of zero flow through the circuit, or at the end of 4 hours. Thrombi were weighed using a scientific balance and preserved in formalin. There was no statistical difference in the mass of the thrombi from either the control or the NO-releasing ECC. We believe this is due to the high sensitivity of platelets, as majority of clotting occurred within the venous angiocatheter and not within the thrombo-chamber (control 112.8 ± 129.5 mg, and NO releasing 91.35 ± 103.5 mg). While it is possible that the thrombus formed in the angiocatheter itself, we maintain the possibility for thrombus formation in the thrombosis chamber, detachment from the ECC walls, and flowing to obstruct the angiocatheter. We believe this is possible due to the high variations in thrombus weight in both control and NO releasing populations. While masses of the collected thrombi were not significantly different, fibrinogen

concentrations in control felines decreased significantly ($p = 0.004$), while no significant differences were seen in NO-releasing ECCs ($p = 0.176$). Time dependent levels of both fibrinogen and platelet counts for the control and ECC loops are shown in **Figure 3.7** and **Figure 3.8** respectively. Plasma fibrinogen levels have been previously reported to decrease from 10-20% in 4 h ECC applications due to the binding of fibrinogen to the ECC surface.[26] As fibrinogen concentrations drop to near 69% of the baseline, this further confirms the increased clotting activity of the feline model when compared rabbits. There was no significant difference between baseline measured coagulation parameters in the NO-releasing or control groups ($p > 0.4$, **Table 3.1**), showing the NO-release from the ECC surface had insignificant effect on the overall clotting kinetics systemically. There was no significant change in any coagulation parameter in the felines with the NO-releasing circuit over the duration of the 4 hours ($p > 0.05$). This is similar to results seen in the previous rabbit models.[10, 17, 26]

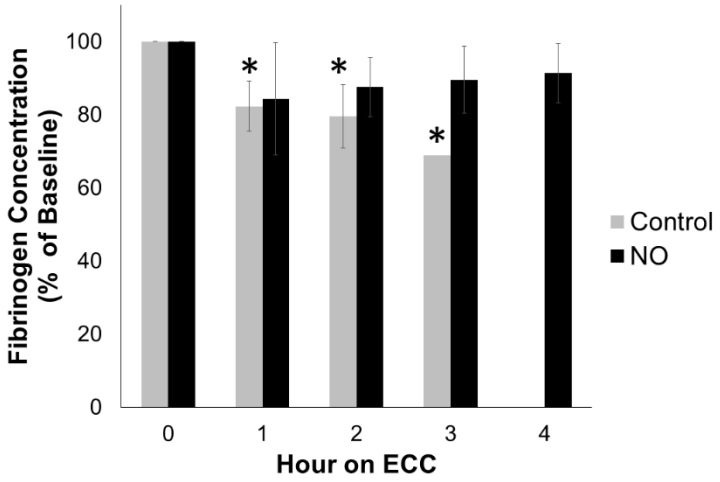


Figure 3.7: Time dependent effects of NO-releasing ECC (5 wt% SNAP) as compared to control ECCC on feline fibrinogen concentration. Control at 3 h has N=1, where none of the controls survived until 4h. *represents significant difference when compared to baseline ($p < 0.05$).

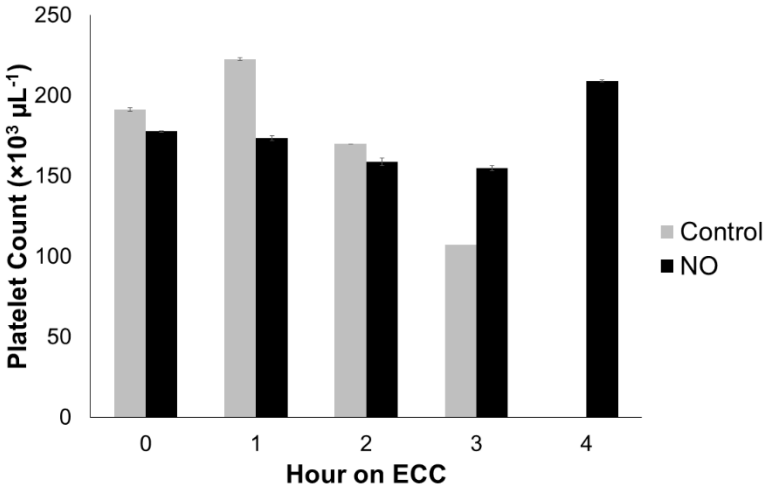


Figure 3.8: Time dependent effects of NO-releasing ECC (5 wt% SNAP) as compared to control ECCC on feline platelet count. Control at 3h has N=1, where none of the controls survived until 4 h.

The control ECC were generally well tolerated, and heart rate and blood pressure were maintained within normal ranges. Initiation of flow through the NO-releasing ECC was accompanied in all cases by severe hypotension (systolic arterial blood pressure < 30 mm Hg) and bradycardia (HR <40 bpm) requiring treatment with atropine. No additional interventions were made to treat the hypotension, other than minimizing the amount of delivered inhalant anesthetic.

Overall, it was confirmed that the hypersensitivity of the platelets in adult felines would result in decreased time to clot for both control and NO releasing loops when compared to previously studied rabbit models. The release of NO from the ECC circuits were successful in improving the hemocompatibility of the ECC loops as observed by drastic increases in the observed time until clotting (11 ± 3.6 min control, 132 ± 93.0 min NO-releasing). However, the increased platelet activity in the feline model led to high variability in clot size, as well as location of the clot.

Table 3.1: Coagulation parameters for control and NO-releasing ECC loops for during 4 h ECC. Activated partial thromboplastin time (aPPT), prothrombin time (PT), (TT), and vonWilebrand Factor activity (vWF). No measurement at 4 hours was taken for control loops as zero loops in the control population reached the 4-hour time point.

| | | **aPTT (s)** | **PT (s)** | **TCT** | **vWF** |
|---|---|---|---|---|---|
| **NO-Releasing** | Baseline | 16.8 ± 4.4 | 18.2 ± 0.6 | 7.3 ± 0.6 | 84.7 ± 28.9 |
| | 1 h | 17.8 ± 7.7 | 19.9 ± 2.3 | 8.3 ± 1.5 | 84 ± 16.6 |
| | 2 h | 17.9 ± 5.8 | 20.1 ± 1.4 | 8.8 ± 2.3 | 95.0 ± 31.2 |
| | 3h | 18 ± 6.3 | 19.7 ± 1.0 | 7.7 ± 1.5 | 96.3 ± 26.6 |
| | 4h | 17.7 ± 5.5 | 20.0 ± 1.3 | 7.5 ± 0.5 | 107.3 ± 30.2 |
| **Control** | Baseline | 14.4 ± 1.1 | 17.8 ± 0.4 | 6.7 ± 1.2 | 73.7 ± 10 |
| | 1 h | 15.8 ± 1.8 | 19.1 ± 1.1 | 8.2 ± 0.8 | 70 ± 16.5 |
| | 2 h (n=1) | 14.3 | 18.4 | 7.5 | 87 |
| | 3h (n=1) | 14.2 | 19.1 | 7.5 | 85 |

## Conclusion

For the first time, leaching of the RSNO SNAP was measured for three various ECC coating configurations in a flow environment. The addition of a top coat was successful in decreasing the total leached SNAP by 38% in the 4-hour period, while further incubation for 12 hours decreased leaching by 66%. These leaching kinetics showed unsteady NO release rates from the ECC surface over the 4-hour application, suggesting large administration of NO systemically should it be used *in vivo.* Incubated ECC loops maintained a flux of 1.83 ± 0.50 ×

$10^{-10}$ mol $min^{-1}$ $cm^{-2}$ for the full 4 h duration, which is well within physiological levels. Top coated ECCs with incubation delivered ca. 1% of the total NO potential over the 4-hour period, where uncoated ECCs delivered over 4.5% of the total NO stored in the film. The incubated ECC design was further tested to examine the hemocompatibility of the NO-releasing ECCs *in vivo* in a feline model. While it was clear the release of NO from the ECC circuit resulted in increased time to clot (11 ± 3.6 min control, 132 ± 93.0 min NO-releasing), no significant differences were seen in platelet count, thrombus weight, prothrombin time (PT), activated partial thromboplastin time (aPTT), thrombin clotting time (TCT), and vonWillebrand Factor (vWF) activity. However, a significant decrease in fibrinogen concentration was seen in the control ECC loops through 3 h, whereas fibrinogen levels were maintained through the 4 h period for NO releasing loops. It was confirmed that the hypersensitivity of the platelets in adult felines would result in decreased time to clot for both control and NO releasing loops when compared to previous rabbit models. While this does prove to be a more rigorous model for assessing the hemocompatibility of materials, the high variability of clot size, as well as inability to be maintained in the desired region, make the feline model inferior to the rabbit model at this time.

**References**


1. J. J. Rouby, American Journal of Respiratory and Critical Care Medicine, 2003, 168, 265-266.
2. G. M. Halpenny and P. K. Mascharak, Anti-Infective Agents in Medicinal Chemistry (Formerly Current Medicinal Chemistry-Anti-Infective Agents), 2010, 9, 187-197.
3. J. Marín and M. A. Rodríguez-Martínez, Pharmacology & Therapeutics, 1997, 75, 111-134.

4. K. Vural and M. Bayazit, European Journal of Vascular and Endovascular Surgery, 2001, 22, 285-293.
5. B. D. Ratner, Journal of Biomaterials Science, Polymer Edition, 2000, 11, 1107-1119.
6. B. D. Ratner, Biomaterials, 2007, 28, 5144-5147.
7. E. J. Brisbois, R. P. Davis, A. M. Jones, T. C. Major, R. H. Bartlett, M. E. Meyerhoff and H. Handa, Journal of Materials Chemistry B, 2015.
8. W. Cai, J. Wu, C. Xi and M. E. Meyerhoff, Biomaterials, 2012, 33, 7933-7944.
9. H. Handa, T. C. Major, E. J. Brisbois, K. A. Amoako, M. E. Meyerhoff and R. H. Bartlett, Journal of Materials Chemistry B, 2014, 2, 1059-1067.
10. T. C. Major, H. Handa, G. M. Annich and R. H. Bartlett, Journal of biomaterials applications, 2014, 29, 479-501.
11. A. M. Skrzypchak, N. G. Lafayette, R. H. Bartlett, Z. Zhou, M. C. Frost, M. E. Meyerhoff, M. M. Reynolds and G. M. Annich, Perfusion, 2007, 22, 193-200.
12. E. J. Brisbois, H. Handa and M. E. Meyerhoff, in Advanced Polymers in Medicine, Springer, 2015, pp. 481-511.
13. T. Hakim, K. Sugimori, E. Camporesi and G. Anderson, Physiological measurement, 1996, 17, 267.
14. A.-S. D. Haitham and A. Ferro, Clinical science, 2000, 98, 507-520.
15. N. Hogg, R. J. Singh and B. Kalyanaraman, FEBS letters, 1996, 382, 223-228.
16. D. L. H. Williams, Accounts of Chemical Research, 1999, 32, 869-876.
17. E. J. Brisbois, H. Handa, T. C. Major, R. H. Bartlett and M. E. Meyerhoff, Biomaterials, 2013, 34, 6957-6966.

18. Y. Wo, Z. Li, E. J. Brisbois, A. Colletta, J. Wu, T. C. Major, C. Xi, R. H. Bartlett, A. J. Matzger and M. E. Meyerhoff, ACS applied materials & interfaces, 2015.

19. S. l. M. Shishido, A. B. Seabra, W. Loh and M. G. de Oliveira, Biomaterials, 2003, 24, 3543-3553.

20. B. K. Oh and M. E. Meyerhoff, Journal of the American Chemical Society, 2003, 125, 9552-9553.

21. M. C. Frost and M. E. Meyerhoff, Journal of the American Chemical Society, 2004, 126, 1348-1349.

22. A. Seabra, A. Fitzpatrick, J. Paul, M. De Oliveira and R. Weller, British Journal of Dermatology, 2004, 151, 977-983.

23. A. Seabra, E. Pankotai, M. Fehér, A. Somlai, L. Kiss, L. Biro, C. Szabo, M. Kollai, M. De Oliveira and Z. Lacza, British Journal of Dermatology, 2007, 156, 814-818.

24. G. E. Gierke, M. Nielsen and M. C. Frost, Science and Technology of Advanced Materials, 2011, 12, 055007.

25. M. M. Reynolds, J. A. Hrabie, B. K. Oh, J. K. Politis, M. L. Citro, L. K. Keefer and M. E. Meyerhoff, Biomacromolecules, 2006, 7, 987-994.

26. H. Handa, E. J. Brisbois, T. C. Major, L. Refahiyat, K. A. Amoako, G. M. Annich, R. H. Bartlett and M. E. Meyerhoff, Journal of Materials Chemistry B, 2013, 1, 3578-3587.

27. T. Stokol, M. Brooks, J. Rush, M. Rishniw, H. Erb, E. Rozanski, M. Kraus and A. Gelzer, Journal of veterinary internal medicine, 2008, 22, 546-552.

28. F. Tablin, T. Schumacher, M. Pombo, C. Marion, K. Huang, J. Norris, K. Jandrey and M. Kittleson, Journal of Veterinary Internal Medicine, 2014, 28, 411-418.

29. C. E. Smith, E. A. Rozanski, L. M. Freeman, D. J. Brown, J. S. Goodman and J. E. Rush, Journal of the American Veterinary Medical Association, 2004, 225, 1237-1241.

30. I. Chipinda and R. H. Simoyi, The Journal of Physical Chemistry B, 2006, 110, 5052-5061.

31. T. C. Major, D. O. Brant, M. M. Reynolds, R. H. Bartlett, M. E. Meyerhoff, H. Handa and G. M. Annich, Biomaterials, 2010, 31, 2736-2745.

32. M. W. Vaughn, L. Kuo and J. C. Liao, American Journal of Physiology-Heart and Circulatory Physiology, 1998, 274, H2163-H2176.

33. I. Megson, S. Morton, I. Greig, F. Mazzei, R. Field, A. Butler, G. Caron, A. Gasco, R. Fruttero and D. Webb, British journal of pharmacology, 1999, 126, 639-648.

34. M. J. Goudie, E. J. Brisbois, J. Pant, A. Thompson, J. A. Potkay and H. Handa, International Journal of Polymeric Materials and Polymeric Biomaterials, 2016, 65, 769-778.

35. A. Dicks, H. Swift, D. Williams, A. Butler, H. AlSadoni and B. Cox, Journal of the Chemical Society, Perkin Transactions 2, 1996, 481-487.

36. D. J. Sexton, A. Muruganandam, D. J. McKenney and B. Mutus, Photochemistry and Photobiology, 1994, 59, 463-467.

37. P. D. Wood, B. Mutus and R. W. Redmond, Photochemistry and Photobiology, 1996, 64, 518-524.

# CHAPTER 4

# LIQUID-INFUSED NITRIC OXIDE-RELEASING (LINOREL) SILICONE FOR DECREASED FOULING, THROMBOSIS, AND INFECTION OF MEDICAL DEVICES[3]

[3] Goudie, M.J., Pant, J., Handa, H. 2017. *Scientific Reports*.

**Abstract**

Recent reports on liquid-infused materials have shown promise in creating ultra-low fouling surfaces, but are limited in their ability to prevent bacterial proliferation and prevent platelet activation in blood-contacting applications. In this work, a liquid-infused nitric oxide-releasing (LINORel) material is created by incorporating the nitric oxide (NO) donor *S*-nitroso-acetylpenicillamine (SNAP) and silicone oil in commercial medical grade silicone rubber tubing through a solvent swelling process. This combination provides several key advantages over previous NO-releasing materials, including decreased leaching of NO donor, controlled release of NO, and maintenance of ultra-low fouling property of liquid-infused materials. The LINORel tubing reduces protein adhesion as observed using fluorescence imaging, and platelet adhesion (81.7 ± 2.5 %) *in vitro* over a 2 h period. The LINORel combination greatly reduces bacterial adhesion and biofilm formation of two most common pathogens responsible for hospital acquired infections: gram-positive *Staphylococcus aureus* and gram-negative *Pseudomonas aeruginosa* (99.3 ± 1.9% and 88.5 ± 3.3% respectively) over a 7-day period in a CDC bioreactor environment. Overall, the LINORel approach provides a synergistic combination of active and passive non-fouling approaches to increase biocompatibility and reduce infection associated with medical devices.

**Introduction**

Blood contacting devices (extracorporeal circuits, catheters, stents, grafts, etc.) are used in thousands of patients every day.[1] Fouling of these devices, either through adsorption of protein leading to thrombus formation, or the adhesion of bacteria resulting in infection, are two of the most common complications seen clinically today.[2-4] The ability to prevent fouling of these devices is critical for the functionality of the device and safety of the patient. While antibiotics

and systemic anticoagulation have drastically improved the safety of procedures, researchers continue to strive for a completely biocompatible surface, where passive and active approaches have been developed.

Common approaches to limit the adsorption of proteins (i.e. fibrinogen) include modification of the material surface such as the immobilization of zwitterionic compounds or polyethylene glycol (PEG) and have been demonstrated to provide substantial decreases in fouling of materials both *in vitro* and *in vivo* for bacterial adhesion and thrombus formation.[5-8] Immobilization of heparin have also been shown to decrease thrombus formation; however, none of these strategies have been shown to be 100% effective. A number of limitations remain with these materials, including the leaching of the surface-bound heparin, decreasing the anticoagulation activity over time, and thus require additional systemic heparin to ensure thrombus formation does not occur.[9-11] While it is the current standard in clinical practice, the systemic administration of heparin can cause morbidity and mortality through post-operative bleeding, thrombocytopenia, and hypertriglyceridemia.[12] In the case of extracorporeal circuits, while systemic anticoagulation is required to preserve the patency of the circuit, platelet consumption is still observed and can drop to <40% of the initial value during the first 1-2 h of use.[13] Due to these complications, the systemic administration of anticoagulants is the leading cause of drug-related deaths from adverse clinical events in the United States.[14] Active materials such as antibiotic-releasing or silver-containing catheters are capable of limiting infection, but do not provide any mechanism for reducing thrombus formation.[15] For this reason developing novel materials that possess ultra-low fouling characteristics with materials that can actively kill bacteria and prevent platelet activation and adhesion could provide a drastic advancement in materials for medical devices.

Nitric oxide-releasing (NORel) materials have been developed over the past 30 years after the discovery of NO as an important signaling molecule in a number of biological processes, of which include acting as a strong bactericidal and antithrombotic agent.[16-18] To mimic the physiological release of NO from the endothelium, various NO donors (such as *S*-nitrosothiols[18-20] and diazeniumdiolates[21-23]) have been developed and can be integrated into polymeric materials for localized delivery of NO. Multiple methods have been used to integrate *S*-nitrosothiols such as *S*-nitroso-*N*-acetylpenicillamine (SNAP) into various medical grade polymers, and include physical blending within the polymer[18,24], immobilization to the polymer backbone[25,26], or swelling into the polymer matrix[27,28]. However, NORel materials have been shown to have increased protein adhesion,[29] which can ultimately increase the likelihood of bacterial or platelet adhesion on the surface.[30] Despite increases in protein adhesion, NO-releasing materials have been shown to significantly reduce thrombus formation and presence of viable bacteria *in vivo.*[23,24,27,31] While NO possesses the ability to kill bacteria and prevent platelet activation, decreasing the degree of protein adsorption can act in a synergistic manner to aid in the prevention of thrombosis and bacterial adhesion. Therefore, the development of non-fouling NO-releasing materials can provide further improvements in the overall biocompatibility of existing materials.

Liquid-infused materials take advantage of capillary forces between the infused liquid and the polymer network, creating a low-adhesion interface between the material and the contacting fluid, such as blood. The idea of these slippery liquid-infused porous surfaces (SLIPS) stems from the lining of the gastrointestinal tract, where a mucous layer protects the tissues from colonization by bacteria.[32,33] These materials have shown drastic improvements in the biocompatibility on several common medical polymers, as well as decreasing the adhesion of

bacteria to the surface. The efficacy of these SLIPs has been previously demonstrated using tethered perfluorocarbons with a liquid perfluorocarbon held on the surface using capillary forces, as well as the infusion of full medical grade tubing with a biocompatible oil.[11,33,34] It is also important to note that silicone oil has been shown to be nontoxic on the cellular and systemic levels in humans, making it a promising liquid for infusion of SLIPs materials.[35]While these materials provide a passive approach to limit protein or bacterial adhesion, even small amount of adsorbed fibrinogen can lead to platelet activation and adhesion, and ultimately the proliferation of bacteria that can lead to biofilm formation and infection. For example, the presence of thin silicone films has been reported to prevent thrombus formation for short durations[36], but are not capable preventing platelet activation and adhesion.[11] The question remains if bacteria or other microorganisms can breach the liquid barrier to the surface, leading to the formation of "beachheads" and enable colonization and biofouling.[37] To overcome bacterial adhesion, the combination of liquid-infused materials and release of a model antimicrobial agent triclosan has demonstrated a synergistic effect of the slippery surface with the active release of antimicrobial agents.[37] One drawback of these materials, however, is these materials do not address issues associated with platelet activation. Incorporating an active release of NO into these materials can aid in the prevention of platelet activation, while also acting as a bactericidal and fungicidal agent to prevent colonization and biofouling on the material surface.[38-41] The use of NO as an antibacterial agent is also attractive as antibiotic-resistant strains of bacteria have been increasingly problematic in the healthcare industry.[42,43]

In this work, fabrication of liquid-infused NO-releasing (LINORel) materials is described, and the synergistic effect of incorporating the NO release with the ultra-low fouling capabilities of liquid-infused materials is demonstrated. The LINORel properties using a two-

stage swelling process of the NO donor SNAP and silicone oil respectively into medical grade Tygon™ 3350 silicone rubber (SR) tubing. The presence of the infused silicone oil not only provides the desired traits of liquid-infused materials, but also acts in a manner to prevent the burst release kinetics typically associated with NO releasing materials. We demonstrate: (i) these LINORel materials show reduced adhesion of the blood coagulation protein fibrinogen despite NO release; (ii) reduced platelet adhesion *in vitro*; (iii) and the increased efficacy of preventing biofilm formation of pathogens associated with hospital-acquired infection over a 7 d period. The LINORel approach is the first of its kind to combine the advantages of liquid-infused materials with the active release of an antibacterial, antifungal, and antithrombotic agent, which may aid in future developments of broad-spectrum solution for complications associated with thrombosis and infection associated with medical devices.

## Results and Discussion

*Physical characterization of silicone tubing from SLIPs perspective*

Commercial silicone tubing was impregnated with the NO donor SNAP using the previously described swelling method.[27] To demonstrate the incorporation of SNAP has an insignificant effect on the lubricating nature of the silicone oil, sliding angle and oil swelling/deswelling were investigated before and after SNAP incorporation.

The infusion of silicone oil into the silicone tubing leads to an expanded state of the polymer tubing, as the polymer chains extend to maximize the polymer-solvent interactions.[33] To observe if the presence of SNAP within the silicone tubing altered the overall swelling capacity or kinetics, the swelling ratio of oil within the tubing was recorded over 72 hours. The presence of SNAP increased the overall swelling ratio, from 1.53 ± 0.003 to 1.59 ± 0.009 **(Figure 4.1A,** $p = 0.012$**)**. The increase in swelling ratio maybe be attributed to unfavorable interactions between

the polymer matrix and crystaline SNAP distrubted throught, leading to higher silicone oil uptake to minimize this interaction. The SR tubing was also capable of maintaining these swelling ratios over the 7 d period at 37°C. The ability for the tubing to maintain this swelling ratio shows that while the swelling ratio is lower than previously reported[33], the diffusion of the oil from the polymer matrix has decreased, which coincides with the increased time to reach maximum swelling. However, the decrease in swelling ratio may result in decreased thickness of the liquid layer, impacting the overall performance of the SLIP surface. Therefore, we hypothesize that there may be a compromise in the functionality of the surface with an overall longevity of the infused oil. The full chemical structure of the silicone tubing will dictate the overall swelling ratio and could pose the possibility of selecting certain swelling ratio kinetics for the desired application.

All sliding angle measurements were taken using a 2 µL droplet, where the sample was raised slowly at one end and the angle was measured with a digital level. The liquid-infused nitric oxide-releasing (LINORel) SR tubing showed a sliding angle of 13.2 ± 5.5°, compared to oil swollen tubing which had an initial sliding angle of 10.8 ± 2.4° ($p > 0.05$). Both methods utilizing the incorporation of silicone oil provided drastic decreases in the observed sliding angle when compared to SR controls, which all showed sliding angles >90°. The sliding angle was observed to slightly increasing over a 7 d period for both NORel-SR and LINORel-SR samples **(Figure 4.1B)**. Previous results of infused silicone report sliding angles in the single digits (2.1°).[33] However, these samples were prepared using the silicone Sylgard 184 and prepared as a flat surface. Therefore, we leave the possibility that the composition of the Tygon™ tubing could lead to increased sliding angle. However, we presume the potential cause of this increase stems from the inability for the commercial tubing to achieve a completely flat surface, creating

regions for pinning. It has been shown previously that the SNAP swelling process has minimal effects on the surface morphology of the silicone tubing, and is supported by the similar sliding angles of LI-SR and LINORel-SR tubing.[27] Overall, the drastic decrease between control and the oil infused tubing are substantial in demonstrating the efficacy of the oil to increase the slippery nature of the tubing.

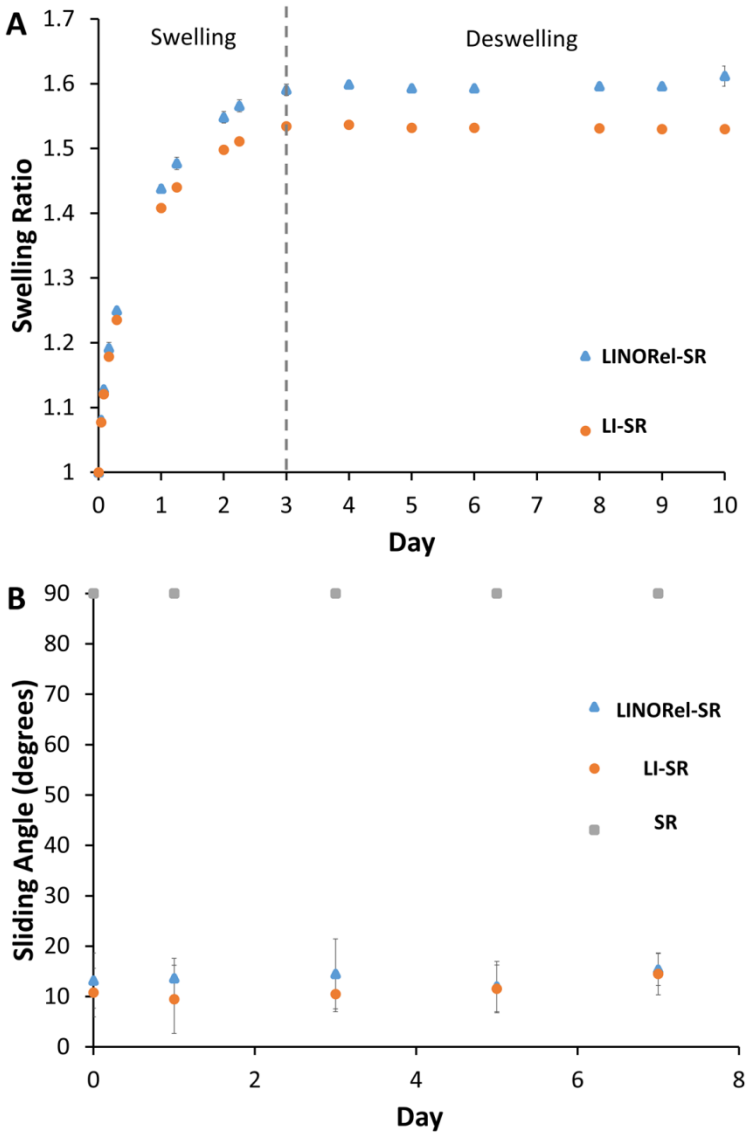

Figure 4.1: **A)** Swelling of silicone rubber tubing with silicone oil in control and SR tubing infused with SNAP. Error bars are on the order of data point size and therefore not shown. **B**) Sliding angle of LI-SR and LINORel-SR tubing over 7 d when stored in phosphate buffered saline at 37°C.

*Characterization of liquid-infused NO releasing silicone rubber from NO perspective*

*Leaching of S-nitroso-acetyl-D-penicillamine*

The leaching of NO donors can have detrimental effects on the release characteristics and overall lifetime of the device. This phenomenon is generally associated with a "burst-release" of NO during the initial hours of use. Methods to limit the leaching of physically incorporated NO donors have included the use of hydrophobic polymers.[18] For NO donor-polymer combinations that have minimal leaching ( < 5% of the total NO donor incorporated), incubation of the device in a solution for an allotted time has been used to control the burst effect when used *in vivo*.[18,31] While the overall leaching of the donor is low compared to the total loading of the NO donor, the timeframe in which the donor is released to the blood stream can still have systemic effects such as vasodilation and decreases in blood pressure. Therefore, even materials that experience minimal NO donor leaching can still exhibit burst-release characteristics at implantation.

The leaching of SNAP from the SR tubing was examined using UV-vis spectroscopy during both the oil swelling (72 h) as well as the first 24 h in PBS under physiological conditions **(Figure 4.2)**. During the infusion of the tubing with silicone oil, the amount of leached SNAP was observed to not increase after the first 8 h ($1.3 \pm 0.1 \times 10^{-5}$ mg SNAP $mg^{-1}$ tubing), which may be attributed to the solubility of SNAP (or the base molecule NAP) in the silicone oil. Solubility of SNAP in silicone oil was found to be 0.4 μg/mL. Therefore, increasing the swelling

time past 8 h should not have significant effects on the levels of SNAP within the SR tubing when compared to NORel-SR that is stored at room temperature. The stability of SNAP within a polymer matrix has been shown to retain 87% of SNAP activity after 6 months at room temperature.[44] Once placed into the aqueous environment at physiological conditions, the LINORel tubing demonstrated significantly lower leaching levels than of the NORel tubing alone over an initial 24 h period ($5.3 \pm 0.4 \times 10^{-4}$ mg SNAP $mg^{-1}$ tubing vs. $2.9 \pm 1.0 \times 10^{-4}$ mg SNAP $mg^{-1}$ tubing, $p = 0.02$). The total leaching of the LINORel tubing (from both oil and PBS incubation) was reduced by ca. 45% than that of NORel tubing alone.

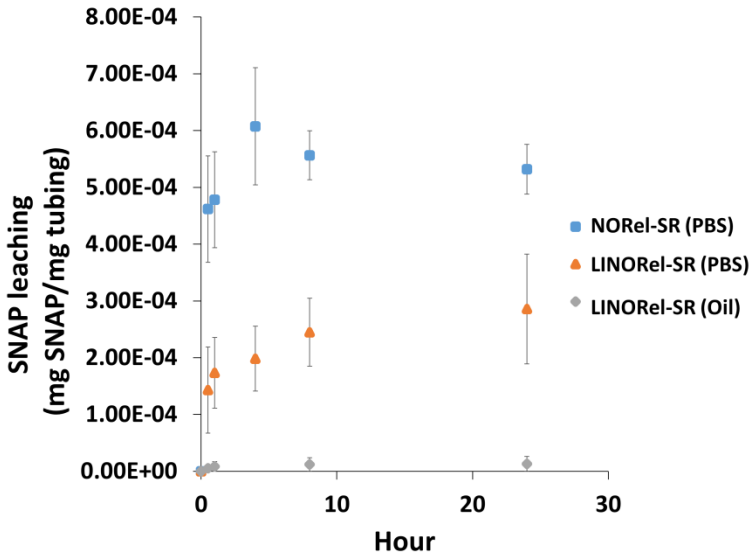


Figure 4.2: Leaching characteristics of SNAP from NORel-SR and LINORel-SR. Leaching was conducted at room temperature for oil swelling, and physiological conditions (PBS, 37C). Samples were protected from light at all times.

*Nitric Oxide release in vitro*

Nitric oxide release was measured over a 7 d period from both NORel-SR and LINORel-SR using a Sievers chemiluminescence nitric oxide analyzer **(Figure 4.3A)**. Release of NO from

the SNAP infused tubing exhibited an NO release profile that is consistent with other previously reported materials, showing higher levels of NO initially, and gradually decreasing until reaching a steady state release.[18,27,44] Controlling this burst release is a prime objective for researchers when developing new NO releasing materials, as the burst can be detrimental to the lifetime of the device. The SNAP swelling concentration of 25 mg $mL^{-1}$ was chosen as it was previously shown to provide physiological levels of NO release and significantly increase the hemocompatibility of SR tubing *in vivo.*[27] However, silicone Foley catheters have been shown to release NO for over 30 d when swollen with 125 mg $mL^{-1}$ SNAP in THF,[28] demonstrating that further optimization of the SNAP swelling concentration can be investigated. The total loading of SNAP using the swelling process was found to be ca. 1 wt% (via chemiluminescence) when a concentration of 25 mg $mL^{-1}$ is used, and is consitent with previous SNAP swelling reports (ca. 5 wt%, 125 mg $mL^{-1}$).[28] Release rates for the NORel-SR tubing decreased from $0.62 \pm 0.09 \times 10^{-10}$ mol $min^{-1}$ $cm^{-2}$ to $0.09 \pm 0.07 \times 10^{-10}$ mol $min^{-1}$ $cm^{-2}$ over the 7 d period. The LINORel-SR tubing demonstrated a consistent release over the 7 d period, with initial and final release rates of $0.34 \pm 0.03 \times 10^{-10}$ mol $min^{-1}$ $cm^{-2}$ and $0.42 \pm 0.06 \times 10^{-10}$ mol $min^{-1}$ $cm^{-2}$, respectively ($p > 0.05$). The while the bactericidal activity was not examine >7 d, LINORel SR was able to provide this sustained release of NO over a 21 d period, making this a plausible approach for long term applications. The cummulative release of NO from the material due to both leaching and degredation of SNAP to NAP is shown in **Figure 4.3B** as a percentage of the total SNAP loaded. Therefore, the incorporation of the silicone oil not only assists with non-fouling capabilities of the tubing but provides a more controlled NO release from the donor as well. This can be attributed to the silicone oil preventing the hydration on the silicone tubing, which can lead to faster release of NO from the donor.[16,18] Further optimization is needed on the swelling method

can be done on the concentration of SNAP within the swelling solution as the release will not only be governed by the total amount of SNAP loading, but also the crystal structure within the silicone matrix.[45] It is also possible that the crystal structure of SNAP within the polymer may be tunable using the rate of solvent evaporation, and may also be influenced by the degree of crosslinking within the polymer. Possiblities for improving the activity of the LINORel SR by increasing the NO release could involve integration of metalic complexes such as copper into the silicone matrix[46], or for non-implanted applications such as extracorporeal circuits stimulation with light may be applied to modulate the NO release[25,47].

*Assessment of fibrinogen adsorption in vitro*

One common method for assessing the hemocompatibility of materials *in vitro* is to examine the ability of the material to resist protein adhesion, more specifically, fibrinogen. The conversion of fibrinogen to fibrin in the common pathway of the coagulation cascade, and the adhesion of platelets through GpIIb/IIIa, lead to the formation of thrombus on the material surface. While the orientation of fibrinogen adsorption has been shown to determine the degree of platelet adhesion, limiting protein adhesion regardless of orientation is generally considered to be an improvement in the hemocompatibility of a material.[48] Apart from aiding in the formation of thrombus, surface bound protein has been shown to increase the level of bacterial adhesion, increasing the chance of biofilm formation and infection.[30] Although NO releasing materials have been shown to significantly reduce platelet activation and adhesion, they have also been shown to adsorb higher levels of fibrinogen.[29] Therefore, developing non-fouling NO-releasing materials could provide drastic improvements in the overall hemocompatibility and antibacterial nature of these materials.

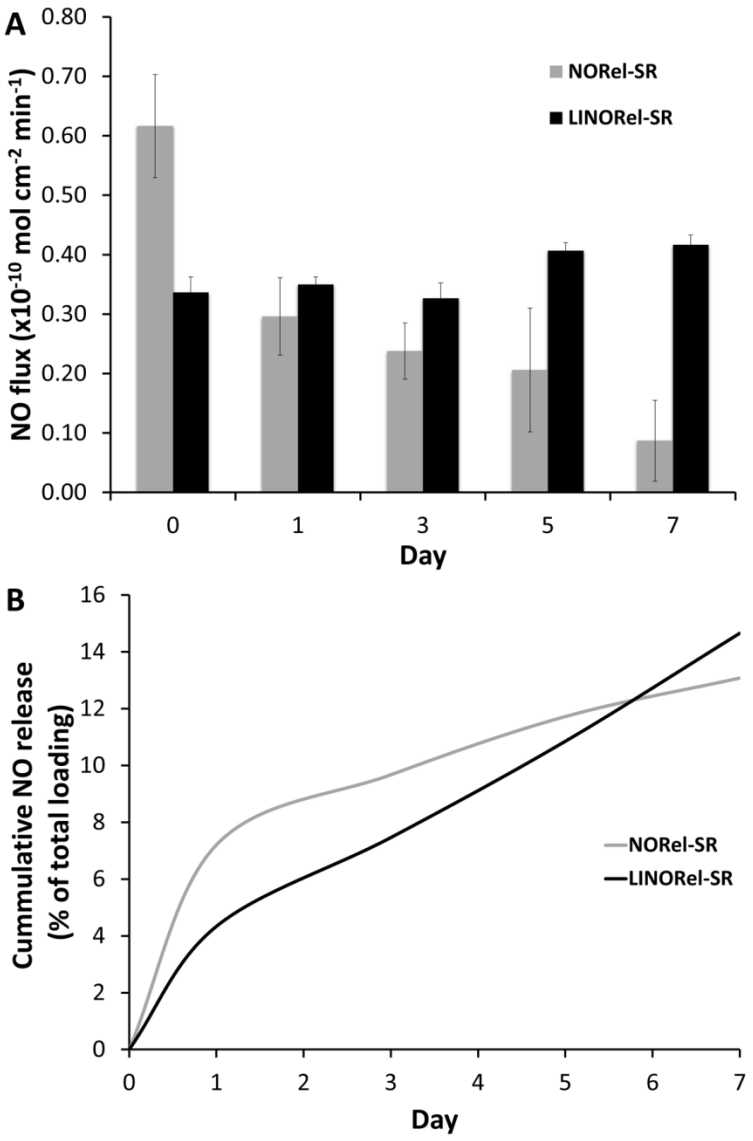


Figure 4.3: A) Average daily nitric oxide release measures from NORel-SR and LINORel-SR tubing over a 7-day period. Measurements were conducted at 37°C using a Sievers Chemiluminescence Nitric Oxide Analyzer. B) Cummulative release of NO from NORel-SR and LINORel at physiological conditions due to leaching and degredation of the NO donor.

To examine if the infusion of silicone oil to provide a slippery surface could overcome the increased protein adhesion observed on NO-releasing materials, 2 h exposure to FITC-labeled fibrinogen was conducted at 37°C **(Figure 4.4)**. NORel-SR was observed to adsorb

comparable amounts of fibrinogen compared to the control SR tubing, which coincides with previously reported results.[29] The presence of the infused oil was observed to greatly reduce protein adhesion in both LI-SR and LINORel tubing. Therefore, the infusion of silicone oil was successful in drastically reducing the adsorption of fibrinogen despite NO release. The adhesion of the protein of the surface was not measured quantitatively, although MacCullum et. al has reported that the measured bacterial adhesion on silicone oil infused tubing can vary drastically with the method that the material is washed.[33] In this study, the authors show that with no wash, ca. 90% reductions in biofilm formation was observed with LI-SR alone; however, it reduced to nearly 100% with both 5 s and 5 min wash times under high shear. The infinite dilution of this method for washing of the material surface ensures minimal shear on the material surface, and therefore we believe represents the highest levels of protein adsorption that would be seen, with much of the protein loosely bound to the surface. The efficacy of these materials in long-term exposure to protein-rich environments is currently under investigation by our group and will vary highly with duration of exposure and applied shear forces, ultimately governing the thickness of the thin film protecting the surface.

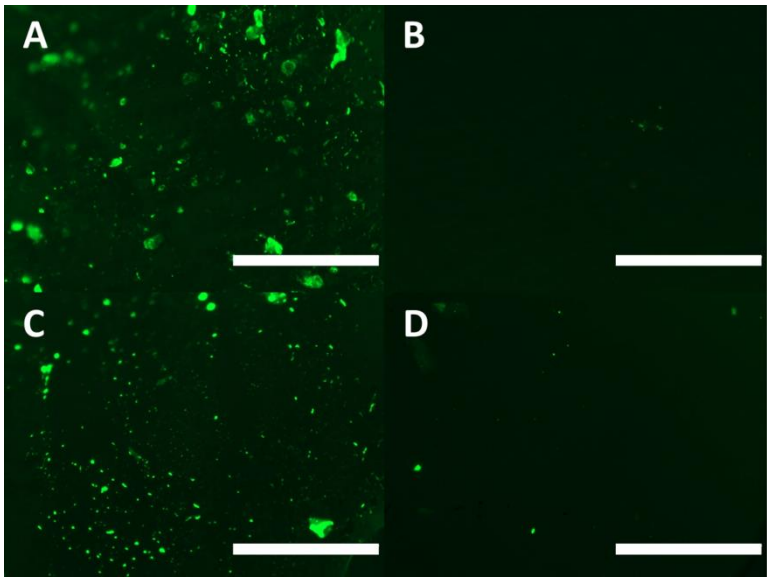

Figure 4.4: Assessment of protein adhesion (FITC labeled fibrinogen) after 2 h incubation on A) SR B) LI-SR, C) NOrel-SR, D) LINORel-SR. Scale bar represents 250 µm.

*Assessment of porcine platelet adhesion in vitro*

Sections of the various modified Tygon™ tubing were exposed to fresh porcine PRP for 2 h at 37°C under mild rocking, where the number of adhered platelets were quantified using a Roche LDH assay **(Figure 4.5)**. The presence of the infused oil provides a lubricating layer, separating the material surface from the liquid to be in contact, as well as drastically reducing the surface roughness.[11,33,34] Presence of the SLIP surface resulted in 27% reduction in the overall adhered platelets ($7.76 \pm 1.70 \times 10^5$ platelets $cm^{-2}$ vs $5.67 \pm 2.58$ $10^5$ platelets $cm^{-2}$, $p>0.05$), while NORel surfaces saw reductions near 44%. Similar reductions in platelet adhesion have been reported for other liquid infused surfaces when exposed to whole blood for 30 min, containing 0.25 U $mL^{-1}$ heparin.[11] The increased platelet adhesion observed in this study can be attributed to the increased exposure time and absence of anticoagulant. The combination of infused oil with a NO releasing donor molecule further reduced the degree of platelets adhered to 81.7±2.5% of control silicone rubber tubing ($7.76 \pm 1.70 \times 10^5$ platelets $cm^{-2}$ vs $1.52 \pm 0.68 \times 10^5$ platelets $cm^{-2}$, $p = 0.03$). The LINORel combination was able to significantly reduce platelet adhesion when compared to LI-SR alone (73.1%, $p = 0.03$), and may be attributed to the presence of the silicone oil as it does not prevent platelet activation. However, the LINORel combination did not provide a significant decrease in platelet adhesion when compared to NORel-SR alone ($p > 0.05$). Washing of each material was done through infinite dilution of the well plate, and therefore provided minimal shear at the material interface. The effectiveness of the washing of these liquid infused materials is highly depended on the shear rate and time of wash, and can attribute to higher platelet counts observed.[33] Few dual-action materials incorporating NO release

have been developed, with even fewer examined for platelet adhesion *in vitro*. Kipper et. al, developed a glycoclyx-inspired NO releasing material on titanium to mimic the natural endothelium, where NO release was provided by nitrosated chitosan thioglycolic acid.[49] These materials showed similar reductions in platelet adhesion to the LINORel tubing when examined using scanning electron microscopy after 2 h exposure to human blood plasma containing platelets and leukocytes. However, the NO release from the materials decreased to below 0.01 × $10^{-10}$ mol $min^{-1}$ $cm^{-2}$ within 20 minutes. The combination of NO with zwitterionic polycarboxybetaine coatings have been reported by Cook et. al with similar platelet adhesion to the LINORel materials describe with 93.1 ± 1.3% reductions in platelet adhesion using NO delivery through a permeable polydimethylsiloxane membrane. While this combination is highly effective, the requirement for sweep gas may limit the direct application. Therefore, the combination of the extended non-fouling nature from the SLIP surface with controlling of the NO release profile make the LINORel approach a promising for long term blood-contacting applications.

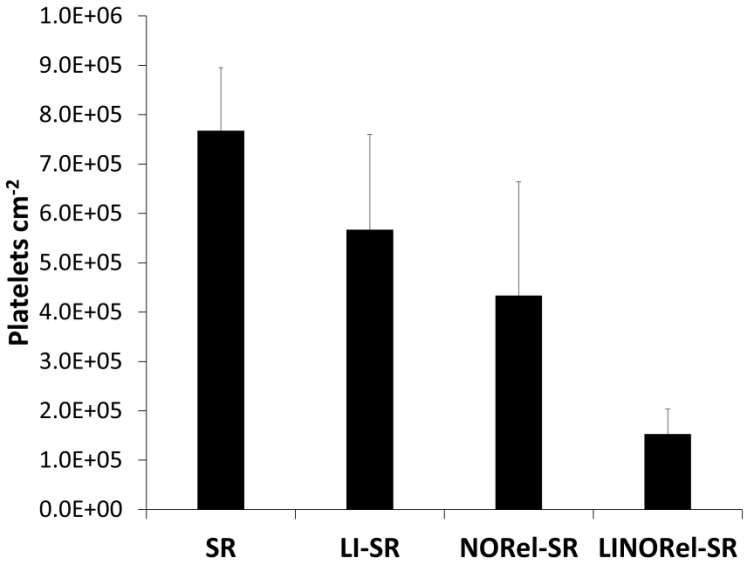

Figure 4.5: Degree of platelet adhesion on various silicone tubing after 2 h exposure to porcine platelet rich plasma as measured using an LDH quantification assay.

*In vitro 7 d bacterial adhesion and viability analysis in a continuous flow CDC bioreactor*

Development of novel materials to reduce bacterial adhesion and growth on materials are generally achieved using one of or a combination of two parameters: (i) the surface characteristics of the material (chemical and physical), and (ii) the antibacterial efficiency attributed to it via the antimicrobial agent. The LINORel approach looks to address each of these parameters by combing an active release of and antibacterial agent (NO) with a liquid-infused surface. While the infused silicone oil provides a super slippery hydrophobic surface for preventing attachment of bacteria on the polymer surface in an environment with shear force (such as CDC bioreactor), the free radical NO provides bactericidal action via lipid oxidation, denaturation of enzymes ,and deamination of DNA.[50] To examine the long-term efficacy of these materials to prevent biofilm formation, exposure to two common pathogens associated with healthcare-acquired infections was done in a CDC bioreactor over a 7 d period with gram-negative *P. aeruginosa* and gram positive *S .aureus*, where *P. aeruginosa* causes 10-15% of nosocomial infections worldwide.[33,51].

In a similar fashion to the protein adhesion studies mentioned above, minimal washing of the surface was done as to not detach loosely bound bacteria from the material surface through shear forces prior to the intentional detachment via homogenization of the film. **Figure 4.6** graphically represents the CFU $cm^{-2}$ attached on the surface of each of modified tubing. Efficacy of each tubing modification is summarized in **Table 4.1**.

Table 4.1: Efficacy of each modification of SR on reducing bacterial adhesion and viability over 7 d in CDC bioreactor.

| | | CFU $\times 10^5$ cm$^{-2}$ | Reduction vs. SR (%) | *p* value vs. SR |
|---|---|---|---|---|
| ***S. aureus*** | **SR** | 7.29±1.11 | - | - |
| | **LI-SR** | 0.25±0.02 | 96.57±0.3 | 0.007 |
| | **NORel-SR** | 0.17±0.04 | 97.61±0.62 | 0.008 |
| | **LINORel-SR** | 0.05±0.01 | 99.31±.15 | 0.007 |
| ***P. aeruginosa*** | **SR** | 13.92±1.22 | - | - |
| | **LI-SR** | 7.95±0.53 | 42.89±3.80 | 0.004 |
| | **NORel-SR** | 2.49±0.02 | 82.08±0.18 | 0.002 |
| | **LINORel-SR** | 1.61±0.14 | 88.44±1.01 | 0.003 |

The presence of the infused silicone oil alone reduced CFU cm$^{-2}$ of *S. aureus* by 96.5 ± 0.30% and *P. aeruginosa* by 42.8 ± 3.8% after 7 d in the CDC environment. The drastic difference in the ability for LI-SR to prevent the attachment of *P. aeruginosa* can be attributed to the differences in the structure of the bacteria, and demonstrate the need for an active release of a bactericidal agent such as NO when used in long-term applications. Previously, infusion of silicone oil was shown to reduce *P. aeruginosa* adhesion to medical grade silicone by >90% after 48 h exposure.[33] Many of the interactions of bacteria with liquid infused materials are not fully understood. This increase in *P. aeruginosa* adhesion at day 7 could stem from the proliferation of few bacteria that had adhered, or overcoming the liquid layer with extended exposure. NORel-SR achieved 97.6 ± 0.6% and 82.1 ± 0.2% reductions against *S. aureus* and *P. aeruginosa* respectively. The NO flux of the tubing dropped from 0.62 ± 0.09 $\times 10^{-10}$ mol min$^{-1}$ cm$^{-2}$ to 0.09 ± 0.07$\times 10^{-10}$ mol min$^{-1}$ cm$^{-2}$ from the initial release to day 7, therefore it would not be unreasonable to predict that the bacterial killing was much higher initially, decreasing over time due to gradual decrease in NO flux.The bacterial killing ability of the NO releasing tubing matches with the

previous reports where the bactericidal activity of NO has been demonstrated against *S. aureus*, *E. coli, Candida albicans, L. monocytogenes, E. faecalis* and *A. baumanni*.[22,41,52,53] However, both the ability of the liquid infused surface to reduce bacterial adhesion and NO to provide bactericidal activity can vary between bacterial strains, and should be investigated further with the bacterial strain that will apply to the intended device. The NO based strategy to prevent infection is not expected to stimulate resistance in the bacterial strains due to its rapid mode of action and very short half-life (<5 sec) unlike antibiotics and silver nanoparticles.[22,54] Further developing these materials to release levels of NO at the upper end of physiological limits would be expected to provide further reductions in long-term viable bacterial adhesion. LINORel-SR achieved a 99.3 ± 1.9% reduction in gram-positive *S. aureus* and 88.5 ± 3.3% reduction in *P. aeruginosa* population on LINORel tubing (CFU $mL^{-1}$) as compared to control SR tubing, and was significantly more effecitvive than LI-SR or NORel-SR tubing alone (**Table 4.2**). The effect of the LINORel combination is clearly demonstrated, where reductions of the combination are near the reductions observed when comparing a singular modification to the unmodified SR.

Integration of biocides into materials to provide antibacterial activity to SLIPs surfaces have been reported by using the combination of triclosan with infused silicone oil in polyethyleneimine/poly(2-vinyl-4,4-dimethylazlactone) (PEI/PVDMA) multilayers, and showed ca. 80% reduction in *C. albicans* after three sequential 24 h exposures to 1 mL cell suspension ($10^6$ CFU/mL).[37] However, the biomimetic nature of NO releasing materials is attractive with the emergence of antibiotic-resistant strains of bacteria, as well having antithrombotic properties. Dual action mechanisms to increase the bactericidal activity of NO releasing materials using the combination of NO release with metallic ions[46,55], quarterinary ammonium compounds[56,57], antibiotics and antimicrobial peptides[58] have also been investigated. While the combination of

bactericidal agents may provide higher bactericidal activity in the short-term, these materials can experience decreases in efficacy with fouling of the material surface. Therefore, adding bactericidal activity to SLIP materials can be advantageous in protein-rich or bacterial-rich environments where the surface can be comprimised quickly.

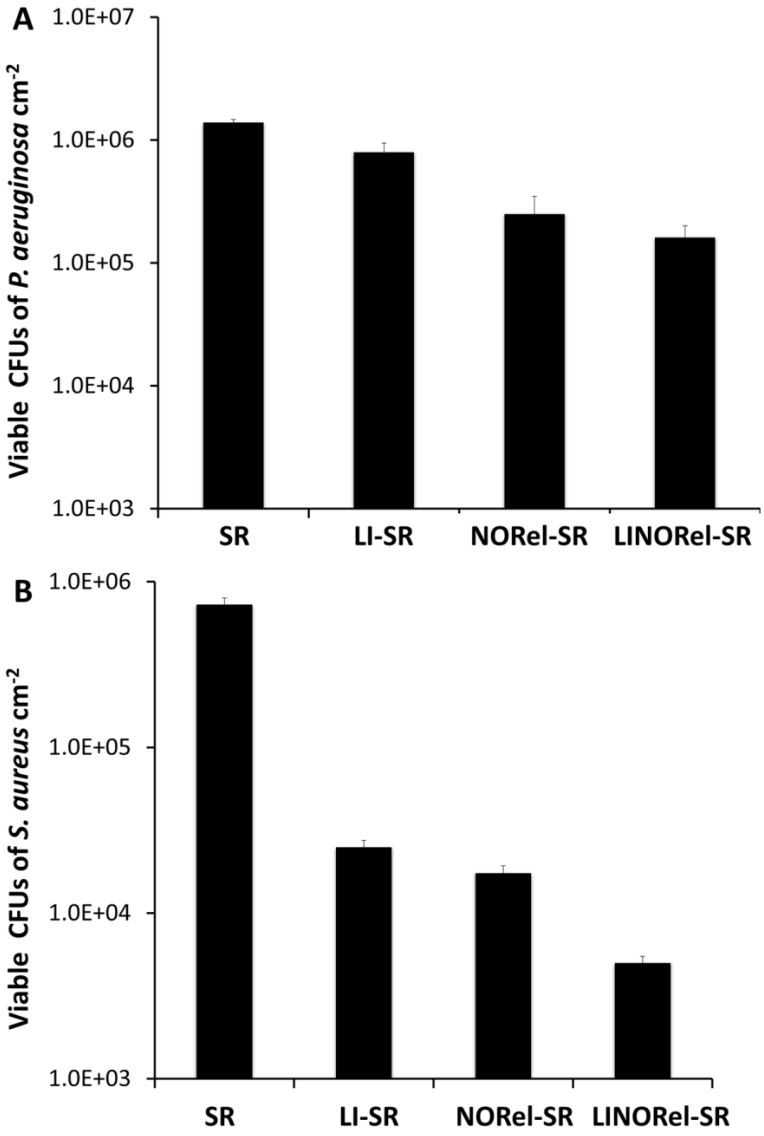


Figure 4.6: Viable bacteria on various silicone tubing after 7 d bacteria exposure in a CDC bioreactor.

Table 4.2: Comparison of LINORel-SR tubing to LI-SR and NORel-SR after 7 d in CDC bioreactor.

| | ***S. aureus*** | | ***P. aeruginosa*** | |
|---|---|---|---|---|
| | **LI-SR vs. LINORel** | **NORel-SR vs. LINORel** | **LI-SR vs. LINORel** | **NORel-SR vs. LINORel** |
| Reduction vs. LINORel (%) | 80.0±4.7 | 71.3±4.9 | 73.2±2.2 | 35.5±5.7 |
| *p* value vs LINORel | 0.001 | 0.044 | 0.003 | 0.004 |

*Cytocompatibility of LINORel-SR tubing*

The CCK-8 assay was performed to the demonstrate the absence of any toxic response of the leachates from NORel-SR and LI-SR tubing towards mouse fibroblast cells. The results demonstrated that neither NORel or LI-SR, nor their combination in the used dosages, , is cytotoxic to the mammalian fibroblast cells. In the past SNAP and Si-oil has been used individually as an active strategy to control the growth of bacteria on the polymeric surface, however, this would be the first report to show that the leachates from the applied concentration of SNAP and Si-Oil intergrated in the tubing is not cytotoxic to the mammalian cells but still very effective in terms of bacterial inhibition and preventing platelet adhesion.

The results demonstrated that not only the leachates not caused any cytotxic respeonse but at the same time also promoted the proliferation of the mouse fibroblast cells. This can be manly due to the cell proliferationg potential of NO that would have released as a result of putting the tubes in contact with cell culture media. **Figure 4.7** shows the cell proliferation capacity of NO-releasing silicone tubes. It was previously shown that SNAP incorporation in the medical grade polymer resulted in no cytotoxicity in a 24 h study *in vitro.*[44,46] This is in line with the recent studies which demonstrated endogenous NO has to be important in mammalian cell proliferation. Ziche et al., reported that NO induces endogenous basic fibroblast growth factor

(bFGF) resulting in upregulation of urokinase-type plasminogen activator (uPA) in coronary venular endothelial cells (CVECs) ultimately resulting in the proliferation of endothelial cells.[59] Another study has shown similar results where endogenous NO was shown to cause an increase in proliferation of endothelial cells from postcapillary venules by promoting DNA synthesis in these cells.[60] However, the current study demonstrated the cell proliferation via NO release from the leachate solution as a result of soaking tubing samples in DMEM medium for 24 h. Theoretically, the NO flux should have been released in the physiological range to show the proliferative response as shown in this study. A further studyis needed to measure the NO flux in the cell culture medium as a result of leachingwhich significantly increased the fibroblast cell proliferation by 60% as compared to control cells without external NO supply ($p < 0.05$).

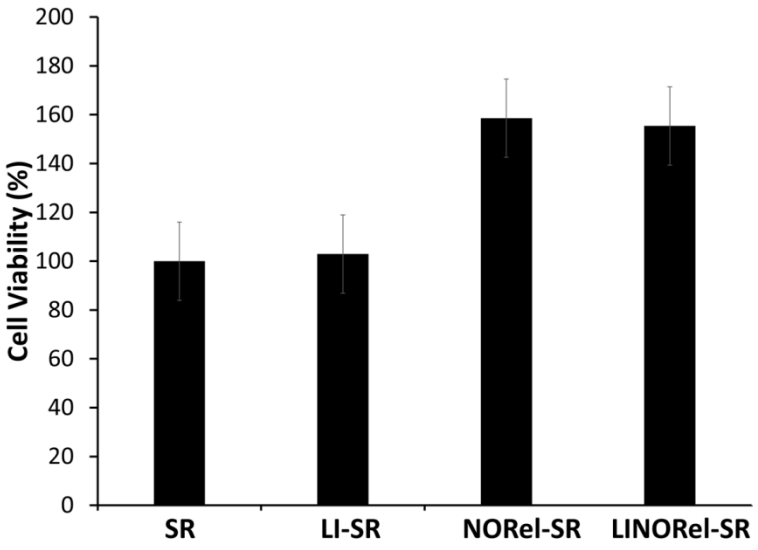


Figure 4.7: Cytocompatbility and cell growth support of various infused SR tubing towards mouse fibroblast cells in 24 h study.

## Conclusion

In this work, the combination of liquid-infused slippery surfaces was combined with NO-releasing capabilities in commercial medical grade silicone rubber tubing through the infusion of silicone oil and the NO donor SNAP. The presence of SNAP in the silicone matrix had no significant negative effects on the slippery nature of the surface, with no significant changes in the swelling ratio or sliding angle over 7 d. However, the infusion of silicone oil assisted in the controlled release of NO due to limiting the hydration of the SR. Silicone tubing infused with SNAP showed a decrease in NO-release from $0.62 \pm 0.09 \times 10^{-10}$ mol $min^{-1}$ $cm^{-2}$ to $0.09 \pm 0.07 \times 10^{-10}$ mol $min^{-1}$ $cm^{-2}$ over the 7 d period, while the LINOrel-SR tubing showed a much more constant release of $0.35 \pm 0.03 \times 10^{-10}$ mol $min^{-1}$ $cm^{-2}$ and $0.42 \pm 0.06 \times 10^{-10}$ mol $min^{-1}$ $cm^{-2}$. The infusion of silicone oil reduced fibrinogen adsorption over a 2 h period for both LI-SR and LINORel-SR tubing. Bacterial adhesion was investigated over a 7 d period using a CDC bioreactor, where $99.3 \pm 1.9\%$ and $88.3 \pm 3.3\%$ reductions in viable cell adhesion were observed for *S. aureus* and *P. aureginosa*, respectively. The combination of SNAP and silicone oil was confirmed to be non-cytotoxic towards mammalian fibroblast cells Instead it resulted in the proliferation of mammalian cells due to the possible presence of NO in the leachouts. Overall, the results suggested that the infusion of SNAP and silicone oil into commercial silicone tubing can potentially increase the biocompatibility for medical applications while preventing infection.

## Experimental Section

All methods were performed in accordance to the University Committee on the Use and Care of Animals, and with university and federal regulations.

*Materials*

*N*-Acetyl-*D*-penicillamine (NAP), sodium chloride, copper chloride, L-cysteine, potassium chloride, sodium phosphate dibasic, potassium phosphate monobasic, ethylenediaminetetraacetic acid (EDTA), tetrahydrofuran (THF), and sulfuric acid were purchased from Sigma-Aldrich (St. Louis, MO). Methanol, hydrochloric acid, silicone oil, and sulfuric acid were obtained from Fisher Scientific (Pittsburgh, PA). Saint-Gobain™ Tygon™ Formula 3350 silicone rubber (SR) tubing was purchased from Fisher Scientific (Pittsburgh, PA). All aqueous solutions were prepared with 18.2 MΩ deionized water using a Milli-Q filter (Millipore Corp., Billerica, MA). Phosphate buffered saline (PBS), pH 7.4, containing 138 mM NaCl, 2.7 mM KCl, 10 mM sodium phosphate, 100 µM EDTA was used for all *in vitro* experiments. Trypsin -EDTA and Dulbecco's modification of Eagle's medium (DMEM) were obtained from Corning (Manassas, VA 20109). The antibiotic Penicillin-Streptomycin (Pen-Strep) and fetal bovine serum (FBS) were purchased from Gibco-Life Technologies (Grand Island NY 14072). The Cell Counting Kit -8 (CCK-8) was obtained from Sigma-Aldrich (St Louis MO 63103). The bacterial strains of *Pseudomonas aeruginosa* (ATCC 27853), *Staphylococcus aureus* (ATCC 6538) and 3T3 mouse fibroblast cell line (ATCC 1658)were originally obtained from American Type Culture Collection (ATCC).

*SNAP Synthesis Protocol*

SNAP was synthesized using a modified version of a previously reported method.[61] Briefly, an equimolar ratio of NAP and sodium nitrite was dissolved in a 1:1 mixture of water and methanol containing 2 M HCl and 2 M $H_2SO_4$. After stirring, the reaction vessel was cooled in an ice bath to precipitate the green SNAP crystals. The crystals were collected by filtration,

rinsed with water, and dried under ambient conditions. The reaction mixture and resulting crystals were protected from light at all times.

*Preparation of NORel and LINORel tubing*

The SNAP swelling solution was prepared by dissolving SNAP in THF using a concentration of 25 mg $mL^{-1}$ as found previously to provide an optimized NO-release.[27] The Saint-Gobain™ Tygon™ SR tubing was soaked in the SNAP swelling solution for 24 h. The tubing was removed, briefly rinsed with PBS, and dried for 48 h under ambient conditions to allow the excess THF to evaporate. After drying, the tubing samples were placed in a 20 mL vial with DI $H_2O$, and placed in a Fisher Scientific 1.9 L sonicating bath for 5 min to remove any crystalized SNAP from the surface of the tubing. The tubing and swelling solutions were protected from light throughout the swelling process. Infusion of silicone oil for LINORel tubing was then acheived through incbuation of NORel SR tubing in silicone oil for 72 h at room temperature, and protected from light.

*Nitric Oxide Release and Total SNAP Loading*

Nitric oxide release from the silicone tubing was measured using a Sievers chemiluminescence Nitric Oxide Analyzer (NOA), model 280i (Boulder, CO). A section of the NORel-SR or LINORel-SR tubing (1 cm) was placed in 4 mL PBS with EDTA buffer at 37 ºC. Nitric oxide purged from the submerging buffer through bubbled nitrogen and was continuously swept from the headspace of the sample cell with a nitrogen sweep gas to the chemiluminescence detection chamber. The nitrogen flow rate was set to 200 mL/min with a chamber pressure of 6 Torr and an oxygen pressure of 6.0 psi. The NO-release from samples is normalized by the surface area using the flux unit ($x10^{-10}$ mol $cm^{-2}$ $min^{-1}$). Both NORel-SR and LINORel -SR samples were incubated at 37°C in 4 mL PBS with EDTA between NO release measurements to

maintain physiological conditions. The buffer was changed daily as to ensure the buffer was not saturated with either SNAP nor silicone oil.

Total loading of SNAP using the swelling process was measured by incubating a small section of the NORel-SR tubing (10-20 mg) in a solution of 50 mM $CuCl_2$ and 10 mM L-cysteine at 37°C.[28] The addition of L-cysteine aids in the catalysis of $Cu^{2+}$ to $Cu^{+}$, which is responsible for the catalytic release of NO from RSNOs such as SNAP.[62] Release rates of NO were then integrated over the duration of the measurement to determine the total NO released.

*Oil swelling*

Swelling and deswelling characteristics of the silicone tubing were investigated. For swelling, silicone tubing and NORel-SR were submerged in silicone oil (Alfa Asar). The mass swelling ratio can be defined as the ratio of the mass of the infused polymer ($M_i$) and the mass of the polymer initially ($M_0$) (equation 1).

$$Swelling\ ratio = \frac{M_i}{M_0} \qquad (1)$$

Deswelling of the oil from the respective tubing was examined through incubation of the swollen tubing in PBS with EDTA at 37°C under mild agitation on a Medicus rocker.

*Sliding angle characterization*

A sliding stage with a digital protractor was used to measure the sliding angle of a 10 µL droplet of water on the surface of each silicone substrate. Tubing samples (ca. 5 cm in length) were cut longitudinally and mounted onto a glass slide to create a flat sheet of silicone. Samples were gently washed with DI $H_20$ and air-dried with nitrogen to remove any dust or contaminants that were initially on the surface. For each measurement, the angle of the sample was slowly increased until the droplet was observed to slide along the surface, and the angle was recorded

using a digital protractor. Each surface was measured at 6 different randomly selected areas. Samples were stored in 50 mL conical tubes containing 40 mL of PBS with EDTA, and maintained at 37°C in a Thermo Fisher water jacketed incubator, under mild agitation on a Medicus blood rocker. The buffer was replaced after each measurement to avoid saturation of the oil in the incubating buffer. Samples were gently blown dry with nitrogen after being removed from the incubating buffer to ensure any water on the surface did not interfere with the sliding angle measurement.

*Leaching of SNAP from NORel-SR and LINORel -SR tubing*

Total leaching of SNAP during the oil swelling and first 24 hours of use were examined at physiological conditions. Nitric oxide releasing tubing were fabricated as described in the Preparation of SNAP Impregnated Tubing section. Phosphate buffered saline (PBS) with 100 mM EDTA was adjusted to a pH of 7.4 was used, where EDTA was used to ensure any metal ions in the PBS solution are neutralized as metallic ions can act as a catalyst for the decomposition of SNAP to release NO. The NO releasing tubing was submerged in 4 mL of PBS-EDTA, and allowed to incubate at 37°C in a Thermo Fisher water jacketed incubator and was protected from light. At each time point, the concentration of SNAP in the PBS-EDTA buffer was measured using a Thermo Scientific Genysis 10S UV-Vis Spectrophotometer and reintroduced to the sample container as to not alter the total incubation volume throughout the measurement period. The SNAP molecule has maxima at 340 and 590 nm, corresponding to the S-NO bond.[18,47,63] Absorbance was recorded for each sample, and concentration was determined using a predetermined calibration curve for known concentrations of SNAP in the PBS/EDTA solution. The pure PBS/EDTA solution was used as a blank for all measurements.

Leaching of SNAP from the silicone tubing was repeated during the oil swelling process as well, to ensure large amounts of SNAP were not lost during the 3-day swelling period. Sections of SNAP impregnated tubing were massed and placed in 4 mL of silicone oil. The absorbance spectra of silicone oil were taken to ensure no interference would be seen between the SNAP maxima and the oil. Pure silicone oil was found to have 0.0 absorbance when PBS-EDTA was used as a blank at 340 nm. Therefore, the same calibration curve of SNAP in PBS-EDTA was used for determining SNAP concentration in the silicone oil. Solubility of SNAP in silicone oil was determined by by adding 10 mg/mL and put on a vortex mixer for 2 min. The suspension was then centrifuged (10 min, 3000 rpm), and a 1 mL sample of the silicone oil was taken for UV vis spectroscopy.

*Adsorption of fibrinogen in vitro*

Levels of protein adhesion were quantified for the fabricated materials using a modified version of a previously reported method.[48] FITC labeled human fibrinogen (13 mg/mL, Molecular Innovations) was diluted to achieve 2 mg $mL^{-1}$ in phosphate buffer solution (pH 7.4). Sections of the various SR tubing were incubated at 37°C for 30 minutes in a 96 well plate, followed by the addition of the stock protein solution to achieve a concentration of 2 mg $mL^{-1}$.[48] During the addition of the stock solution, the tip of the pipette was held below the air-water interface to avoid denaturing of the protein. Following 2 hours of incubation, infinite dilution of the wells' contents was carried out to wash away the bulk and any loosely bound protein from the materials. Samples were then imaged under an EVOS FL fluorescent microscope to qualitatively assess the degree of protein adhesion on the surface. All images were taken at an equal light intensity.

*Assessment of platelet adhesion in vitro*

All protocols pertaining to the use of whole blood and platelets were approved by the Institutional Animal Care and Use Committee. Freshly drawn porcine blood was drawn into a BD 60 mL syringe with 3.4% sodium citrate at a ratio of 9:1 (blood: citrate) through a blind draw.

Immediately following the draw, the anticoagulated blood was centrifuged at 1100 rpm for 12 min using the Eppendorf Centrifuge 5702. The platelet rich plasma (PRP) portion was collected carefully with a pipet as to not disturb the buffy coat. The remaining samples were then spun again at 4000 rpm for 20 min to achieve platelet poor plasma (PPP). Total platelet count in both the PRP and PPP fractions were determined using a hemocytometer (Fisher). The PRP and PPP were combined in a ratio to give a final platelet concentration ca. $2 \times 10^8$ platelets $mL^{-1}$. Calcium chloride ($CaCl_2$) was added to the final platelet solution to achieve a final concentration of 2.5 mM.[48]

Sections of each respective tubing were cut into small sections (0.5 cm long) and placed in a 48 well plate. Approximately 1.5 mL of the calcified PRP was added to each well containing a catheter sample, with one sample per well, and incubated at 37°C for 90 min with mild rocking (25 rpm) on a Medicus Health blood tube rocker. Following the incubation, the wells were infinitely diluted with 0.9% saline.

The degree of platelet adhesion was determined using the lactate dehydrogenase (LDH) released when the adherent platelets were lysed with a Triton-PBS buffer (2% v/v Triton-X-100 in PBS) using a Roche Cytotoxicity Detection Kit (LDH). A calibration curve was constructed using known dilutions of the final PRP, and the platelet adhesion on the various tubing samples was determined from the calibration curve.

*In vitro bacterial adhesion and growth in a continuous flow CDC bioreactor*

The ability of the LINORel-SR tubing to prevent bacterial binding and growth on the polymeric surface was tested *in vitro* in a continuous flow CDC bioreactor against gram-positive (*Staphylococcus aureus*) and gram negative (*Pseudomonas aeruginosa*). The use of CDC bioreactor provides a highly favorable environment for bacterial growth and biofilm formation through a continuous supply of nutrients so that antimicrobial efficacy of LINORel-SR tubing can be tested for a prolonged time interval. In this study, we examined the long-term performance of the SNAP-Si oil and control (without SNAP and/or Si-oil coat) tubing in a 7-day model. A single isolated colony of the bacterial strains was incubated overnight in LB medium for 14 h at 150 rpm at 37 ºC. The optical density (O.D) was measured at 600 nm (OD600) using UV-vis spectrophotometer. All samples (SR, LI-SR, NORel-SR, and LINORel-SR; N=3 each) were sterilized with UV irradiation under a Biosafety Cabinet (BSC) and fitted inside the CDC bioreactor. The CDC bioreactor was sterilized using high pressure saturated steam for 30 min at 121ºC in an autoclave. The CDC bioreactor (working volume 1000 mL) with 400 mL of LB medium (2 g $L^{-1}$) was inoculated with the bacterial culture in a manner that the final OD600 falls in the range of $10^7$-$10^9$ CFU $mL^{-1}$ to simulate the chronic infection conditions. The CDC bioreactor on one end was connected to a feed bottle having a continuous supply of sterile LB medium (2 g $L^{-1}$) and to a sealed container to collect the wash out in a sterile manner on the other end. After 7 days, samples were removed under a BSC and gently rinsed with PBS, pH 7.4 in order to remove any loosely bound bacteria. The rinsed films were then transferred to a 15 mL tube with 2 mL sterile PBS and homogenized for 60 sec using an OmniTip homogenizer.[23] The shear force from the homogenizer tip ensured the transfer of the bound bacterial strains from the tubing to the PBS solution. Thereafter, serial dilution ($10^{-1}$ to $10^{-5}$) were made suing sterile PBS

and bacterial strains were plated on Petri-dishes solid LB-agar medium using an L-spreader. The antimicrobial efficacy of the LINOrel-SR tubing was measured relative to the SR control rubing using equation 2.

$$\%\ Bacterial\ inhibition = \frac{\left(\frac{CFU}{cm^2} in\ control - \frac{CFU}{cm^2} in\ test\right) X100}{\frac{CFU}{cm^2}\ in\ control} \qquad (2)$$

*In vitro cytocompatibility*

The ability of the NORLI-SR tubing to generate any cytotoxic responses was tested on mouse fibroblast cells (ATCC-1658) using cell counting kit-8 (CCK-8) assay in accordance with ISO 10993 standard. The CCK-8 assay is based on the reduction of highly water-soluble tetrazolium salt. WST-8 [2-(2-methoxy-4-nitrophenyl)-3-(4-nitrophenyl)-5-(2,4-disulfophenyl)-2H-tetrazolium monosodium salt] by dehydrogenases present in viable mammalian cells to give formazan (an orange color product) in direct proportion to the number of viable cells when detected at a wavelength 450 nm. Mouse fibroblast cells were cultured in a humidified atmosphere with 5% $CO_2$ at 37ºC in 75 $cm^2$ T-flask containing premade DMEM medium (Thermo Fischer) with 10% fetal bovine serum (FBS) and 1% penicillin-streptomycin. After the confluency reached 80%-90%, cells were removed from the flask using 0.18% trypsin and 5 mM EDTA, counted using bromphenol blue in a hemocytometer and 100 µL of 5000 cells $mL^{-1}$ were seeded in 96 well plates. The leachates from the each sample (control SR, NORel-SR, LI-SR and LINORel-SR) was obtained by soaking 10 mg of tubing sample in 10 mL DMEM medium for 24 h at 37 ºC in the amber vial (N=5 each). To each of the wells containing fibroblast cells, 10 µL of the CCK-8 solution was added and cells with CCK-8 dye were incubated for 3 h. Negative controls containing 5000 cells/ml were grown in 5 separate wells for reference to compare with

the cells treated with leachates. Absorbance values were measured at 450 nm and the relative cell viability of mammalian cells exposed to the respective leachates were compared. 100 µL of the DMEM medium without cells was added in 5 of the wells and used as blank to adjust the background interference from DMEM media. Results were reported as percentage cell viability difference between the leachate treated cells relative to the negative control (without leachate treatment) using equation 3.

$$\%\ Cell\ Viability = \frac{Absorbance\ of\ the\ test\ samples}{Absorbance\ of\ the\ control\ samples} \times 100 \qquad (3)$$

*Statistical analysis*

Data is reported as the mean ± standard deviation. Statistical significance was determined using a two-tailed t-test assuming unequal variances with $\alpha = 0.05$. All measurements were conducted with N=3 samples unless otherwise stated.

**References**


1. E. J. Brisbois, H. Handa and M. E. Meyerhoff, in Advanced Polymers in Medicine, Springer, 2015, pp. 481-511.
2. A. Vertes, V. Hitchins and K. S. Phillips, Analytical chemistry, 2012, 84, 3858-3866.
3. N. P. O'Grady, M. Alexander, E. P. Dellinger, et al., Clinical infectious diseases, 2002, 35, 1281-1307.
4. M. L. Paden, S. A. Conrad, P. T. Rycus, et al., ASAIO journal, 2013, 59, 202-210.
5. R. S. Smith, Z. Zhang, M. Bouchard, et al., Science translational medicine, 2012, 4, 153ra132-153ra132.
6. S. Zheng, Q. Yang and B. Mi, Applied Surface Science, 2016, 363, 619-626.
7. K. Kovach, M. LaBarbera, M. Moyer, et al., Lab on a Chip, 2015.

8. K. M. Kovach, J. R. Capadona, A. Sen Gupta, et al., Journal of Biomedical Materials Research Part A, 2014.
9. N. A. Peppas and R. Langer, Science, 1994, 263, 1715-1720.
10. O. Larm, R. Larsson and P. Olsson, Biomaterials, medical devices, and artificial organs, 1983, 11, 161-173.
11. D. C. Leslie, A. Waterhouse, J. B. Berthet, et al., Nature biotechnology, 2014, 32, 1134-1140.
12. R. E. Cronin and R. F. Reilly, 2010.
13. G. Annich, Journal of Thrombosis and Haemostasis, 2015, 13.
14. G. Shepherd, P. Mohorn, K. Yacoub, et al., Annals of Pharmacotherapy, 2012, 46, 169-175.
15. Y.-M. Chen, A.-P. Dai, Y. Shi, et al., International Journal of Infectious Diseases, 2014, 29, 279-286.
16. J. Pant, M. Goudie, E. Brisbois, et al., in Advances in Polyurethane Biomaterials, Elsevier, 2016, pp. 471-550.
17. Y. Hou, A. Janczuk and P. Wang, Current Pharmaceutical Design, 1999, 5, 417-442.
18. E. J. Brisbois, H. Handa, T. C. Major, et al., Biomaterials, 2013, 34, 6957-6966.
19. J. M. Joslin, S. M. Lantvit and M. M. Reynolds, ACS applied materials & interfaces, 2013, 5, 9285-9294.
20. D. A. Riccio, P. N. Coneski, S. P. Nichols, et al., ACS applied materials & interfaces, 2012, 4, 796-804.
21. M. M. Reynolds, J. A. Hrabie, B. K. Oh, et al., Biomacromolecules, 2006, 7, 987-994.
22. E. M. Hetrick and M. H. Schoenfisch, Biomaterials, 2007, 28, 1948-1956.

23. E. J. Brisbois, T. C. Major, M. J. Goudie, et al., Acta Biomaterialia, 2016.

24. E. J. Brisbois, R. P. Davis, A. M. Jones, et al., Journal of Materials Chemistry B, 2015.

25. G. E. Gierke, M. Nielsen and M. C. Frost, Science and Technology of Advanced Materials, 2011, 12, 055007.

26. P. N. Coneski, K. S. Rao and M. H. Schoenfisch, Biomacromolecules, 2010, 11, 3208.

27. E. J. Brisbois, T. C. Major, M. J. Goudie, et al., Acta biomaterialia, 2016, 37, 111-119.

28. A. Colletta, J. Wu, Y. Wo, et al., ACS biomaterials science & engineering, 2015, 1, 416-424.

29. S. M. Lantvit, B. J. Barrett and M. M. Reynolds, Journal of Biomedical Materials Research Part A, 2013, 101, 3201-3210.

30. G. W. Charville, E. M. Hetrick, C. B. Geer, et al., Biomaterials, 2008, 29, 4039-4044.

31. M. J. Goudie, B. M. Brainard, C. W. Schmiedt, et al., Journal of Biomedical Materials Research Part A, 2016.

32. J. W. Costerton, Z. Lewandowski, D. E. Caldwell, et al., Annual Reviews in Microbiology, 1995, 49, 711-745.

33. N. MacCallum, C. Howell, P. Kim, et al., ACS Biomaterials Science & Engineering, 2014, 1, 43-51.

34. T.-S. Wong, S. H. Kang, S. K. Tang, et al., Nature, 2011, 477, 443-447.

35. S. Bondurant, V. Ernster and R. Herdman, Journal, 1999.

36. R. C. Hartmann, C. L. Conley and E. L. Poole, Journal of Clinical Investigation, 1952, 31, 685.

37. U. Manna, N. Raman, M. A. Welsh, et al., Advanced Functional Materials, 2016, 26, 3599-3611.

38. M. A. De Groote and F. C. Fang, Clinical Infectious Diseases, 1995, 21, S162-S165.

39. M. L. Jones, J. G. Ganopolsky, A. Labbé, et al., Applied microbiology and biotechnology, 2010, 88, 401-407.

40. D. O. Schairer, L. R. Martinez, K. Blecher, et al., Virulence, 2012, 3, 62-67.

41. B. J. Privett, S. T. Nutz and M. H. Schoenfisch, Biofouling, 2010, 26, 973-983.

42. L. Dijkshoorn, A. Nemec and H. Seifert, Nature Reviews Microbiology, 2007, 5, 939-951.

43. R. H. Sunenshine, M.-O. Wright, L. L. Maragakis, et al., Emerg Infect Dis, 2007, 13, 97-103.

44. M. J. Goudie, E. J. Brisbois, J. Pant, et al., International Journal of Polymeric Materials and Polymeric Biomaterials, 2016, 65, 769-778.

45. Y. Wo, Z. Li, E. J. Brisbois, et al., ACS applied materials & interfaces, 2015.

46. J. Pant, M. J. Goudie, S. P. Hopkins, et al., ACS Applied Materials & Interfaces, 2017.

47. M. C. Frost and M. E. Meyerhoff, Journal of the American Chemical Society, 2004, 126, 1348-1349.

48. B. Sivaraman and R. A. Latour, Biomaterials, 2010, 31, 832-839.

49. R. Simon-Walker, R. Romero, J. M. Staver, et al., ACS Biomaterials Science & Engineering, 2016.

50. F. C. Fang, Journal of Clinical Investigation, 1997, 99, 2818-2825.

51. C. L. Abad and N. Safdar, Infectious Disease Special Edition, 2011, 14.

52. E. J. Brisbois, J. Bayliss, J. Wu, et al., Acta Biomater., 2014, 10, 4136-4142.

53. J. Sundaram, J. Pant, M. J. Goudie, et al., Journal of agricultural and food chemistry, 2016.

54. M. Feelisch, Naunyn-Schmiedeberg's archives of pharmacology, 1998, 358, 113-122.

55. S. M. Deupree, B. J. Privett, C. J. Backlund, et al., Molecular pharmaceutics, 2010, 7, 2289.

56. B. V. Worley, D. L. Slomberg and M. H. Schoenfisch, Bioconjugate chemistry, 2014, 25, 918-927.

57. J. Pant, J. Gao, M. J. Goudie, et al., Acta Biomaterialia, 2017.

58. H. Ren, J. Wu, A. Colletta, et al., Frontiers in Microbiology, 2016, 7.

59. M. Ziche, A. Parenti, F. Ledda, et al., Circulation Research, 1997, 80, 845-852.

60. M. Ziche, L. Morbidelli, E. Masini, et al., Biochemical and biophysical research communications, 1993, 192, 1198-1203.

61. I. Chipinda and R. H. Simoyi, Journal of Physical Chemistry B, 2006, 110, 5052-5061.

62. A. Dicks, H. Swift, D. Williams, et al., Journal of the Chemical Society, Perkin Transactions 2, 1996, 481-487.

63. S. l. M. Shishido, A. B. Seabra, W. Loh, et al., Biomaterials, 2003, 24, 3543-3553.

# CHAPTER 5

# SURFACE TETHERED NITRIC OXIDE DONOR FOR DUAL-FUNCTION NON-FOULING AND BACTERICIDAL SURFACES[4]

[4] Goudie, M.J., Singha, P., Hopkins, S.P., Handa, H. To be submitted to *Advanced Materials*.

**Abstract**

Two major challenges faced by medical devices are thrombus formation and infection. In this work, surface tethered nitric oxide (NO) releasing molecules have been presented as a solution to combat infection and thrombosis with a robust release capacity of ca. 1 month while simultaneously improving the non-fouling nature of the material by preventing protein, bacteria, and platelet adhesion. Nitric oxide's potent bactericidal function has been implemented by a facile surface crosslinking method to fabricate a triple action surface - **s**urface **im**mobilized **S**-nitroso-*N*-acetylpenicillamine (SIM-S). Comparison of NO load amongst the unbranched and branched SIM-S materials (unbranched SIM-S1, branched: SIM-S2 and SIM-S4) is shown through the NO release kinetics over time and the cumulative NO release. Biological characterization is done using fibrinogen protein and *Staphylococcus aureus*. The highest NO releasing material, SIM-S2, is able to reduce protein adhesion by 65.8 ± 8.9% when compared to unbranched SIM-S1. SIM-S2 demonstrates a 99.99% (i.e. ~4 log) reduction for *Staphylococcus aureus* over 24 h. The various functionalized surfaces were also shown to significantly reduce platelet adhesion *in vitro*, for both NO releasing and non-NO releasing surfaces (up to 89.1 ± 0.9%). Hence, this study demonstrates the importance to fabricate more of such materials that retain antifouling characteristics even after the bactericidal agent load is exhausted.

**Introduction**

Fouling of materials used in medical devices leads to increased risk of infection and device failure, and is the result of the adherence of proteins, bacteria, or thrombus formation. These complications can lead to large increases in healthcare costs and mortality.[1, 2] While heparin is often administered to aid in the prevention of thrombus formation, its prolonged use can result in morbidity and mortality while providing no activity to prevent infection.[3] In

addition to this, the increasing use of antibiotics has led to the development of resistant strains of bacteria, which can be attributed to the high dosages required to be effective against established biofilms.[4] The degree that bacteria or platelets can bind to the surface of these materials can be highly influenced by the ability to prevent protein adhesion to the materials surface.[5-7] A number of strategies have been used to develop adhesion resistant materials, such as increasing the hydrophilicity,[5, 8] super hydrophobic or patterned surfaces,[9-12] liquid-infused materials,[13, 14] or grafting of polymer brushes.[15-22] While these materials are suitable for decreasing the adhesion of protein and bacteria through "passive" mechanisms, they provide no "active" mechanism to prevent platelet activation and adhesion, or any bactericidal activity towards bacteria that have adhered, which lead to proliferation and biofilm formation.

Nitric oxide (NO) is an endogenous, gaseous, free radical that is produced naturally by macrophages and by endothelial cells lining the vascular walls, and is involved in various biological processes, such as preventing platelet activation and adhesion, while also being a potent, broad spectrum bactericidal agent.[23] To take advantage of these properties, NO donors (e.g. s-nitrosothiols or diazeniumdiolates) have been developed to allow for the storage and localized delivery of NO, and are particularly advantageous for polymeric materials typically used for medical devices, such as polyurethanes, silicones, or polyvinyl chloride.[24, 25] The addition of these donors at various levels also provides a simple method for controlling the level of NO that is delivered from the materials.[26] Materials releasing NO have been shown to significantly reduce thrombus formation in both extracorporeal-circuit and vascular catheter models, and have been shown to provide significant reductions in bacteria during long term catheterization.[2, 27, 28]

In this work, we demonstrate the ability of a material to not only offer an increase in steric ability to prevent bacterial and protein adhesion through a passive mechanism but also utilize the active biocidal mechanism of NO. In addition to combining these mechanisms, the antifouling capability of the material is retained after all NO has been released from the surface, making it attractive for long term applications. Specifically, this is done by the immobilization of the NO donor precursor *N*-acetyl-D-penicillamine (NAP) to silicone surfaces using an alkylamine spacer (**Figure 5.1**). As shown in figure 5.1, increasing the grafting density of free amines was done through branching of the initial spacer. Following immobilization, the grafted donor is nitrosated to its NO-rich form *S*-nitroso-*N*-acetyl-D-penicillamine (SNAP). SIM-N1 and SIM-S1 correspond to unbranched polymers that are non-nitrosated (product of C in figure 5.1) and nitrosated (product of D in figure 5.1), respectively. SIM-N2 and SIM-S2 correspond to branched polymers that are non-nitrosated (product of G in figure 1) and nitrosated (product of H on figure 5.1), respectively. Finally, SIM-N4 and SIM-S4 correspond to branched polymers that are non-nitrosated (product of K in figure 5.1) and nitrosated (product of L in figure 5.1), respectively. From here on, these will be referred to as is for all the experiments, in addition to the unmodified silicone surface which will be considered as the control.

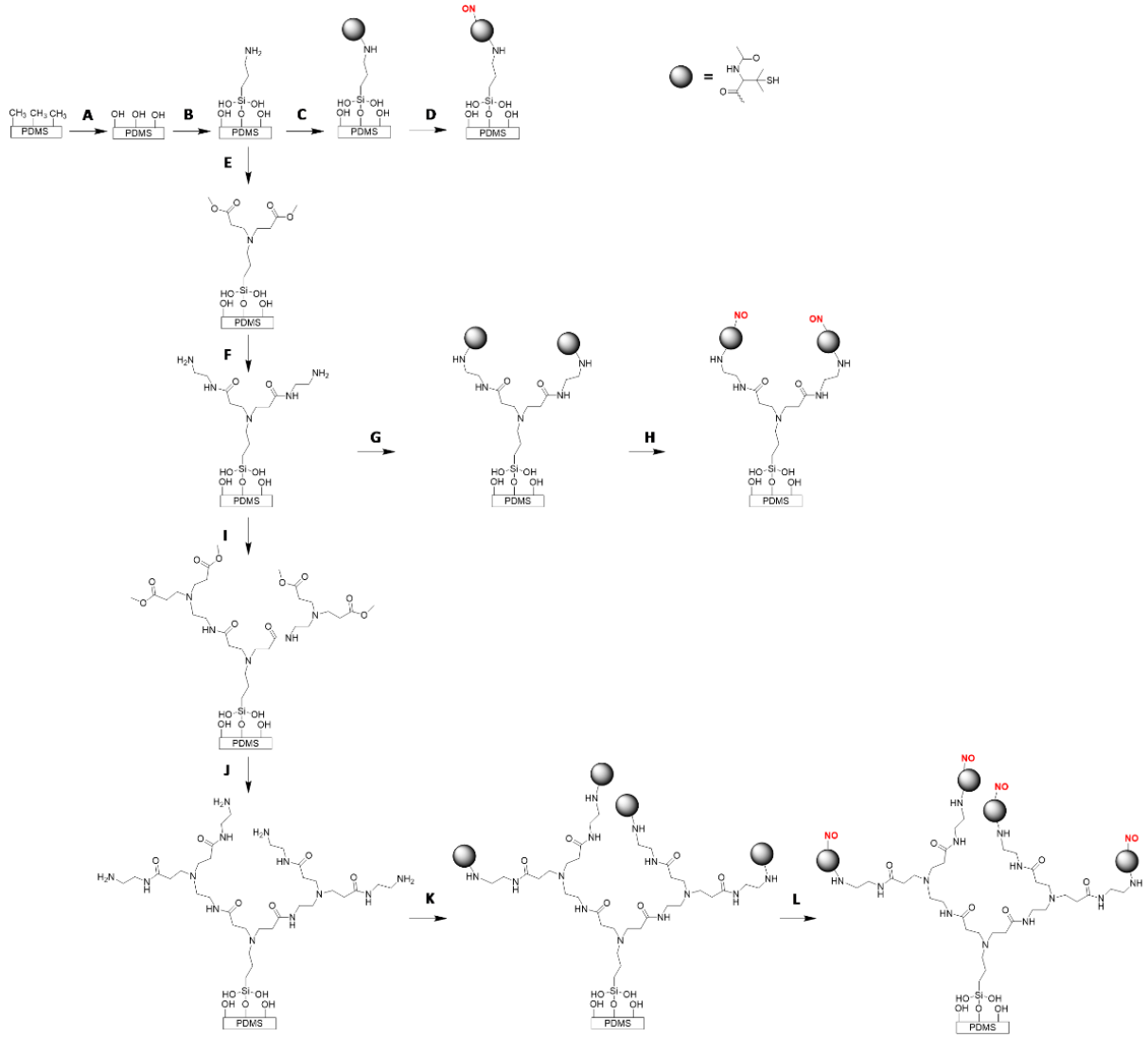


Figure 5.1: Preparation of PDMS surface bound SNAP with NO releasing capabilities A) Functionalization of PDMS surface with hydroxyl groups by submerging it in 50:50 ratio of 13 N HCl : 30 wt% $H_2O_2$ in $H_2O$ B) Treatment with APTMES for amine functionalization C) Ring-opening reaction of NAP-thiolactone with free amine groups to produce free thiol groups D) Nitrosation of thiol groups with tert-butyl nitrite E) branching of primary amine via reaction with methyl acrylate F) Amine functionalization of branched site using ethylene diamine

**Results**

As seen in our design strategy, we varied the NO-load and release capacity of the materials by branching of the initial akyl spacer to increase the number of free amines. This variation in NO-load and release capacity was measured by using a chemiluminescence nitric oxide analyzer (NOA). NOA is the gold standard for measurement of NO flux from materials and is a very efficient and sensitive instrument which can analyze NO release down to ppb.[29] One of the theoretical expectations was to see increasing NO-load and release measurements with an increase in branching. However, as seen in **Figure 5.2**, NO release measurements were significantly higher for SIMS-2 (cumulative release: $43442.53 \times 10^{-10}$ mol cm$^{-2}$) when compared to SIM-S4 (cumulative release: $23319.98 \times 10^{-10}$ mol cm$^{-2}$) over the 25-d period. There could be two possible explanations for this: steric hindrance in case of higher branching and hence NAP thiolactone was not able to completely bind to the amine groups, or/and more branching increases the probability of chain interactions within the polymer before the free amine groups can react with NAP thiolactone, as supported by the measurement of free amines via Ellman's assay (**Figure 5.3**). Therefore, from this study we were able to conclude that branching increasingly doesn't necessarily increase NO-load or release and we were also able to design a surface that can release NO up to 25 days at endogenous flux levels. This increasing branching method is a novel technique to increase NO release characteristics much like the function of metal ions when added to NO releasing polymers. However, this material proves to be more advantageous as it also imparts antifouling characteristics to the material as seen in the following studies conducted. To ensure NO release was not from the bulk material due to swelling of the diamine during the reaction period, control measurements were used on samples using the same reaction scheme without immobilization of the aminosilane. Due to the large decrease in NO

release capabilities, the SIM-S4 and SIM-N4 were not evaluated for their biological activity and non-fouling characteristics.

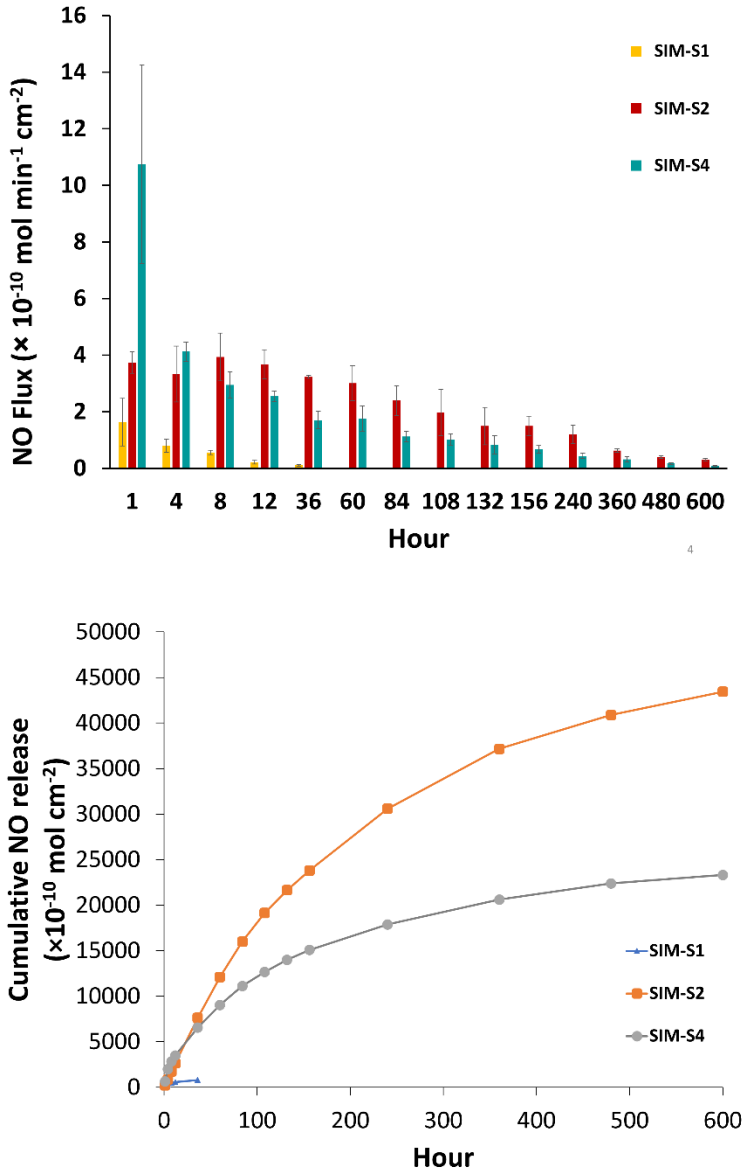


Figure 5.2: Nitric oxide release characteristics over 25 d for various SIM-S surface configurations.

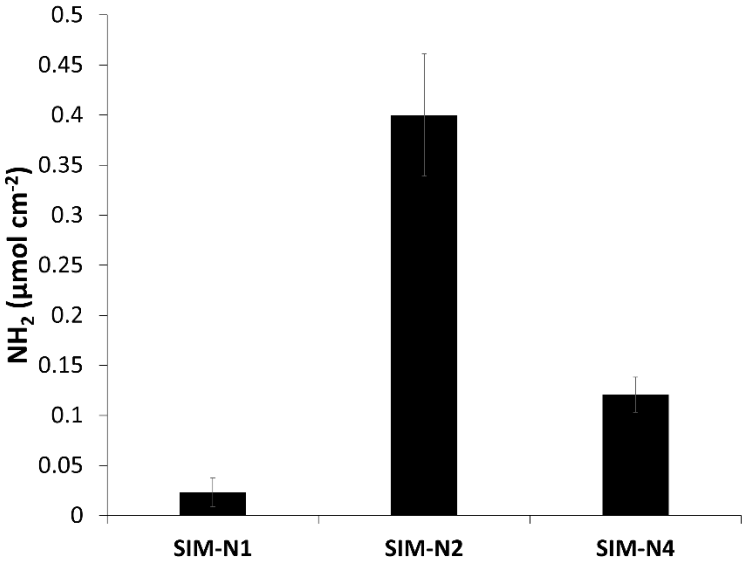


Figure 5.3: Quantification of primary amine grafting density on various branching configurations.

One common method for assessing the fouling of materials *in vitro* is to examine the ability of the material to resist non-specific protein adhesion, or if intended for blood contacting applications more specifically, fibrinogen (Fg). The adsorption of Fg to the material surface greatly aids in the ability for activated platelets or bacteria to bind to the surface, leading to higher risks of thrombus formation or infection.[6] While the orientation of Fg adsorption has been shown to determine the degree of platelet adhesion, limiting protein adhesion regardless of orientation is generally considered to be an improvement in the hemocompatibility of a material.[7] Developing NO-releasing materials that can reduce protein adsorption could provide drastic improvements in the overall hemocompatibility and antibacterial nature of these materials. To examine if the surface immobilized NO donors (both nitrosated and non-nitrosated) can provide a decrease in protein adhesion observed on NO-releasing materials, 2 h exposure to FITC-labeled fibrinogen (2 mg $mL^{-1}$) was conducted at 37°C **(Figure 5.4)**. While minimal changes in contact angle were observed, increasing the branched nature of the surface grafted NAP groups

decreased the degree of Fg adsorption, and is hypothesized to result from increases in steric hindrance. However, altering the chemistry of the linkages to the amine functionalized surface could greatly increase the non-fouling ability of these materials. Moreover, the optimization of immobilization of NAP to the free amines may not be trivial as the solvent-surface interaction will be critical for high conversion, as was observed above in the Ellman's/nitric oxide release comparisons. Overall, reductions in protein adsorption were observed to reach 65.8 ± 8.9% for SIM-S2 when compared to the unmodified SR (**Table 5.1**). It is also interesting to note that the release of NO from the surface had no significant effect on the amount of adsorbed Fg.

Table 5.1: Ability of various surface modified PDMS substrates to reduce nonspecific protein adsorption over 2 h.

| | **SR** | **SIM-N1** | **SIM-S1** | **SIM-N2** | **SIM-S2** |
|---|---|---|---|---|---|
| Fg Adsorption (μg $cm^{-2}$) | 72.4 ± 16.4 | 74.5 ± 13.7 | 51.0 ± 15.5 | 33.0 ± 11.0 | 24.7 ± 3.2 |
| Reduction (%) | - | - | 29.6 ± 26.7 | 54.4 ± 18.3 | 65.8 ± 8.9 |
| p value vs control | - | NS | 0.024 | $1.94 \times 10^{-4}$ | $6.59 \times 10^{-5}$ |
| p value vs SIM-S2 | $6.59 \times 10^{-5}$ | $1.43 \times 10^{-5}$ | 0.027 | NS | - |

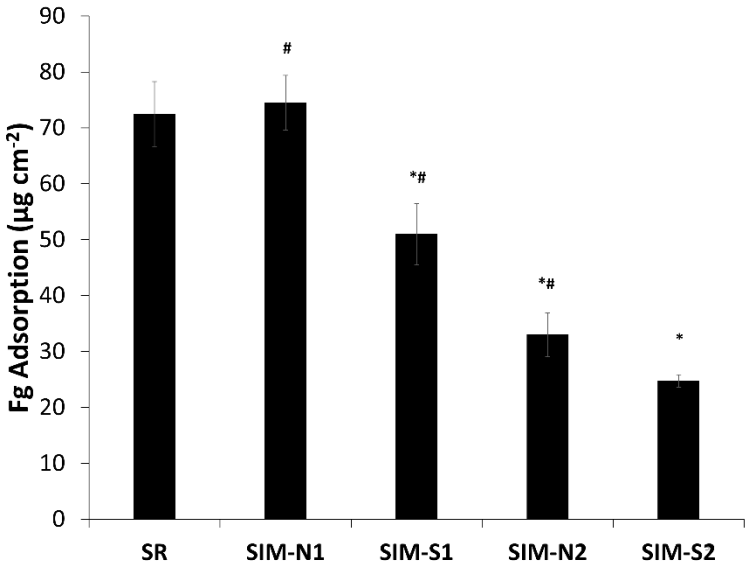

Figure 5.4: Adsorption of fibrinogen to modified PDMS surfaces over a 2 h period. Values are expressed as mean ± standard error. Measurements were conducted using N=8 per group. * - significantly different compared to unmodified SR. # - significantly different compared to SIM-S2 configuration.

Bacterial adhesion, which often results in biofilm formation, is a prevalent issue in moist and humid environment, which is found in implanted devices. The basic nutrients important for bacterial growth may be resourced from the device material, bodily proteins that attach post-implantation or other bodily macromolecular contaminants that adhere to the surface of the device. Antimicrobial efficacy of the designed test samples was compared to the control samples to confirm their superior bactericidal and bacterial repulsion properties. The samples were soaked in bacterial solutions containing ~$10^{7}$-$10^{8}$ CFU $mL^{-1}$ of *S. aureus* or *P. aeruginosa*, which are two of the most commonly found nosocomial infection bacteria at 37°C for 24 h.[13, 30] These infections are most commonly associated with cardiac devices, intravascular catheters and urinary catheters among other prosthetic devices. This high prevalence of *S. aureus* along with its known affinity to proteins [31, 32] that foul medical devices has made it a very important pathogen studied for antimicrobial efficacy of medical device materials. Keeping this information in mind, bacterial adhesion study of the SIM-S polymer developed was done with *S. aureus*. As mentioned in the introduction of the paper, our theoretical expectation was that the NO molecules would actively kill bacteria and the immobilized structure was expected to repel proteins and enhance the biocompatibility of the material even after all the NO load was exhausted. The antimicrobial efficacy of the designed test samples was clearly observed after 24 hours of incubation, the crucial time for initiation of bacterial infection. The CFU $cm^{-2}$ of *S. aureus* adhered to each material is shown on **Table 5.2**. SIM-S2 showed a bactericidal efficiency

of 99.91 ± 0.06 % (**Figure 5.5**) compared to the control samples where a growth of ~$10^8$ CFU $cm^{-2}$ was observed. This reduction is higher compared to samples with only NAP thiolactone functionalization (SIM-N1= 82.14 ± 22.20 % and SIM-N2= 96.86 ± 0.49 %) and SIM-S1 (85.71 ± 24.74 %). It can also be concluded from the results that NAP thiolactone functionalized surfaces alone could only reduce bacteria adhesion because it cannot kill bacteria. However, because NO is not a contact active antimicrobial but a biocide that can travel to the bacteria's location and kill it before the bacteria even comes in contact with the substrate, NO by itself can also reduce bacterial adhesion significantly. In summary, the synergistic effect of the modifiable NO-release kinetics from SR's surface and prevention of protein and/or bacterial adhesion due to the surface chemistry can help significantly reduce undesired clinical consequences post-implantation of a medical device.

Table 5.2: Viable bacterial adhesion on various SIM surfaces after 24 h incubation.

| | **SR** | **SIM-N1** | **SIM-S1** | **SIM-N2** | **SIM-S2** |
|---|---|---|---|---|---|
| CFU of *S. aureus* $cm^{-2}$ | 4.63 x$10^7$ | 8.58 x$10^4$ | 7.15 x$10^4$ | 2.14 x$10^5$ | 3.89 x$10^2$ |
| Reduction (%) | - | 82.14 ± 22.20 | 85.71 ± 24.74 | 96.86 ± 0.49 | 99.99 ± .002 |

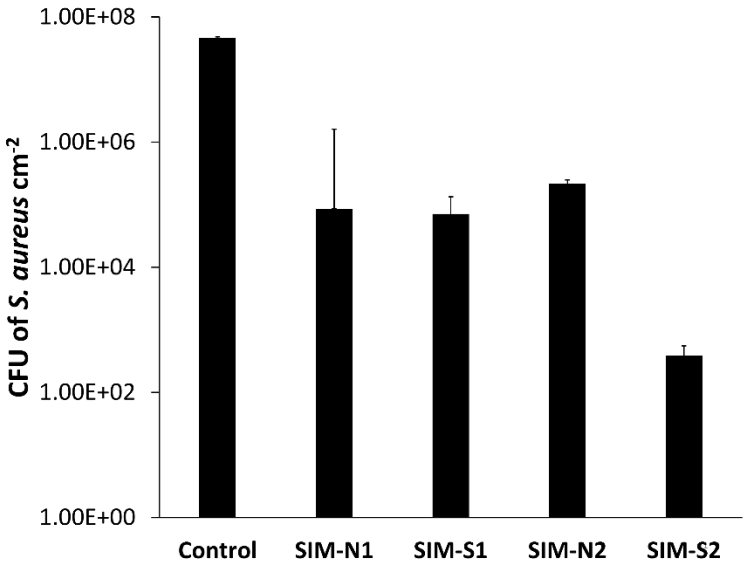


Figure 5.5: Relative adhesion of *S. aureus* on various SIM surfaces after 24 h exposure.

Platelet activation and adhesion are important considerations when determining the hemocompatibility of materials. Upon activation, platelets release several coagulation agonists such as phospholipase $A_2$ (which is then converted into thromboxane $A_2$), furthering platelet activation and the coagulation cascade and increasing thrombin generation.[33] One key predecessor of platelet activation is the adsorption of fibrinogen to the materials surface, where changes in the protein confirmation allows for binding to the platelets Gp IIb/IIIa receptors. Therefore, reducing protein adhesion alone can act as a mechanism to reduce platelet activation. The aim of this study was to confirm that while NO releasing materials have been shown to significantly reduce platelet adhesion, the functionality of the modified surface is not lost after all the loaded NO has been released. In fact, small molecules with free thiol groups (similar to NAP) have been shown to provide potent thrombolytic effects when administered systemically by binding to von Willebrand factor crosslinks of adhered platelets in arterial thrombi.[34] Both nitrosated and non-nitrosated surfaces were incubated in porcine platelet rich plasma for 90 min at 37°C, where platelet adhesion was then determined using an lactate dehydrogenase (LDH)

assay. The degree of platelet adhesion for all materials is shown in **Figure 5.6**. Each variation of the surface modifications was able to provide significant reductions in platelet adhesion when compared to unmodified SR controls (**Table 5.3**). The SIM-N1 and SIM-S2 modifications provided the highest reductions, but were not statistically significant when compared to each other (p value > 0.5). However, as the brush size increased from the SIM-N1 to the SIM-N2 configuration, the ability to prevent adhesion begins to decrease ($p = 0.001$). We believe this may stem from the chemical structure of the methacrylate and diamine linkages, where the composition of these may be varied in future studies to provide more hydrophilic surface and possibly allow for further reduction in protein adhesion as the degree of polymerization at the surface increases. While the SIM-S2 configuration did not provide significant reductions in platelet adhesion when compared to SIM-N1 or SIM-S1, the significant increase in NO release can provide increased bactericidal activity for extended durations.

Table 5.3: Efficacy of various SIM surfaces at reducing platelet adhesion over a 2 h period.

| | **SR** | **SIM-N1** | **SIM-S1** | **SIM-N2** | **SIM-S2** |
|---|---|---|---|---|---|
| Platelets $cm^{-2}$ ($\times 10^6$) | 13.5 ± 0.4 | 1.5 ± 0.1 | 2.8 ± 0.1 | 3.6 ± 0.2 | 1.6 ± 0.1 |
| Reduction (%) | - | 89.1 ± 0.9 | 79.1 ± 1.0 | 73.4 ± 1.3 | 87.7 ± 0.7 |
| p value ($\times 10^{-6}$) | - | 0.1 | 1.7 | 0.5 | 0.2 |

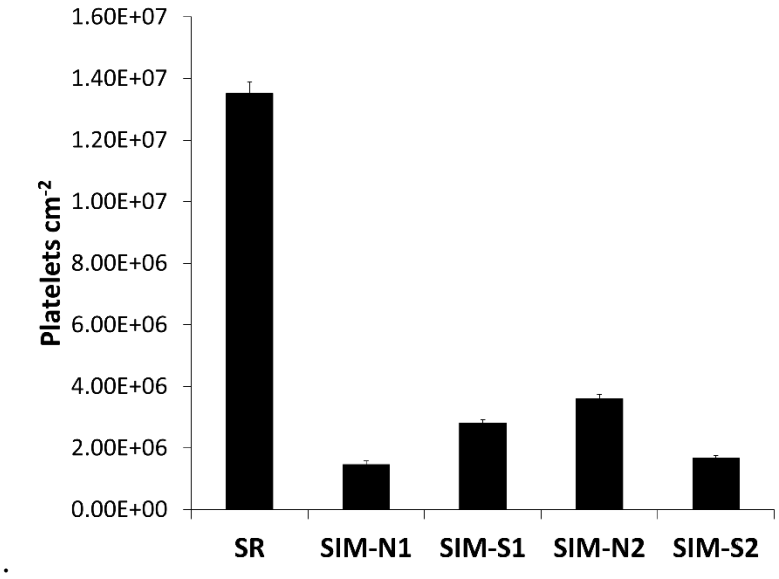


Figure 5.6: Reduction in platelet adhesion over 90 min period for NO releasing and non-NO releasing substrates.

**Conclusion**

In summary, we have presented a facile method to attach various amounts of the nitric oxide releasing donor, SNAP to any polymer material for provide both bactericidal/antiplatelet activity while adding a non-fouling nature to the material surface. This method will be highly applicable for biomedical device materials that are prone to infections and thrombosis related failures, and can easily be coupled with existing NO-releasing polymers. The SIM-S2 configuration was successful in releasing NO at relevant levels for 25 d. Both NO releasing and non-NO releasing surface treatments reduced protein adhesion (~66%), platelet adhesion (88%), and bacterial adhesion (99%) *in vitro*.

## Experimental Section

### *Materials*

*N*-Acetyl-*D*-penicillamine (NAP), sodium chloride, potassium chloride, sodium phosphate dibasic, potassium phosphate monobasic, phosphate buffered saline (PBS, pH 7.4 at 25°C), ethylenediaminetetraacetic acid (EDTA), tetrahydrofuran (THF), tert-butyl nitrite, and sulfuric acid were purchased from Sigma-Aldrich (St. Louis, MO). Aminopropyl trimethoxy silane was purchased from Gelest. All silicone substrates were fabricated with polydimethylsiloxane Sylgard 184 (Dow Corning). Methanol, hydrochloric acid, and sulfuric acid were obtained from Fisher Scientific (Pittsburgh, PA). All aqueous solutions were prepared with 18.2 MΩ deionized water using a Milli-Q filter (Millipore Corp., Billerica, MA). Trypsin-EDTA and Dulbecco's modification of Eagle's medium (DMEM) were obtained from Corning (Manassas, VA 20109). The antibiotic Penicillin-Streptomycin (Pen-Strep) and fetal bovine serum (FBS) were purchased from Gibco-Life Technologies (Grand Island NY 14072). The Cell Counting Kit -8 (CCK-8) was obtained from Sigma-Aldrich (St Louis MO 63103). The bacterial strains were originally obtained from American Type Culture Collection (ATCC): *Pseudomonas aeruginosa* (ATCC 27853), *Staphylococcus aureus* (ATCC 5538). Luria Agar (LA), Miller and Luria broth (LB), Lennox were purchased from Fischer BioReagents (Fair Lawn, NJ).

### *Synthesis of SIM material*

Silicone films were first fabricated by mixing Sylgard 184 base to curing agent (ratio of 10:1). The solution was cast into Teflon molds and placed under vacuum for degassing. The casted solution was then placed in an oven (80°C, 90 min) for curing. To create a hydroxyl group functionalized surface, the silicone films were submerged in a mixture of 13 N HCl : 30 wt.%

$H_2O_2$ (50:50) in $H_2O$ under mild agitation (15 min). The surfaces were then rinsed with DI $H_2O$ and dried under vacuum. The amine functionalization was then achieved by submerging the hydroxyl-functionalized surfaces in 5 wt.% APTMES in extra dry acetone for 2h. Films were then rinsed with extra dry acetone to remove any non-covalently attached silane from the surface, and vacuum dried for 24h. Branching of the immobilized moieties was achieved through incubation of the amine functionalized surface in 2:1 (v/v) methanol:methyl acrylate (24h) followed by 2:1 (v/v) methanol: ethylenediamine (24h) as shown in **Figure 5.1**. Samples were rinsed twice with methanol (20 mL) between incubating solutions. Amine-functionalized surfaces were then submerged in 10 mg $mL^{-1}$ NAP-thiolactone in toluene for 24h, allowing for the ring opening reaction of thiolactone to bind to free amines. The samples were then air-dried for 5h to completely remove any residual solvent. Nitrosation of the immobilized NAP was achieved by incubation in neat tert-Butyl nitrite for 2h. The resultant SIMS samples were stored at -20°C for further experiments.

*Contact angle and FTIR analysis*

Surface properties and proof of attachment of nitric oxide donors to silicone surfaces was analyzed using contact angle measurements and FTIR. Static contact angle was measured using Krüss DA 100 drop shape analyzer. A 3 µL droplet of water was placed on various silicone films, and the average of left and right contact angles were measured via the Krüss software.

*Free Amine Quantification*

Quantification of APTMES attachment to the surface of the PDMS was done using an ATTO-TAG (3-2-(furoyl quinoline-2-carboxaldehyde)) (FQ) derivatization kit. Each primary

amine forms a conjugate with the FQ reagent which can then be fluorescently detected. Fluorescent count was measured using a Biotek Synergy microplate reader (Winooski, VT). The tested samples of APTMES functionalized PDMS were first carefully measured before being placed in a solution containing 15 µL of 10 mM potassium cyanide (KCN), 25 µL of 0.01 M PBS (pH = 7.4), and 10 µL of 10 mM FQ solution (in methanol). The samples were then protected from light and allowed to react for 1h. The solutions containing the samples were then gently agitated to ensure all of the florescent product is removed from the surface. The sample pieces were then discarded and the solutions with the fluorescent product were placed in a 96-well plate to be measured at excitation and emission wavelengths of 480 nm and 590 nm, respectively. Calibration curves were done using prepared using glycine to directly relate the fluorescent count with primary amine concentration.

*Sulfhydryl Group Quantification*

The covalent attachment of NAP-thiolactone can be directly related to the amount of free sulfhydryl groups on the surface of the PDMS. Measurement of these functional groups was done using Ellman's assay, which reacts 5,5'-dithio-*bis*-(2-nitrobenzoic acid) (DTNB) with free sulfhydryl groups to form conjugated disulfide and 2-nitro-5-thiobenzoic acid (TNB). While in solution, TNB's extinction coefficient has been recorded to be $14{,}150 M^{-1}$ at 412 nm.[35, 36] Surface functionalized NAP-PDMS films were first cut to a recorded surface area before being placed in a solution containing 50 µL of DNTB stock solution (50 mM sodium acetate and 2 mM DTNB in DI water), 100 µL of PBS, and 850 µL of DI water. The samples were then thoroughly mixed and allowed to incubate at room temperature for 5 minutes. Optical absorbance was then

recorded at 412 nm using a UV-Vis spectrophotometer. A standard calibration curve using acetyl cysteine was made to correlate thiol concentration with absorbance.

*Nitric Oxide Release Characteristics*

Nitric oxide release from the films containing SNAP was measured using a Sievers Chemiluminescence Nitric Oxide Analyzer (NOA) 280i (Boulder, CO). The Sievers chemiluminescence Nitric Oxide analyzer is considered as the gold standard for detecting nitric oxide and is widely used due to its ability to limit interfering species, such as nitrates and nitrites, as they are not transferred from the sample vessel to the reaction cell. Films were then placed in the sample vessel immersed in PBS (pH 7.4) containing 100 mM EDTA. Nitric oxide was continuously purged from the buffer and swept from the headspace using nitrogen sweep gas and bubbler into the chemiluminescence detection chamber.

*Protein Repulsion Quantification*

Levels of protein adhesion were quantified for the various materials using a modified version of a previously reported method.[7] FITC-human fibrinogen (13 mg/mL, Molecular Innovations) was diluted to achieve 2 mg $mL^{-1}$ in PBS (pH 7.4). Silicone disks were incubated at 37°C for 30 min in a 96-well plate, followed by the addition of the stock protein solution to achieve a concentration of 2 mg $mL^{-1}$.[7] Following 2h of incubation, infinite dilution of the well contents was carried out to wash away the bulk and any loosely bound protein from the materials. The fluorescence of each well (n=8) was then measured using a 96-well plate reader (Biotek), and the amount of protein adsorbed was determined via a calibration curve.

*Bacterial Adhesion Assay*

The ability of the samples to inhibit growth and promote killing of the adhered bacteria on the polymer surface was tested following guidelines based on American Society for Testing and Materials E2180 protocol with the commonly found nosocomial pathogen, Gram-positive *S. aureus* (ATCC 6538). A single colony of bacteria was isolated from a previously cultured LB-agar plate and incubated in LB Broth (37°C,150 rpm, 14-16h). The optical density of the culture was measured at a wavelength of 600 nm using a UV-vis spectrophotometer (Thermoscientific Genesys 10S UV-Vis) to ensure the presence of ~$10^6$-$10^8$ CFU $mL^{-1}$. The overnight culture was then centrifuged at 2500 rpm for 7 min to obtain the bacterial pellet. The bacterial pellet obtained was resuspended in sterile PBS. The polymer samples (SR control, SIM-N1, SIM-S1, SIM-N2 and SIM-S2) were then incubated in the bacterial suspension (37 °C, 24h, 200 rpm). After incubation, samples were removed from the bacterial suspension and rinsed with sterile PBS to remove any unbound bacteria. They were then sonicated for 1 min each using an Omni Tip homogenizer for 1 min to collect adhered bacteria in sterile PBS. To ensure proper homogenization of the collected bacteria, the samples were vortexed for 45s each. The solutions were serially diluted, plated on LB agar medium and incubated at 37°C. After 24h, the total CFUs for serially diluted and plated bacterial solutions were counted.

*Platelet Adhesion Assay*

Freshly drawn porcine blood was purchased from Lampire Biologicals. The anticoagulated blood was centrifuged (1100 rpm, 12 min) using the Eppendorf Centrifuge 5702. The platelet rich plasma (PRP) portion was collected carefully with a pipet as to not disturb the buffy coat. The remaining samples were then centrifuged (4000 rpm, 20 min) to retrieve platelet poor plasma (PPP). Total platelet counts in both PRP and PPP fractions were determined using a

hemocytometer (Fisher). The PRP and PPP were combined in a ratio to give a final platelet concentration ca. 2 x $10^8$ platelets $mL^{-1}$. Calcium chloride ($CaCl_2$) was added to the final platelet solution to achieve a final concentration of 2.5 mM.[7] Disks of each respective surface were placed in a 5 mL blood tube. Approximately 4 mL of the calcified PRP was added to each tube and incubated (37°C, 90 min) with mild rocking (25 rpm). Following the incubation, the tubes were infinitely diluted with normal saline. The degree of platelet adhesion was determined using the lactate dehydrogenase (LDH) released when the adherent platelets were lysed with a Triton-PBS buffer using a Roche Cytotoxicity Detection Kit (LDH). The silicone disks were then incubated in 1 mL of Triton-PBS buffer. After 25 min, 100 μL was transferred to a 96-well plate and combined with 100μL of the LDH reagent buffer per the supplier specifications. The absorbance of each well (duplicates of n=6) was then measured using a 96-well plate reader (Biotek), and the number of platelets adhered was determined using the calibration curve.

*Acknowledgements*

M.G. and P.S. contributed equally to this work. The authors acknowledge the financial support of the National Institutes of Health (K25HL111213 and RO1HL134899), and the University of Georgia start-up funds. MG would like to thank the ARCS Foundation of Atlanta for their support. The authors also appreciate the support of Jason Locklin for use of the Krüss drop shape analyzer and FTIR.

**References**

1. B. D. Ratner, Biomaterials, 2007, 28, 5144-5147.
2. E. J. Brisbois, R. P. Davis, A. M. Jones, et al., Journal of Materials Chemistry B, 2015.

3. R. E. Cronin and R. F. Reilly, 2010.
4. N. Høiby, O. Ciofu, H. K. Johansen, et al., International journal of oral science, 2011, 3, 55.
5. P. Singha, J. Pant, M. J. Goudie, et al., Biomaterials Science, 2017.
6. G. W. Charville, E. M. Hetrick, C. B. Geer, et al., Biomaterials, 2008, 29, 4039-4044.
7. B. Sivaraman and R. A. Latour, Biomaterials, 2010, 31, 832-839.
8. L.-C. Xu and C. A. Siedlecki, Biomaterials, 2007, 28, 3273-3283.
9. X. Hou, X. Wang, Q. Zhu, et al., Colloids and Surfaces B: Biointerfaces, 2010, 80, 247-250.
10. E. Ueda and P. A. Levkin, Advanced healthcare materials, 2013, 2, 1425-1429.
11. L. C. Xu and C. A. Siedlecki, Journal of Biomedical Materials Research Part B: Applied Biomaterials, 2017, 105, 668-678.
12. E. J. Falde, S. T. Yohe, Y. L. Colson, et al., Biomaterials, 2016, 104, 87-103.
13. N. MacCallum, C. Howell, P. Kim, et al., ACS Biomaterials Science & Engineering, 2014, 1, 43-51.
14. D. C. Leslie, A. Waterhouse, J. B. Berthet, et al., Nature biotechnology, 2014, 32, 1134-1140.
15. N. A. Alcantar, E. S. Aydil and J. N. Israelachvili, Journal of biomedical materials research, 2000, 51, 343-351.
16. K. Holmberg, K. Bergström and M.-B. Stark, in Poly (Ethylene Glycol) Chemistry, Springer, 1992, pp. 303-324.
17. C.-G. Gölander, J. N. Herron, K. Lim, et al., in Poly (ethylene glycol) Chemistry, Springer, 1992, pp. 221-245.

18. J. H. Lee, H. B. Lee and J. D. Andrade, Progress in Polymer Science, 1995, 20, 1043-1079.

19. J. Andrade, V. Hlady and S.-I. Jeon, Polymeric Materials: Science and Engineering, 1993, 60-61.

20. J. M. Harris, Poly (ethylene glycol) chemistry: biotechnical and biomedical applications, Springer Science & Business Media, 1992.

21. E. J. Brisbois, H. Handa and M. E. Meyerhoff, in Advanced Polymers in Medicine, Springer, 2015, pp. 481-511.

22. T. Kolobow, E. Stool, P. Weathersby, et al., Transactions-American Society for Artificial Internal Organs, 1974, 20, 269.

23. M. A. De Groote and F. C. Fang, Clinical Infectious Diseases, 1995, 21, S162-S165.

24. M. J. Goudie, E. J. Brisbois, J. Pant, et al., International Journal of Polymeric Materials and Polymeric Biomaterials, 2016, 65, 769-778.

25. E. J. Brisbois, T. C. Major, M. J. Goudie, et al., Acta Biomaterialia, 2016, 44, 304-312.

26. M. W. Vaughn, L. Kuo and J. C. Liao, American Journal of Physiology-Heart and Circulatory Physiology, 1998, 274, H2163-H2176.

27. E. J. Brisbois, T. C. Major, M. J. Goudie, et al., Acta biomaterialia, 2016, 37, 111-119.

28. E. J. Brisbois, T. C. Major, M. J. Goudie, et al., Acta Biomaterialia, 2016.

29. E. J. Brisbois, H. Handa and M. E. Meyerhoff, in Advanced Polymers in Medicine, ed. F. Puoci, Springer International Publishing Switzerland, Switzerland, 2015.

30. S. Y. Tong, J. S. Davis, E. Eichenberger, et al., Clinical microbiology reviews, 2015, 28, 603-661.

31. D. Ní Eidhin, S. Perkins, P. Francois, et al., Molecular Microbiology, 1998, 30, 245-257.

32. T. Boland, R. A. Latour and F. J. Stutzenberger, in Handbook of Bacterial Adhesion, Springer, 2000, pp. 29-41.

33. J. J. Ferguson, R. A. Harrington and N. A. Chronos, Antiplatelet Therapy in Clinical Practice, Taylor & Francis, 1999.

34. S. M. de Lizarrondo, C. Gakuba, B. A. Herbig, et al., Circulation, 2017, CIRCULATIONAHA. 117.027290.

35. G. L. Ellman, Archives of biochemistry and Biophysics, 1958, 74, 443-450.

36. G. L. Ellman, Archives of biochemistry and biophysics, 1959, 82, 70-77.

# CHAPTER 6

# CONCLUSIONS AND FUTURE DIRECTIONS

The drive to develop a truly biocompatible material has resulted in a variety of approaches to combat the issues of thrombosis while mitigating the risk of infection over the past 40 years. These approaches include attachment of polymer brushes, zwitterionic materials, direct and indirect thrombin inhibitors (such as agatroban or heparin), liquid-infused materials, hydrogel coatings, antibiotic releasing materials, and fibrinolytic materials; each having their own advantages and disadvantages. While each of these approaches have provided great strides in increasing the safety of medical materials, it is clear that there is no single solution to solving the issues of thrombosis and device related infection.

This dissertation examines the characteristics of nitric oxide releasing materials both for their antithormbogenic and antimicrobial properties, as well as their clinical applicability and translation from the bench top to the bedside. The efficacy of these materials was then further improved using two separate approaches: i) integration of NO releasing materials with ultra-low fouling liquid-infused materials, and ii) covalent attachment of NO donors as a polymer brush for a non-fouling NO releasing surface. These materials not only greatly reduce the adhesion of protein and bacteria that lead to thrombosis and infection, but can actively prevent platelet activation and biofilim formation responsible for serious complications.

The results outlined in this dissertation set the ground work for the next class of medical materials, which utilize multiple mechanisms to limit thrombus formation and infection. Future work could include the combination of nitric oxide release with direct/indirect thrombin

inhibitors, or examining the materials described in this dissertation in further detail in animal models. It is also not fully understood at this time how liquid-infused materials interact with blood proteins such as albumin and fibrinogen, with a similar understanding for the surface immobilization of nitric oxide donors (specifically nitrosothiols). The details in the protein-surface or protein-liquid interface can provide vital information on the activity of these materials and their ability to limit platelet adhesion and activation. Similarly, the fundamental interaction between liquid-infused materials and bacterial colonization can be further investigated.